

**A novel series of titanocene dichloride derivatives:
synthesis, characterization and assessment of their
cytotoxic properties**

by

Gregory David Potter

A thesis submitted to the Department of Chemistry
in conformity with the requirements for
the degree of Doctor of Philosophy

Queen's University

Kingston, Ontario, Canada

May, 2008

Copyright © Gregory David Potter, 2008

Abstract

Although *cis*-PtCl₂(NH₃)₂ (cisplatin) has been widely used as a chemotherapeutic agent, its use can be accompanied by toxic side effects and the development of drug resistance. Consequently, much research has been focused on the discovery of novel transition metal compounds which elicit elevated cytotoxicities coupled with reduced toxic side effects and non-cross resistance. Recently, research in this lab has focused on preparing derivatives of titanocene dichloride (TDC), a highly active chemotherapeutic agent, with pendant alkylammonium groups on one or both rings. Earlier results have demonstrated that derivatives containing either cyclic or chiral alkylammonium groups had increased cytotoxic activities.

This research therefore investigated a new series of TDC complexes focusing specifically on derivatives bearing cyclic and chiral alkylammonium groups. A library of ten cyclic derivatives and six chiral derivatives were synthesized and fully characterized. These derivatives have undergone *in vitro* testing as anti-tumour agents using human lung, ovarian, and cervical carcinoma cell lines (A549, H209, H69, H69/CP, A2780, A2780/CP and HeLa). These standard cell lines represent solid tumour types for which new drugs are urgently needed. The potencies of all of the Ti (IV) derivatives varied greatly (range from 10.8 μM - >1000 μM), although some trends were observed. In general, the dicationic analogues exhibited greater potency than the corresponding monocationic derivatives. Additionally, the cyclic analogues bearing 1,3- and 1,4-

substituted pyridines displayed potent cytotoxic activities ($IC_{50} > 20 \mu M$). It was also found at concentrations of $\sim 30 \mu M$ that the derivatives bearing an ephedrine derived substituent were cytotoxic. Conversely, analogues substituted with piperidinyl, morpholinyl or primary alkylammonium groups were inactive ($> 200 \mu M$) against the cancer cell lines assayed.

Acknowledgements

There have been a lot of people that have played a significant role in my life over the past few years while I was at Queen's. First and foremost, I would like to thank my supervisor and mentor Mike Baird. He has always been caring, patient and a diligent driving force for me to improve myself. I always appreciated his dedication to his students and their professional development. His passion for chemistry has always been inspiring. I would also like to acknowledge all of the past and present members of the Baird lab. Most notably I wish to thank John Brownie, Goran Stojcevic and Emily Mitchell all of whom have made this experience more enjoyable. I also wish to thank my co-supervisors Dr. Susan P.C Cole and Dr. Philip G. Jessop. As well, I wish to thank Marina Chan and Kathy Sparks for their work with the MTT assays.

Thank you to all of my friends that I have made at Queen's over the past few years. I am grateful for all of the support and words of encouragement from my friends and family outside of the lab. I would also like to acknowledge all of the past students that I have taught throughout my tenure in graduate school. I have always enjoyed teaching and my relationship with the students has made this experience far more rewarding.

Most importantly, I wish to thank my caring and supportive girlfriend Jennifer. I don't know how you put up with me over these past years, but I am sure glad that you did. Thank you for always being there when I needed you the most.

Statement of Co-Authorship and Originality

Unless specifically stated otherwise, the author under the supervision of Professor Michael C. Baird and Professor S.P.C Cole performed all of the research presented in this thesis.

This research reports the synthesis, characterization and cytotoxic activity of a series of sixteen TDC derivatives bearing cyclic and chiral alkylammonium groups against various cancer cell lines.

Table of Contents

Abstract.....	ii
Acknowledgements	iv
Statement of Co-Authorship and Originality	v
Chapter 1: Introduction	1
1.1 Cancer and the need for new treatments	1
1.2 Discovery and development of cisplatin as a chemotherapeutic agent ..	2
1.3 Mechanism of action of cisplatin.....	3
1.4 The pursuit of more effective analogues of cisplatin.....	6
1.5 Development of metallocenes as chemotherapeutic agents	7
1.6 Aqueous chemistry of titanocene dichloride	9
1.7 The uptake and delivery of titanocene dichloride <i>in vivo</i>	13
1.8 Interactions of titanocene dichloride with DNA	17
1.9 Radiolabeling using Titanium-45	19
1.10 Titanocene dichloride analogues with varied anionic ligands	21
1.11 Modification of the cyclopentadienyl ligands	24
1.12 Preparation of TDC derivatives containing alkylammonium groups	33
1.13 Different methodology in preparing titanocene dichloride derivatives...	35
1.14 Research Objectives	37
Chapter 2: Experimental.....	41

2.1	General	41
2.2	X-Ray Crystal Structure Determination	42
2.3	Preparation and Characterization of Compounds	43
2.4	MTT bioassay protocol	82
Chapter 3: Results and Discussion.....		85
3.1	Synthesis of (1R, 2S)- <i>N</i> -Methylephedrine	85
3.2	Chlorination of (1R, 2S)- <i>N</i> -Methylephedrine and Alaninol.....	86
3.2	Syntheses of Cyclic Aminoalkylcyclopentadienes (14a – 20a).....	89
3.3	Results from the syntheses of Lithium Cyclic Aminoalkylcyclopentadienide salts (14b – 20b).....	94
3.4	Results from the syntheses of monocationic titanocene dichloride analogues (14c – 20c).....	99
3.5	Results for the syntheses of the dicationic titanocene dichloride analogues (14d – 20d).....	105
3.6	Characterization by NMR Spectroscopy of the monocationic titanocene dichloride complexes 14c – 20c	112
3.7	NMR spectroscopic characterization of the dicationic titanocene dichloride complexes 14d – 20d	120
3.8	Characterization of mono- and dicationic complexes (14c,d – 20c,d) by elemental analysis.	129
3.9	Characterization of Mono- and Dicationic derivatives (14c,d – 20c,d) by Mass Spectrometric Analysis.	130

3.10	Characterization of mono- and dicationic titanocene dichloride derivatives by X-ray crystallography.	134
3.11	Summary of the Results for the Syntheses and Characterization of the Mono- and Dicationic titanocene dichloride derivatives.	140
3.12	Determination of Cytotoxicity for the Titanocene Dichloride Derivatives by MTT <i>in vitro</i> assays.	141
3.13	Effect of substitution on Cytotoxicity of Titanocene Dichloride Derivatives 14c,d – 20c,d	149
	Chapter 4: Summary and Conclusions	152
	References	154

List of Figures

Figure 1	<i>cis</i> -Diamminedichloroplatinum(II).	2
Figure 2	A representation of a DNA strand highlighting the four bases, and the preferred binding sites of cisplatin. ¹⁷	4
Figure 3	Structures of platinum containing compounds (carboplatin 1 , oxaliplatin 2). The <i>cis</i> leaving groups are highlighted in red. ²⁸	6
Figure 4	Bis (η^5 -Cp) titanium(IV) dichloride, or titanocene dichloride (TDC). 8	8
Figure 5	Chloride hydrolysis equilibria for TDC. ^{50,51}	9
Figure 6	Hydrolysis of the Cp ligand generates cyclopentadiene and a titanium hydroxide species.	10
Figure 7	The complex equilibria resulting from the dissolution of TDC in water at physiological pH ~ 7.4. ⁵³	11
Figure 8	Preparation of the clinical formulation of MKT-4. ⁵⁶	12
Figure 9	One lobe of the apo (left) and the holo form (right) of transferrin. The holo form contains iron as well as the carbonate ion. ⁶¹	14
Figure 10	Metal binding site of transferrin showing coordination of Fe ³⁺ with the CO ₃ ⁻ anion. Relevant amino acid residues that bind Fe ³⁺ are shown. ⁶⁵	15
Figure 11	N,N'-ethylene bis(O-hydroxyphenylglycine) (EHPG), an excellent mimic of the metal binding site in transferrin.	16
Figure 12	Proposed mechanism of action of hydrolyzed TDC binding to the highlighted phosphate backbone of DNA in an intrastrand fashion. ^{76,79}	18
Figure 13	Irradiation of ⁴⁵ Sc with a proton leads to the ejection of a neutron and the production of ⁴⁵ Ti which is unstable. ⁸⁰	19

Figure 14	The annihilation of a positron and an electron producing two collinear γ -rays of 511 keV each.....	20
Figure 15	A titanocene cyclodextrin dimer bound by a thio-1,2-dicyanoethylenylthio-ethyl bridge. ⁸⁵	23
Figure 16	Titanocene chloride derivatives containing benzothieryl (left) and dibenzothieryl (centre and right) ligands. ⁸⁶	24
Figure 17	TDC derivatives where the Cp ligands bear electron withdrawing groups. Cp' represents either η^5 -C ₅ H ₅ or η^5 -C ₅ H ₄ R where R is the corresponding ester.	25
Figure 18	Stabilization of the reactive, vacant site on titanium by the reversible coordination of a lone pair of electrons on the pendant alkylammonia group. ⁹²	26
Figure 19	Air and water stable TDC ammonium derivative prepared by Jutzi and coworkers to be used for polymerization catalysis. ⁹³	27
Figure 20	TDC derivatives bearing piperidinyl groups prepared by McGowan and coworkers. ⁴⁹	28
Figure 21	An extended library of piperidinyl substituted titanocene derivatives prepared by McGowan and coworkers. ⁹⁶	29
Figure 22	A library of monocationic and dicationic TDC derivatives prepared by Baird and coworkers. Cp' represents either η^5 -C ₅ H ₅ or η^5 -C ₅ H ₄ R where R is the corresponding alkylammonium. ⁴⁸	30
Figure 23	The most cytotoxic TDC derivatives prepared by Baird and coworkers. ⁴⁸	31
Figure 24	TDC analogues prepared by Tacke and coworkers. ¹⁰⁰	32
Figure 25	Synthetic scheme of the preparation of TDC derivatives bearing alkylammonium groups.	34
Figure 26	A novel methodology in preparing TDC derivatives. ¹⁰⁷	36

Figure 27	An amino acid functionalized (12) and a fluorescence-labeled (13) TDC derivatives prepared from the acid chloride building block, 8 . ¹⁰⁷	36
Figure 28	An example of a steroid substituted TDC prepared from the reaction of the acid chloride building block with the corresponding alcohol. ¹⁰⁷	37
Figure 29	A small library of dicationic and monocationic TDC derivatives containing cyclic alkylammonium groups. Cp' represents either η^5 -C ₅ H ₅ or η^5 -C ₅ H ₄ R where R is the corresponding alkylammonium. 38	
Figure 30	TDC derivatives containing chiral centres. Cp' represents either η^5 -C ₅ H ₅ or η^5 -C ₅ H ₄ R where R is the corresponding alkylammonium. 39	
Figure 31	Labeling scheme for the molecules used in this research. R represents varying alkylammonia groups.	85
Figure 32	Preparation of (1R, 2S)- <i>N</i> -methylephedrine using formalin (37% wgt formaldehyde in water) and formic acid.	86
Figure 33	The chlorination of (1R, 2S)- <i>N</i> -methylephedrine using thionyl chloride resulted in the formation of the (1S, 2S) and (1R, 2S) diastereomers in a ratio of 85:15, respectively.	87
Figure 34	Chlorination of (S) and (R)-Alaninol.	88
Figure 35	Representative reaction scheme for the synthesis of the cyclic aminoalkylcyclopentadiene, 15a	89
Figure 36	Equilibrium of the regioisomers of 17a	92
Figure 37	¹ H NMR spectrum of a picolyl-substituted cyclopentadiene (17a) in CDCl ₃ . The pattern between δ 6.5 – 5.9 ppm is characteristic for all aminoalkyl-cyclopentdienes in this series (14a – 20a).	94
Figure 38	Representative reaction between methyl lithium and a cyclic aminoalkylcyclopentadiene (18a) in hexanes at 0 °C which affords the air and water sensitive lithium salt 18b	95

Figure 39	^1H NMR spectrum of the lithiated salt 18b in pyridine- d_5 . The region between δ 3.1 – 2.7 is expanded to show the triplet splitting pattern.....	98
Figure 40	Representative reaction scheme for the synthesis of 14c	100
Figure 41	Structures of the monocationic aminoalkylsubstituted TDC derivatives (14c – 20c).....	104
Figure 42	Representative reaction scheme for the preparation of (S,S)- 20d	106
Figure 43	The four possible stereoisomers of complex 20d present in (Mix)- 20d	107
Figure 44	Structures of the dicationic aminoalkylsubstituted TDC derivatives (14d – 20d).	109
Figure 45	^1H NMR spectrum of the titanocene derivative 16c in DMSO- d_6 . The region between δ 6.4 – 6.9 ppm is expanded to show the triplets on the substituted Cp ring.....	113
Figure 46	Structure of the chiral complex 19c showing the diastereotopic N,N-methyls and diastereotopic methines on the substituted Cp ring.	115
Figure 47	^1H NMR spectrum and full assignment of 19c showing the diastereotopic methine protons on the Cp ring and diastereotopic N,N-dimethyl proton resonances.....	116
Figure 48	The substituted Cp ligand of 19c illustrating three and four bond coupling.....	117
Figure 49	2D ^1H – ^1H COSY spectrum of 19c in D_2O between 6.2 – 7.0 ppm. Red and blue circles denote ^3J and ^4J coupling, respectively.	118
Figure 50	^{13}C NMR spectrum of 19c illustrating the three pairs of diastereotopic carbons.	119
Figure 51	^1H NMR spectrum of 14d in DMSO- d_6 with all labeled assignments.	121

Figure 52	^1H NMR spectrum of (R,R)- 20d in DMSO- d_6 illustrating the diastereotopic protons 4 and 4'	123
Figure 53	^{13}C NMR spectrum of (R,R)- 20d with insets illustrating the diastereotopic carbons on the Cp ring.....	124
Figure 54	Comparison of the ^1H NMR signals of 4' in (R,R)- 20d (a) and (Mix)- 20d (b) spectra. The red asterisks represent the peaks assigned to 4' in (R,S)- 20d	128
Figure 55	The predicted (a) and measured (b) isotopic patterns for the protonated molecular ion $[\text{M}+\text{H}]^+$ of 15c	132
Figure 56	Molecular structure of 14d showing two molecules per unit cell and two molecules of ethanol; thermal ellipsoids are shown at 50% probability level.	136
Figure 57	Molecular structure of 16c ; thermal ellipsoids are shown at 50% probability level.	136
Figure 58	The crystal structure of 18d ; thermal ellipsoids are shown at 50% probability level.	137
Figure 59	The molecular structure of 19c showing two molecules per unit cell; thermal ellipsoids are shown at 50% probability level.	137
Figure 60	(a) Representative dose response curves for cisplatin (\circ) and TDC (\bullet) against A549 lung tumour cells; (b) Representative dose response curves for TDC derivatives 15c (\bullet) and 15d (\circ) against A549 lung tumour cells.....	143
Figure 61	The two constitutional isomers making up 15e	147

List of Tables

Table 1	¹ H NMR data (δ), assignments for the hydrochloride salts 19 , 20 . 88
Table 2	Summary of reaction conditions used in the preparation of cyclic aminoalkyl-substituted cyclopentadienes (14a – 20a)..... 90
Table 3	Summary of ¹ H NMR data (δ) for compounds 14a – 20a 93
Table 4	Summary of reaction conditions, yields and ¹ H, ¹³ C NMR Data (δ) for the lithiated salts 14b – 18b 96
Table 5	Summary of reaction conditions, yields, and ¹ H, ¹³ C NMR Data (δ) for the lithiated salts 19b – 20b 97
Table 6	Summary of reaction conditions and yields for the generation of monocationic TDC complexes 14c – 20c 102
Table 7	Summary of reaction conditions and yields for the generation of dicationic TDC complexes 14d – 20d 111
Table 8	¹ H and ¹³ C NMR Data (δ) for titanocene derivatives (14c – 18c). 114
Table 9	¹ H and ¹³ C NMR Data (δ) for titanocene derivatives (19c – 20c). 120
Table 10	¹ H and ¹³ C NMR Data (δ) for titanocene derivatives (14d – 18d). 122
Table 11	¹ H and ¹³ C NMR Data (δ) for titanocene derivatives (19d – 20d). 126
Table 12	Elemental analytical data for monocationic complexes 14c – 20c 129
Table 13	Elemental analytical data for dicationic complexes 14d – 20d 130
Table 14	Mass spectral data for the monocationic complexes 14c – 20c . . 133
Table 15	Mass spectral data for the dicationic complexes 14d – 20d 133
Table 16	Crystallographic data for compounds 14d , 16c , 18d and 19c 138

Table 17	List of selected bond distances and angles of 14d , 16c , 18d , 19c and TDC.....	140
Table 18	Effect of cyclic TDC analogues on human tumour cell viability ...	145
Table 19	Effect of chiral TDC analogues on human tumour cell viability....	146

List of Abbreviations

COSY	$^1\text{H} - ^1\text{H}$ correlation spectroscopy
Cp	cyclopentadienyl
Cp ⁻	cyclopentadienide anion
d	doublet
DMEM	Dulbecco's Modified Eagle Medium
DMF	<i>N,N</i> -dimethylformamide
DMSO	dimethyl sulfoxide
ES	electrospray
HMBC	Heteronuclear Multiple Bond Correlation
HSQC	Heteronuclear Single Quantum Coherence
m	multiplet
MTT	[4,5-dimethyl(thiazol-2-yl)-3,5-diphenyl]tetrazolium bromide
NMR	nuclear magnetic resonance
Ph	phenyl
q	quartet
SD	standard deviation
t	triplet
THF	tetrahydrofuran
TMS	trimethylsilyl

Chapter 1: Introduction

1.1 Cancer and the need for new treatments

Cancer is a group of diseases that can be categorized as aggressive, invasive, metastatic and/or benign. Cancer cells that uncontrollably grow and divide constitute aggressive cancer; cancer cells that invade and destroy neighbouring, healthy cells are described as invasive; and cancer cells that migrate to other areas of the body and form new tumours are called metastatic.¹ The current clinical modalities of treatment for cancer consist of radiation therapy, chemotherapy and surgery. Often a combination of all of these approaches is used. The cancer statistics presented in the following paragraph are taken from “National Cancer Institute of Canada: Canadian Cancer Statistics 2007, Toronto, Canada, 2007.”

Only recently surpassing cardiovascular disease, cancer is now the leading cause of death in Canada, accounting for almost 33% of all deaths.² In 2003, it was estimated that over 1,006,000 potential years of what were lost due to cancer related deaths. The Canadian Cancer Society (CCS) estimates that there will be 159,900 new cases of cancer and 72,700 deaths from cancer this year.² The three most lethal forms of cancer are lung, breast and prostate. Cancer is considered a disease of the elderly and, since the “baby boomer” generation is entering its senior years, this illness will become more and more prevalent. This and the lack of efficacy of current drugs have created an increased demand for new and innovative treatments. Our research has focused

on developing new drugs that may be useful for treating lung (small cell and non-small cell), ovarian and cervical cancer because of the urgent need for improved chemotherapy against these and other solid tumour types. The five year survival rates of lung, ovarian and cervical cancers are 15%, 40% and 75%, respectively. These cancers have much lower five year survival rates compared to the more publicized breast (85%) and prostate (95%) cancers. ²

1.2 Discovery and development of cisplatin as a chemotherapeutic agent

The whole field of medicinal chemistry involving the use of transition metal complexes as chemotherapeutic agents was born from the serendipitous discovery of the chemotherapeutic activity of cis-diamminedichloroplatinum(II), also called cisplatin (Figure 1).³ Rosenberg and coworkers were studying the effects of electrical currents on the growth of *Escherichia coli* (*E. coli*) cells using a platinum electrode in an ammonium chloride solution. This inhibited of *E. coli* cell division. After a series of experiments, they discovered that the cause of the inhibition was cisplatin and not the electrical current. Subsequent studies determined that cisplatin had potent anticancer activity, and consequently it entered clinical trials.^{4,5}

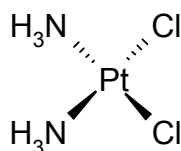


Figure 1 *cis*-Diamminedichloroplatinum(II).

The discovery of cisplatin has spawned the preparation and evaluation of thousands of platinum-based compounds, although few have actually entered clinical use.^{6,7} It is estimated that platinum based chemotherapeutic agents account for approximately US \$2 billion in annual sales.^{8,9} Even though its activity was discovered over thirty years ago, it is still one of the most widely used drugs for the treatment of bladder, ovarian, and head and neck cancers.^{6,7,10,11} Furthermore, cisplatin is responsible for curing over 90% of testicular cancer cases.¹⁰

1.3 Mechanism of action of cisplatin

When cisplatin is administered to the patient intravenously via the bloodstream, it encounters a relatively high chloride concentration in the blood plasma (approximately 100 mM) that hinders substitution of the chloride ligands by water.⁸ Cisplatin migrates into cancer cells by diffusing through the cell membrane¹² and since the chloride concentration is relatively low (4-20 mM)⁸ inside the cell, the mutually *cis* chloride ligands are substituted with water. The dicationic moiety [*cis*-Pt(H₂O)₂(NH₃)₂]²⁺ is a “soft acid” and if able to get into the nucleus, it can readily react with DNA accordingly. Instead of binding to the phosphate backbone (“hard base”) of DNA, it reacts with the softer bases (preferably guanine at N7) forming a monofunctional adducts^{13,14}. A schematic representation of DNA is shown in Figure 2 highlighting the bases and preferred binding sites of cisplatin. Rapid intrastrand ring closure then occurs upon reaction of the monofunctional adduct with an adjacent base.^{15,16} These

intrastrand cisplatin-DNA complexes *in vitro* have been confirmed by x-ray crystallography.¹⁷ The majority of cisplatin-DNA adducts occur with two adjacent

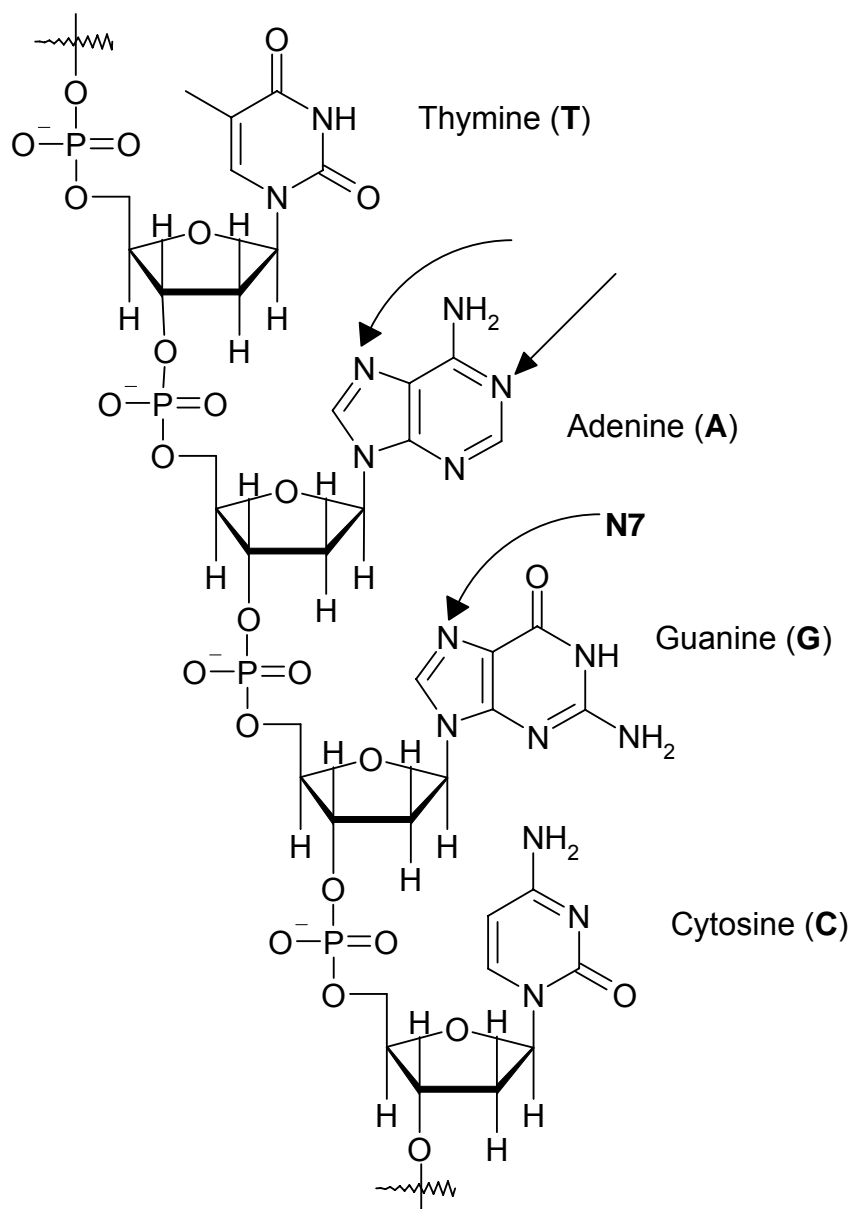


Figure 2 A representation of an oligodeoxynucleotide strand highlighting the four bases, and the preferred binding sites of cisplatin.¹⁷

guanine units (65%), with a small amount as adenine-guanine adducts (25%).^{18,19} The cisplatin-DNA adducts are significantly distorted which in turn inhibits DNA transcription and/or replication, leading to cell death.

Despite its remarkable success, cisplatin has several disadvantages. One problem cisplatin faces is that once it is administered in the bloodstream, it may be bound by proteins found in the blood, reducing the free concentration of drug that may be taken up into cancer cells. In particular, proteins rich in thiol or thioether groups (containing cysteine or methionine amino acids) have been shown to strongly bind cisplatin.²⁰⁻²² This protein binding deactivates the drug^{21,23,24} and decreases its effectiveness. The side effects associated with cisplatin are severe and may include nephrotoxicity, neurotoxicity, nausea, vomiting, hair loss and hearing difficulties.^{7,20,23,24} The toxic side effects of cisplatin limit the dose and frequency with which the drug can be given to patients.^{7,20,23,24}

The effectiveness of cisplatin is also limited by drug resistance. Several tumours are inherently relatively resistant to cisplatin (eg. colon cancer), while others develop a resistance after exposure to the drug over time (eg. ovarian cancer)²⁵, thereby limiting its clinical usefulness.¹⁵ Moreover, tumours that are exposed to cisplatin may develop cross resistance to other similarly acting drugs thereby reducing the effectiveness of other treatments.¹⁵ These particular limitations have driven the search for new compounds exhibiting potent cytotoxic activity along with reduced side effects and non-cross resistance.

1.4 The pursuit of more effective analogues of cisplatin

Despite the widespread success of cisplatin, there has been a lot of research to prepare novel platinum drugs that will perform better in the clinic. Subsequent developments of cisplatin derivatives focused on either improving upon the above mentioned limitations or the ability to be administered orally.¹⁰ Structure-activity studies performed by Cleare and coworkers^{26,27} established some desirable criteria in the platinum compounds: they should have two leaving groups that are *cis* with respect to one another, be chemically neutral, and the leaving groups should be moderately easy to remove.⁷ Following these criteria, a plethora of new cisplatin analogues was prepared and tested for cytotoxic activity.⁷

Carboplatin (Figure 3, **1**) was one of the first derivatives prepared and was found to be less cytotoxic than cisplatin and caused fewer and less severe toxic side effects.¹⁰ It is the only platinum-containing compound aside from cisplatin to have gained widespread use against a variety of different cancers.²⁸ The reduction in toxicity of carboplatin has been partly attributed to the bidentate cyclobutanedicarboxylate leaving groups that have been shown to be less labile than the chlorides present in cisplatin.^{7,10,28} Oxaliplatin (Figure 3, **2**) is the only

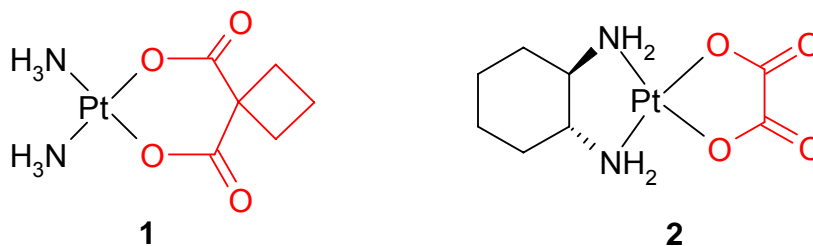


Figure 3 Structures of platinum containing compounds (carboplatin **1**, oxaliplatin **2**). The *cis* leaving groups are highlighted in red.²⁸

known platinum-containing compound that displays activity against colorectal cancer and has been recently approved for clinical use.^{7,28,29}

1.5 Development of metallocenes as chemotherapeutic agents

Since the mode of action of cisplatin involves coordination of DNA to cisplatin in a *cis* fashion, a great deal of research has focused on a variety of transition metal complexes bearing labile *cis* chlorides or similar ligands.³⁰ Among the candidate drugs, the pseudotetrahedral metallocene complexes of the type $(C_5H_5)_2MCl_2$ represent a seemingly logical extension of cisplatin derivatives and have received much attention. These complexes are made up of a metal core consisting of early transition metals from the subgroups 4, 5 or 6 of the periodic table ($M = Ti^{31}, V^{32}, Nb^{33}, Mo^{34}, W^{35}$ etc). The coordination sites of the metal are occupied by two cyclopentadienyl rings ($C_5H_5^-$ or Cp^-) and two labile ligands (ie Cl^-) in a “cis” fashion. The five-membered aromatic Cp rings each bear a negative charge and are coordinated to the metal centre via pentahapto fashion generating an “open sandwich” complex. Köpf-Maier and coworkers³⁶ investigated the antitumour activities of a whole series of metallocene dichloride complexes (varying the transition metal) *in vivo* using simple animal tumour models. From this research, they found that titanocene dichloride (TDC, Figure 4) exhibited the most promising chemotherapeutic activity among all of the other metallocenes tested.³⁷

TDC has been shown to be effective against Ehrlich ascites tumour, B16 melanoma, colon B adenocarcinoma, Lewis lung carcinoma and sarcoma 180

cells and to date, is the only metallocene dihalide to have entered clinical trials.³⁸⁻

⁴¹ In phase I clinical trials, TDC was shown to have significantly fewer toxic side-effects than cisplatin.⁴²⁻⁴⁵ The dose-limiting side effect of TDC was found to be

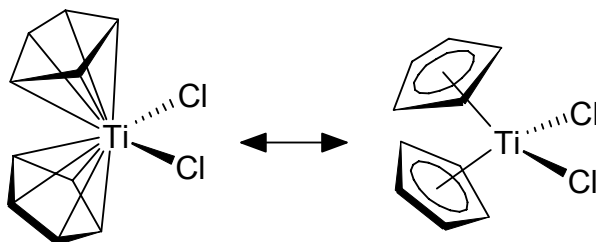


Figure 4 Bis (η^5 -Cp) titanium(IV) dichloride, or titanocene dichloride (TDC).

hepato (liver) toxicity which was found to be reversible. This is unlike cisplatin which has a dose-limiting side effect of nephro (kidney) toxicity. TDC was entered into two phase II clinical trials with patients that had advanced renal cell carcinoma and metastatic breast carcinoma.^{46,47} The results reported included using TDC as a single agent in chemotherapy, but were not sufficiently promising to warrant further investigation and further clinical trials involving TDC were abandoned.⁴⁷

Although TDC has shown significant cytotoxic activity, the active titanium containing species and its mechanism of action is poorly understood. Inherently, TDC has poor aqueous stability. It has been shown, however, to exhibit chemotherapeutic activity, suggesting biomolecules may be involved in its uptake and transport to cancer cells. Furthermore, studies showed that in spite of its structural similarity to cisplatin, it is quite effective against cisplatin resistant cancer cell lines, suggesting that TDC has a different mechanism of action.^{48,49}

1.6 Aqueous chemistry of titanocene dichloride

In order to better understand the mechanism of action of TDC *in vivo*, one must first determine its reactivity in aqueous media. Upon dissolution in water, the chloride ligands of TDC rapidly hydrolyze and this hydrolysis has been shown to be an order of magnitude faster than that of cisplatin.^{50,51} The loss of the first chloride ligand is too fast to be easily measured and occurs as soon as TDC is dissolved in water, whereas the second chloride hydrolyzes with a half-life of approximately 50 min at 35 °C.⁵⁰ This results in a complex series of equilibria involving four hydrolyzed titanocene derivatives that are dependent on both the pH and chloride concentration of the solution (Figure 5).⁵⁰ The rate of hydrolysis is expected to decrease at low pH values and at high chloride concentrations since the equilibrium will favour TDC.

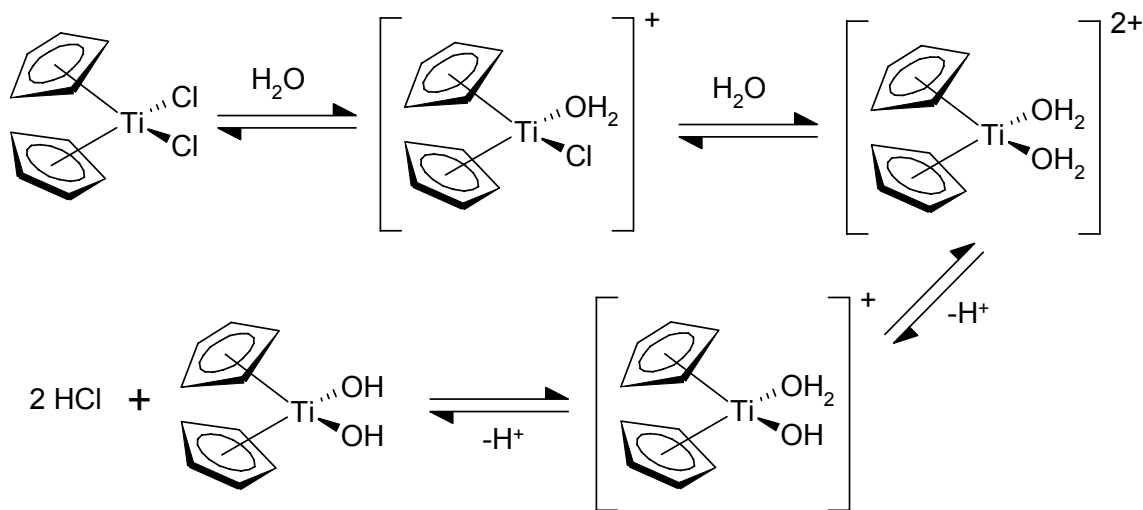


Figure 5 Chloride hydrolysis equilibria for TDC.^{50,51}

Freshly prepared solutions of TDC in water exhibit pH values of 2 – 3, depending upon the concentration of TDC. The most acidic titanocene is the diaquo species $[\text{Cp}_2\text{Ti}(\text{H}_2\text{O})_2]^{2+}$ which has a measured $\text{pK}_{\text{a}1}$ of 3.51 and a $\text{pK}_{\text{a}2}$ of 4.35. In physiological conditions of $\text{pH} \sim 7.4$, the predominant form is the dihydroxyl titanocene species $[\text{Cp}_2\text{Ti}(\text{OH})_2]$. In addition to the hydrolysis of the chloride ligands of TDC, the Cp rings can also undergo hydrolysis. Titanocene can react with water to produce a hydroxyl titanium species and free cyclopentadiene (Figure 6).

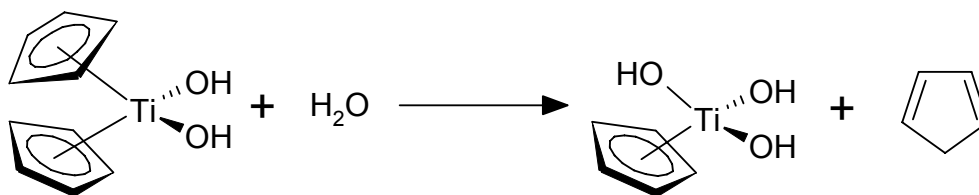


Figure 6 Hydrolysis of the Cp ligand generates cyclopentadiene and a titanium hydroxide species.

Free cyclopentadiene initially forms following first order kinetics and the half-life of the first Cp ring loss has been shown to be approximately 57 h at 37 °C in unbuffered D_2O .⁵⁰ At low pH values, the Cp rings have been shown to be stable over several days.⁵² However, under physiological conditions ($\text{pH} \sim 7.4$), ring hydrolysis becomes much more facile.⁵² In comparison, the hydrolysis of the Cp ligand is significantly slower than that of the chloride ligands.

As a result of these hydrolysis reactions, the aqueous chemistry of TDC is very complex and has been shown to involve more than 14 possible species containing Ti(IV)-bound cyclopentadienide (Figure 7). The equilibria associated

with these species is heavily dependent upon pH and chloride concentration. Ultimately, the hydrolysis of either the Cp or the chloride ligands leads to the formation of insoluble precipitates and biologically inactive products. The precipitates have been attributed to such products as TiO_2 and polymeric species (eg. $[(\text{CpTiO})_4\text{O}_2]_n$) which form through the equilibria shown in Figure 7.⁵³

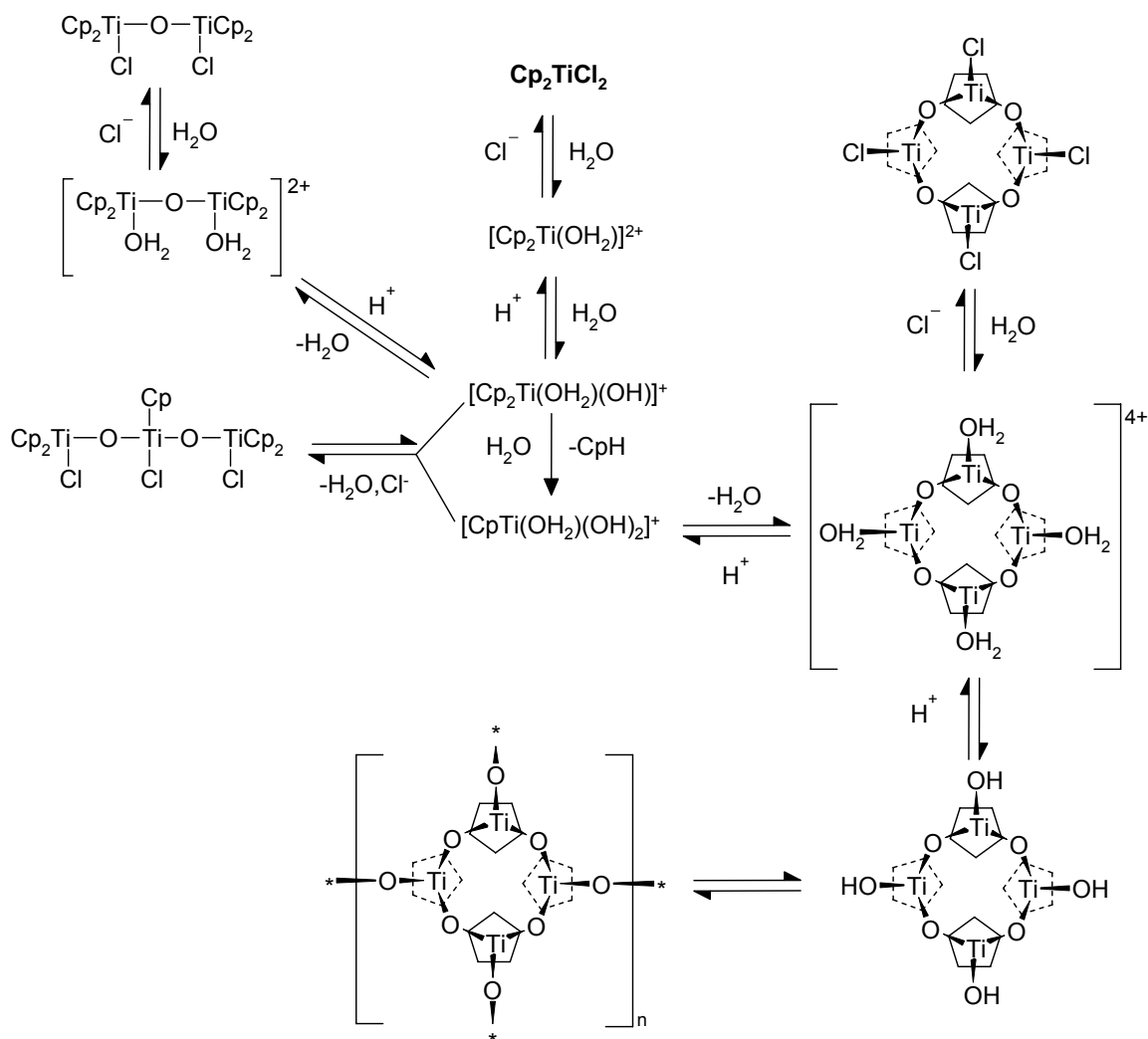


Figure 7 The complex equilibria resulting from the dissolution of TDC in water at physiological pH ~ 7.4 .⁵³

As mentioned previously, TDC has poor, inherent solubility in aqueous solutions. Small amounts of dimethylsulfoxide (DMSO, up to 10%), are typically added in order to improve the solubility of TDC in saline solutions. However, it has been shown that even small amounts of DMSO increase the rate of ring hydrolysis.^{54,55} The reason for this effect is not yet understood. These disadvantages have prompted the development of clinical formulations of TDC that are resistant to hydrolysis and precipitation reactions for use in clinical trials. One particular formulation (MKT-4) is a lyophilized TDC that is prepared by heating a solution of TDC in water with sodium chloride and d-mannitol (Figure 8).⁵⁶ The resulting orange coloured solution is frozen to -50 °C and the water is removed by sublimation under reduced pressure, resulting in a peach coloured precipitate. Other sugars such as sucrose, lactose, glucose or sorbitol have also been used to prepare similar formulations.⁵⁶ This procedure generates air-stable solids that are readily soluble in water and easy to administer by injection. This formulation and others have been used in phase II clinical trials.⁴⁶

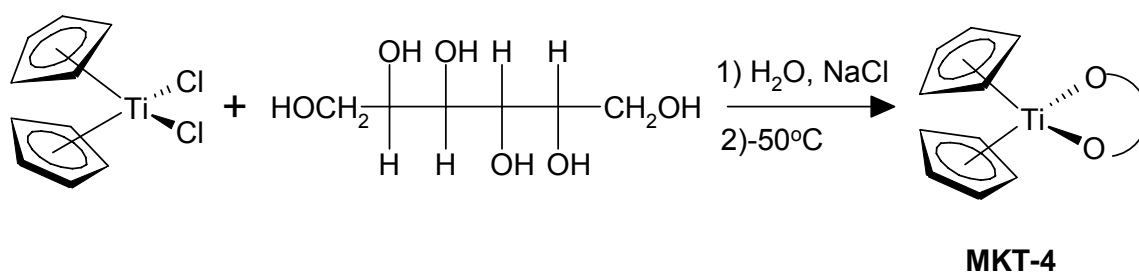


Figure 8 Preparation of the clinical formulation of **MKT-4**.⁵⁶

There has been some recent research done with regard to the aging of TDC in organic solvents. Osella and coworkers⁵⁷ prepared solutions of TDC in methanol, ethanol and DMSO. The solutions were kept at 4 °C in the dark and studied by conductivity measurements and ¹H NMR spectroscopy over a period of fourteen days. The chloride anions were shown to be fully substituted after 10 days in all of the solvents. The rates of chloride substitution by solvent were not reported and therefore cannot be compared to previously reported data. DMSO was shown to be the only solvent that caused significant Cp ring hydrolysis (60% over 10 days) in solution. The “aged” titanocene products in methanol and ethanol were shown to have increased cytotoxicity against human colon adenocarcinoma cells (HCT116), whereas the products aged in DMSO did not.⁵⁷ This observation implies that the Cp ligands play some role in the cytotoxic activity of TDC.

1.7 The uptake and delivery of titanocene dichloride *in vivo*

At a physiological pH ~ 7.4, TDC has been shown in the previous section to be relatively unstable and hydrolyzes to form precipitates over a period of days.⁵³ In spite of this, when TDC is administered intravenously, titanium-containing species are still effective at killing cancer cells. This suggests that stabilization and/or transport of the titanium containing species *in vivo* through the blood stream to the tumour must occur through the use of biomolecules. Until recently, the biomolecule involved with the uptake and release of Cp₂TiCl₂ to cancer cells has remained a mystery. Research by Sadler⁵⁸ and coworkers

has demonstrated that TDC and other titanium containing species strongly interact with the protein transferrin. Their work has provided evidence indicating that transferrin is involved with the delivery of titanium and its uptake into the cancer cell.

Transferrin is an 80 kDa protein comprised of 678 amino acids. The folded protein has two lobes, each containing a binding site deep inside a cleft. The relative binding affinities, concentrations in blood plasma, as well as the amino acids exposed on the surface of the protein all influence the binding of various metals.⁵⁹ This protein is primarily used by the body for the transport of iron from uptake in the gut into the blood stream to utilization sites. The blood plasma concentration of transferrin is approximately 35 μM and is only 30%

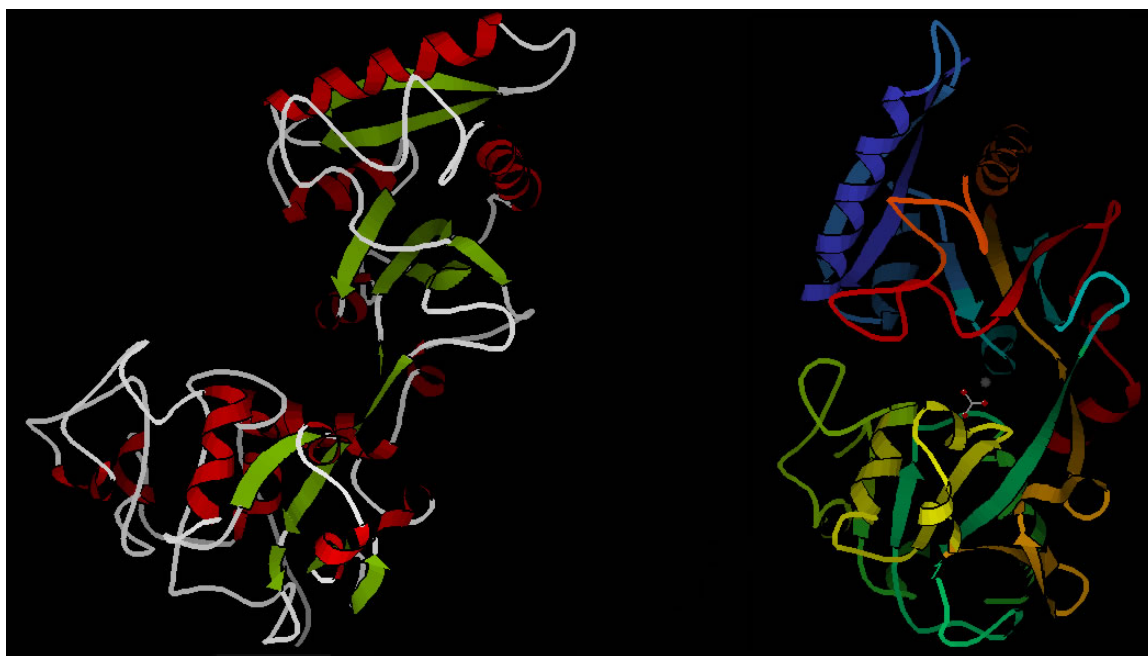


Figure 9 One lobe of the apo (left) and the holo form (right) of transferrin. The holo form contains iron as well as the carbonate ion.⁶¹

Fe(III) saturated *in vivo*.⁶⁰ The x-ray crystal structures of both the apo (iron-free) and holo (iron-bound) forms of transferrin have been elucidated and are shown in Figure 9.^{61,62} Transferrin undergoes a complete conformational change upon binding iron. In the apo form, the binding site is wide open and exposed, whereas the holo form is completely closed around the bound iron atom (ion).⁶¹

During clinical trials, pharmacokinetic studies were performed and showed that greater than 70% of serum titanium (which was administered as TDC) was bound by proteins following intravenous injection.⁴⁴ Sadler and coworkers have shown *in vitro*, that both Cp ligands are displaced and titanium(IV) is taken up by the vacant iron(III) binding sites in transferrin at blood plasma pH values.^{40,58,63,64} A schematic representation of iron(III) along with a carbonate ion inside the binding cavity of transferrin is shown in Figure 10.⁶⁵ Iron(III) is bound with

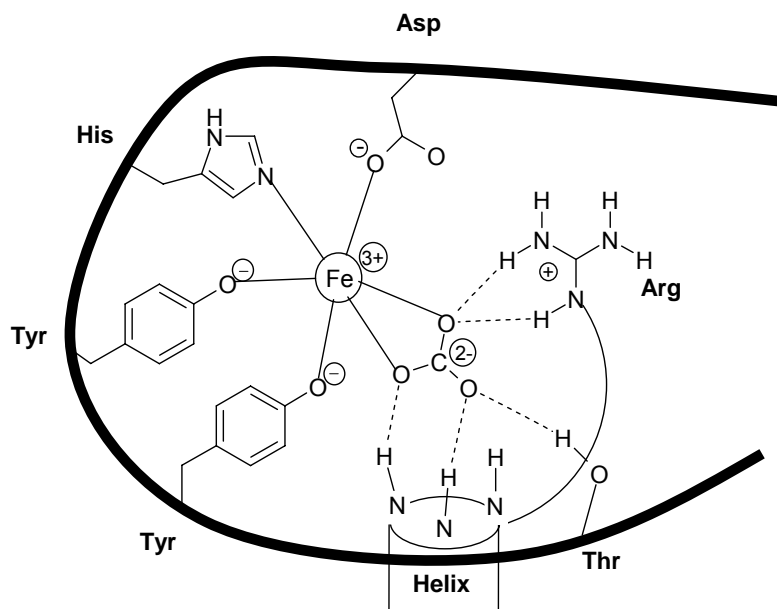


Figure 10 Metal binding site of transferrin showing coordination of Fe^{3+} with the CO_3^{2-} anion. Relevant amino acid residues that bind Fe^{3+} are shown.⁶⁵

octahedral coordination inside the cavity by four amino acids: two tyrosine, a histidine and an aspartate. Transferrin contains two such cavities and they have been shown to bind more than 30 other metal ions.⁵⁹ Moreover, research by Valentine *et al.*⁶⁶ has shown that titanium(IV) (from Ti(IV) citrate complex) binds more strongly to transferrin than does iron(III), illustrating the possible importance of transferrin in the biological chemistry of titanium. Complementary research demonstrated that at pH 7, TDC reacts with N,N'-ethylene bis(O-hydroxyphenylglycine) which behaves as an excellent mimic of the metal binding properties of transferrin (Figure 11).^{67,68}

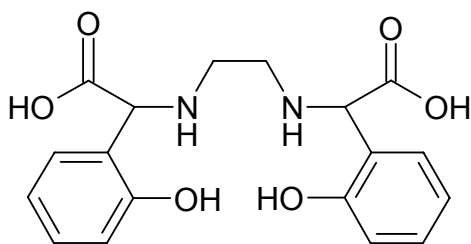


Figure 11 N,N'-ethylene bis(O-hydroxyphenylglycine) (EHPG), an excellent mimic of the metal binding site in transferrin.

Transferrin is taken up into all cells via receptor-mediated endocytosis. Holo-transferrin binds to specific transferrin receptors on the cell surface and is internalized by clathrin-coated vesicles into endosomes.⁵⁸ The environment inside the endosomes is more acidic (pH 5 – 5.5) and it is postulated that the low pH cause a conformational change in transferrin which in turns releases titanium.⁶⁹ Once released, titanium is left to act inside the cell, whereas transferrin is cycled out of the cell to start the delivery cycle all over again.⁷⁰

Tumour cells have an increased requirement for nutrients (such as iron) to allow for rapid growth and cell division.⁷¹ Therefore tumour cells often express increased levels of transferrin receptors compared to normal, healthy cells. This explains the difference in chemosensitivities of platinum-based chemotherapeutic agents versus TDC towards various types of cancers. Cisplatin and related platinum agents have been shown to migrate to cancer cells by passive biodistribution whereas, titanium containing species are transported via the metal binding protein, transferrin. Transferrin acts as a quasispecific delivery agent to cancerous cells rather than normal, healthy cells, thereby at least in theory, reduces the potential side effects and increases the range of therapeutic dosing.^{71,72}

1.8 Interactions of titanocene dichloride with DNA

It is widely accepted that, once it enters the cell, titanium containing species accumulates in the nucleic acid rich regions of the nucleus.⁷³⁻⁷⁵ Full characterization of the nature of titanocene-DNA interactions at the molecular level has been hindered by the hydrolytic instability of TDC under physiological conditions. At present, there has not been a reported crystallographic structure of a TDC-DNA complex. However, there have been several studies involving proton and phosphorus NMR spectroscopy that have provided some insight into the TDC-DNA interactions.⁷⁶⁻⁷⁸ Titanium(IV) is a “hard” Lewis acid and would be expected to bind preferentially to the “hard” oxygens on the phosphate backbone. In support of this argument, NMR studies have shown that TDC binds very

weakly to the base nucleotides and very strongly to the negatively charged phosphate backbone of DNA.^{40,76,79} The binding has been shown to be stronger at low pH values than at neutral pH values. A schematic representation of how the titanocene moiety binds to the phosphate backbone of DNA, at least *in vitro*, in an intrastrand fashion is shown in Figure 12. The corresponding DNA-TDC adducts are postulated to inhibit DNA transcription/replication at least of genes where the adducts are formed, leading to cell death. It is worth mentioning that although TDC has been shown to react with DNA *in vitro*, there is still some uncertainty regarding the composition of the biologically active titanium species responsible for the cytotoxic activity.

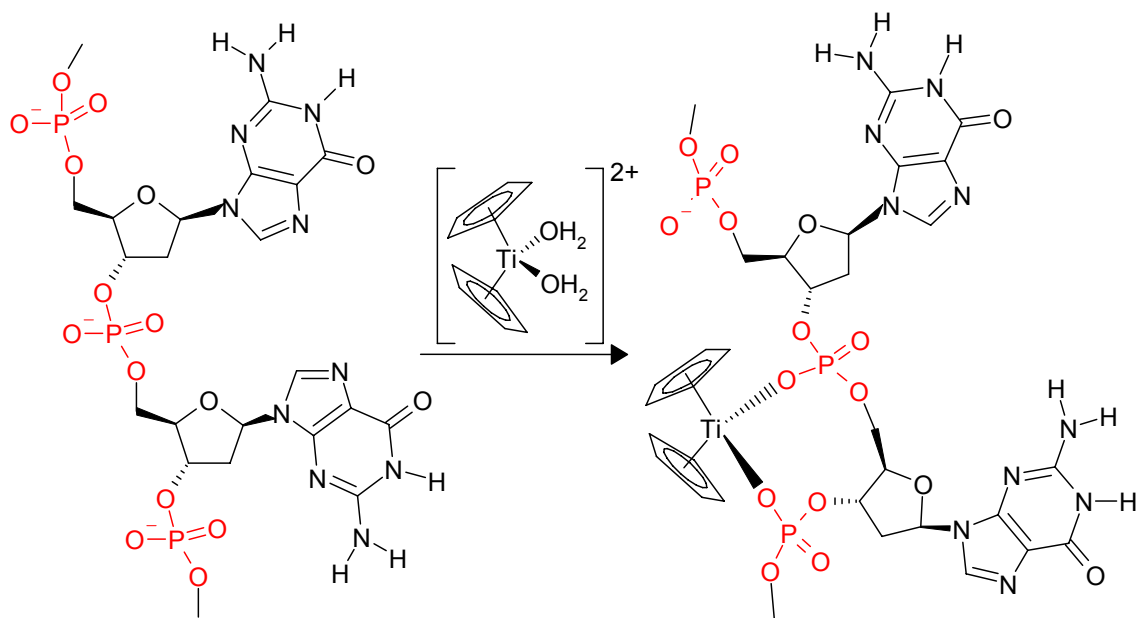


Figure 12 Proposed mechanism of action of hydrolyzed TDC binding to the highlighted phosphate backbone of DNA in an intrastrand fashion.^{76,79}

This chemical behaviour of TDC contrasts that of cisplatin and related platinum based analogues, which as described earlier, predominantly bind to the nitrogen atoms of the nucleotide bases (preferentially adjacent guanine residues). The different targets of the two chemotherapeutic agents may explain, in part, why TDC is active against cisplatin resistant cancer cell lines.

1.9 Radiolabeling using Titanium-45

While NMR spectroscopic methods have had some success at determining the mechanism of drug action of TDC, there are still many unanswered questions concerning its biodistribution. This has led to the development and application of “alternative” methods of investigation such as radioactive labeling. Fortunately, titanium has an isotope (^{45}Ti) that is ideal for radiochemical studies *in vivo*. The titanium isotope is prepared by proton bombardment of a natural scandium foil target, inducing a proton-neutron

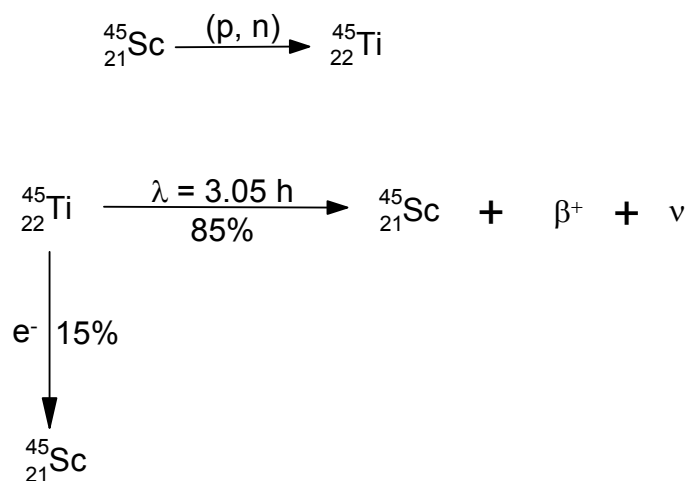


Figure 13 Irradiation of ^{45}Sc with a proton leads to the ejection of a neutron and the production of ^{45}Ti which is unstable.⁸⁰

exchange reaction: $^{45}\text{Sc} (p,n) ^{45}\text{Ti}$ (Figure 13).⁸⁰ Titanium-45 has a half-life of 3.09 h and decays 85% by positron emission with the other 15% decaying by electron capture producing stable ^{45}Sc . The high yielding nuclear chemistry along with the fact that scandium (^{45}Sc) is 100% abundant, make titanium-45 very economical to produce.

Radioactive nuclei that have an excess of protons undergo decay by positron emission. In this type of radioactive decay, a proton is converted into a neutron, a neutrino (ν) and a positron (β^+) (Figure 13). The high percentage of decay through positron emission makes ^{45}Ti a suitable candidate for positron emission tomography (PET). The emitting positrons, being anti-electrons, interact with electrons and annihilate, converting the mass of the two particles into energy.⁸¹ This energy is emitted as two collinear gamma ray photons (511 keV each) that travel in opposite directions (180°) and are detectable using PET (Figure 14). The intensity of the 2 gamma photons emitted is low enough to

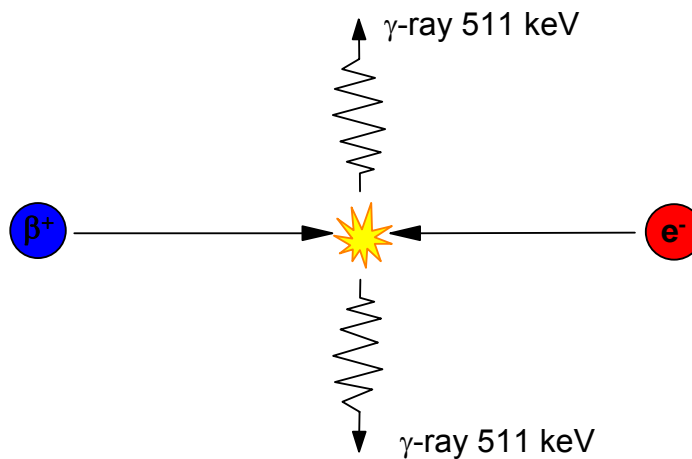


Figure 14 The annihilation of a positron and an electron producing two collinear γ -rays of 511 keV each.

prevent the subject from overexposure to radiation, but energetic enough to emerge from the body and allow for detection. Moreover, the half-life of ^{45}Ti is long enough for chemical manipulation and *in vivo* accumulation, but short enough to minimize radiation exposure to the subject.

Welch and coworkers⁸² have had significant success using this method in producing ^{45}Ti . Processing and isolating the ^{45}Ti involves dissolving the irradiated metal in 6 N hydrochloric acid and passing it through a cation-exchange column in order to separate it from unreacted scandium.⁸² The isolated ^{45}Ti species is obtained after manipulation as $^{45}\text{TiOCl}_2$. Upon treatment with apotransferrin, Welch and coworkers found that they had successfully formed ^{45}Ti -transferrin complexes and that these complexes were stable *in vivo*. Biodistribution studies of the ^{45}Ti -transferrin complexes in mice showed that tumours had increased uptake of ^{45}Ti compared to other organs reflecting higher levels of transferrin receptor.^{82,83} Furthermore, the amount of activity in the tumour (% injected dose/g) was found to remain constant between 4 and 24 h after administration, which is highly desirable for imaging. The percentage injected dose per gram is the amount of radioactivity per gram of animal tissue. These values were compared to a weighed, counted standard solution.

1.10 Titanocene dichloride analogues with varied anionic ligands

All evidence thus far has shown that the primary mode of attack by titanium-based anticancer drugs involves the direct coordination of some titanium species to the phosphate backbone of DNA and that its delivery *in vivo* may be

achieved by the serum protein transferrin and its receptor. Accordingly, considerable research has focused on improving the ability of TDC to bind to the binding sites of transferrin and/or the “hard” phosphate backbone, as well as improving upon some of the shortcomings of TDC such as its inherently poor solubility in aqueous media and its hydrolytic stability. Initial modifications of TDC involved replacing the chlorides with different anions such as other halides, thiocyanate, azide, phenoxide derivatives and carboxylates.³⁸ Changing the nature of the anion was shown to have a negligible effect on the antitumour activity, which is to be expected if the anions rapidly hydrolyze in aqueous media.

Recently, there has been a revival in the investigation of the anion effects on TDC activity. As mentioned above, research focused on the “aging” of TDC in various solvents has shown some marked improvement of TDC activity in methanol and ethanol solvents.⁵⁷ Other work involved the development of titanocene derivatives that were bound to two β -cyclodextrin molecules using a thio-1,2-dicyanoethylenylthioethyl bridge (Figure 15).^{84,85} The β -cyclodextrin molecules were intended to act as a delivery vehicle of the titanocene moiety that would increase the inherent solubility of TDC. Cyclodextrins are well known to act as hosts for hydrophobic molecules (such as Cp_2TiR_2) in aqueous solutions, thereby increasing their solubility. The resulting complexes were found to be soluble in water. The complexes were subsequently tested for cytotoxic activity against the human breast cancer cell line, MCF-7 and displayed higher potency than the parent TDC.

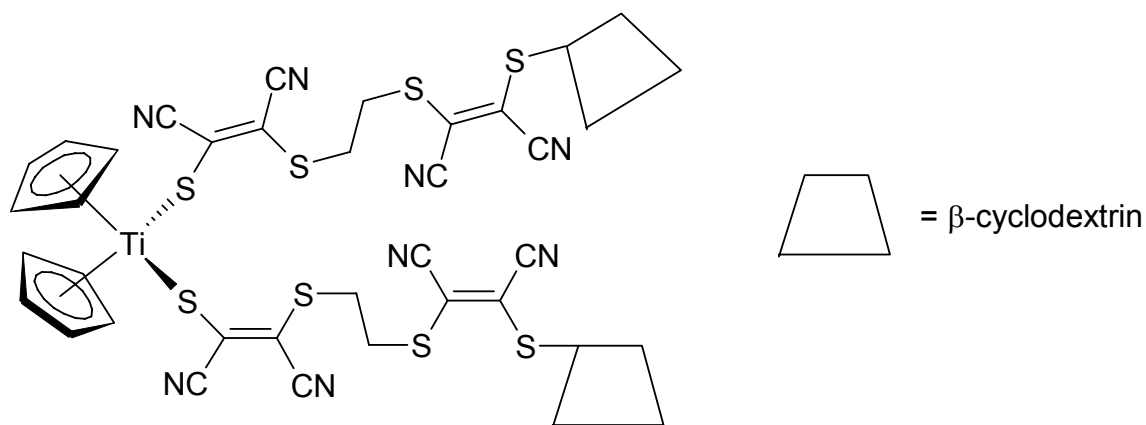


Figure 15 A titanocene cyclodextrin dimer bound by a thio-1,2-dicyanoethylenylthio-ethyl bridge.⁸⁵

Other research involving the modification of the anionic ligands has focused on the development of derivatives containing heteroaromatic rings (Figure 16). It was anticipated that the anionic ligands would dissociate under physiological conditions and Lotz and coworkers attempted to use this to their advantage.⁸⁶ It is known that certain planar heteroaromatic rings (pyridine, thiophenes, etc.) display antitumour activity as they can insert or intercalate into the grooves of double-stranded DNA. This is believed to result in the distortion and unwinding of the DNA structure.⁸⁷ Coupled with the effects of the titanocene moiety on the phosphate backbone, the novel titanocene derivatives may display improved cytotoxic activity through this two pronged attack. The heteroaromatic rings that were used for this study were benzothiophene and dibenzothiophene since these molecules have been shown to interact quite strongly with the adenine-thymine (AT) or guanine-cytosine (GC) base pairs of DNA. The resulting complexes were tested against the human colon adenocarcinoma cell

line COLO 320DM and the cervical carcinoma cell line HeLa. All of the species showed only a slight improvement in potency compared to the parent TDC. The most potent of the derivatives was the complex containing a dibenzothiényl ligand with a sulphur bridge (centre, Figure 16).⁸⁶

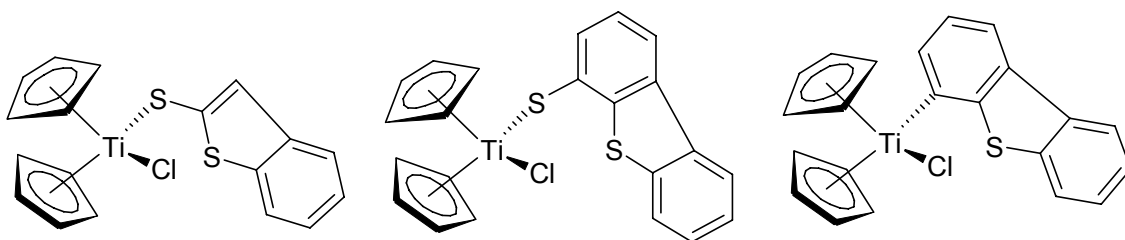


Figure 16 Titanocene chloride derivatives containing benzothiényl (left) and dibenzothiényl (centre and right) ligands.⁸⁶

1.11 Modification of the cyclopentadienyl ligands

Within the past decade, the development of novel TDC analogues has centered on the functionalization of the Cp ligands. Original methodologies had focused on modifying the donor abilities of the Cp ligands by preparing analogues bearing either electron donating or withdrawing groups. TDC derivatives containing electron donating groups such as methyl, ethyl, and trialkylsilyl groups showed a marked decrease in potency.³⁸ Since it has been shown that TDC strongly binds to the phosphate backbone of DNA, an increase in the Lewis acidity of the titanium centre by preparing Cp ligands bearing electron withdrawing groups seemed the next logical step in derivatization.^{64,88} Research in our lab involved the preparation of mono- and di-substituted TDC derivatives with methyl, *t*-butyl or phenyl esters (Figure 17). The resulting methyl ester complexes were found to exhibit significant toxicity against a human small

cell lung cancer cell line (H209),⁸⁸ but a subsequent extension involving complexes containing phenyl and *t*-butyl ester substituents against other human tumour cell lines showed little cytotoxic activity and so this approach was abandoned.⁸⁹

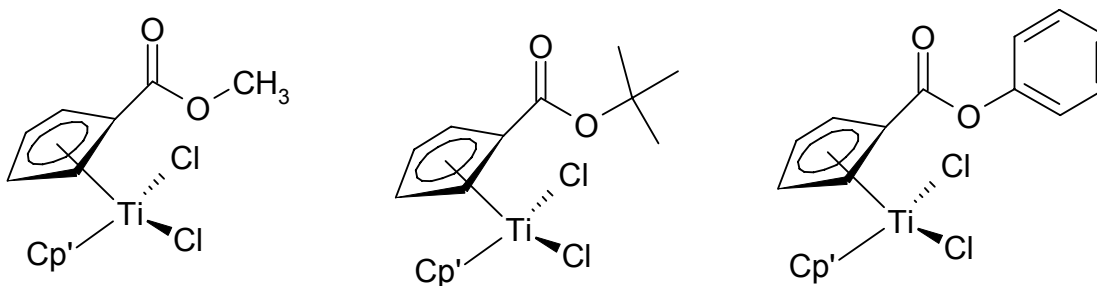


Figure 17 TDC derivatives where the Cp ligands bear electron withdrawing groups. Cp' represents either $\eta^5\text{-C}_5\text{H}_5$ or $\eta^5\text{-C}_5\text{H}_4\text{R}$ where R is the corresponding ester.

Inspiration for other types of cytotoxic TDC derivatives came from research involving the improvement of the catalytic activity of TDC. Metallocenes are well known for their catalytic activity in the polymerization of ethylene and other simple olefins.⁹⁰ In an effort to optimize the catalytic activity of TDC, several derivatives incorporating donor functionalities onto the Cp ligand such as -NR_2 , -PR_2 , -OR , or -SR groups have been developed.⁹¹ The corresponding complexes have shown dramatic increases in catalytic activities of ethylene in toluene. The increases in catalytic activity have been rationalized by the stabilization of the active site on titanium through the reversible coordination by a donor atom bearing a lone pair of electrons (Figure 18).⁹² Normally, nitrogen containing ligands are considered to be weakly coordinating to hard Lewis acid

metals such as those in the early transition metal groups like titanium. However, the amines are attached to the Cp group through a short alkyl chain creating a bidentate chelating ligand that can reversibly coordinate to the titanium centre (Figure 18).

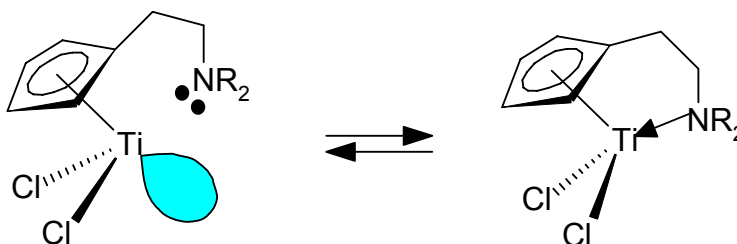


Figure 18 Stabilization of the reactive, vacant site on titanium by the reversible coordination of a lone pair of electrons on the pendant alkylammonia group.⁹²

These types of uncoordinated titanocene complexes have been shown to be extremely air sensitive. They immediately precipitate upon treatment with aqueous solutions. In order to improve the stability of these complexes (and thereby improve their ease of handling), Jutzi and coworkers protonated the nitrogen donor atom using hydrochloric acid.⁹³ The resulting hydrochloride salts were found to be stable in dry air for extended periods of time (Figure 19). They were also found to have pronounced solubilities in all polar protic solvents, and were even shown to be stable in aqueous media for extended periods of time (>3 days).⁹¹ The active catalyst could then be regenerated by the addition of an equal molar amount of methyllithium to deprotonate the alkylammonium salt. This methodology prompted a whole new direction in which novel anti-tumour TDC derivatives could be made.

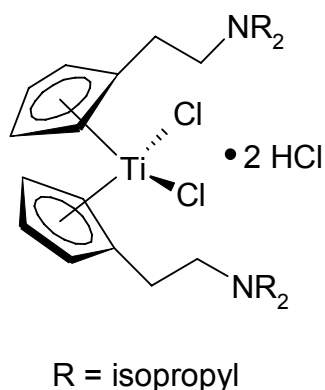


Figure 19 Air and water stable TDC ammonium derivative prepared by Jutzi and coworkers to be used for polymerization catalysis.⁹³

As mentioned earlier, some of the limiting features of TDC were its poor inherent solubility in water, followed by its instability in aqueous media due to hydrolysis reactions. The complexes prepared by Jutzi and coworkers improved upon both of these limitations and so subsequent research on the modification of the Cp rings followed this methodology. McGowan and coworkers⁹⁴ were the first to follow this up by preparing water soluble and air stable TDC derivatives bearing piperidine groups. The amines were converted to tertiary or quaternary ammonium groups upon reaction with either hydrochloric acid or methyl iodide, respectively (Figure 20).^{49,95} The resulting ionic TDC derivatives were found to be readily soluble in aqueous media and their cytotoxic activities were subsequently tested against a variety of human cancer cell lines: ovarian cancer A2780 and A2780/CP (cisplatin resistant variant), colon cancer LoVo and breast cancer MCF-7.⁴⁹ The results were compared to cisplatin and TDC. Although the TDC derivatives were not nearly as potent as cisplatin, these complexes did provide a promising start. It was also observed that the TDC derivatives

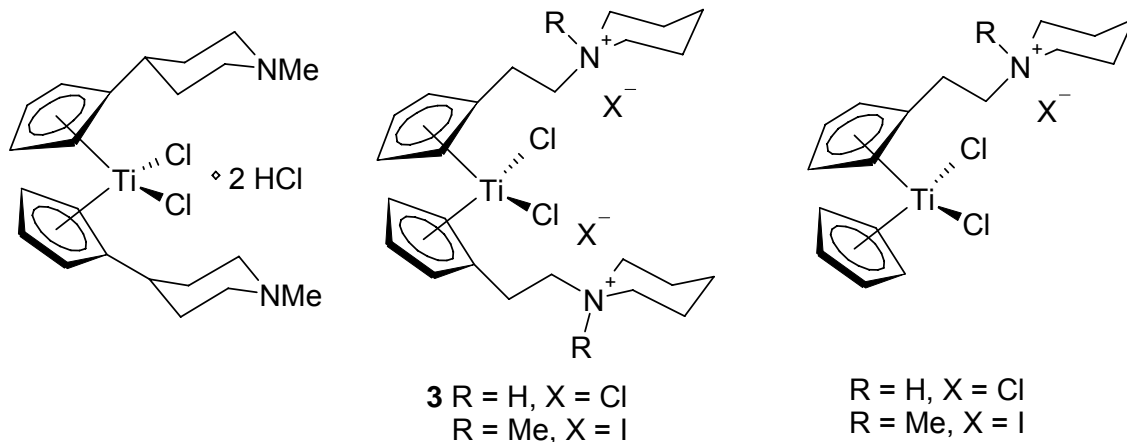


Figure 20 TDC derivatives bearing piperidinylligands prepared by McGowan and coworkers.⁴⁹

exhibited comparable potencies against the ovarian cell line A2780 and its cisplatin resistant variant A2780/CP. This provides additional evidence confirming that TDC derivatives kill tumours through a different mechanism of action than cisplatin. The most active derivative found was the dihydrochloride salt (**3**) shown in Figure 20.

Continuing with their success, McGowan and coworkers developed several complexes extending from their most potent TDC derivative (**3**, Figure 20) in an effort to establish some structure-activity relationships.⁹⁶ The dihydrobromide salt of a titanocene dibromide derivative was prepared along with some trimethylcyclopentadienyl substituted monocationic derivatives (Figure 21). The most potent complex found was the bis(trimethylsilyl) substituted monocationic analogue (**4**, Figure 21) displaying IC_{50} values of $19.7 \mu\text{M}$ against A2780 versus an IC_{50} of $0.36 \mu\text{M}$ for cisplatin.⁹⁶

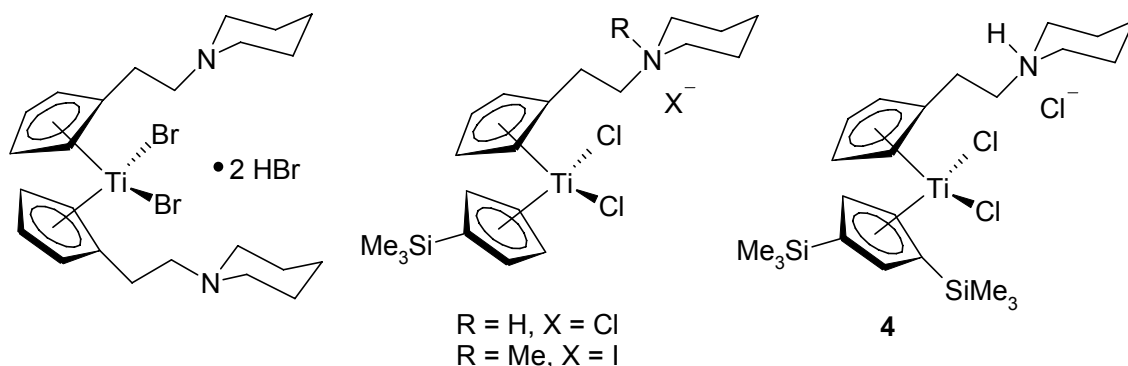


Figure 21 An extended library of piperidinylyl substituted titanocene derivatives prepared by McGowan and coworkers.⁹⁶

Previous work in our lab involved the preparation of a library of dicationic and monocationic TDC derivatives bearing a variety of alkylammonium functional groups (Figure 22).⁴⁸ The majority of the analogues contained alkylammonium side chains varying in length from 2 – 3 carbons. The nature of the nitrogen atom in these linear alkylammonium salts varied from primary to tertiary. In one case a monocationic pentamethylcyclopentadienyl was also prepared. The remaining analogues contained cyclic alkylammonium (piperidinylyl side groups) or a chiral centre. In the case of the TDC derivative containing a stereocenter, the isolated product actually consisted of a statistical mixture of the stereoisomers. Thus the monocationic analogue consisted of a 1:1 racemic mixture of both the R and S enantiomer, whereas the dicationic mixture was made up of the R,R, R,S and S,S isomers in the ratio 1:2:1, respectively. This library consisted of a diverse suite of different alkylammonium substituents allowing for a thorough structure-activity analysis.

X-ray crystallographic structures of eight of the below complexes were determined, but these revealed few differences between the complexes and that of TDC although their cytotoxic activities varied greatly. The analogues were tested against a variety of human cancer cell lines: lung cancer (A549 and H209), and ovarian cancer (A2780) representing a mix both of standard cell lines where many benchmarks of drug potencies exist and that represent solid tumour types for which more effective drugs are urgently needed. In addition, selected complexes were also evaluated against the cisplatin resistant variants of cell

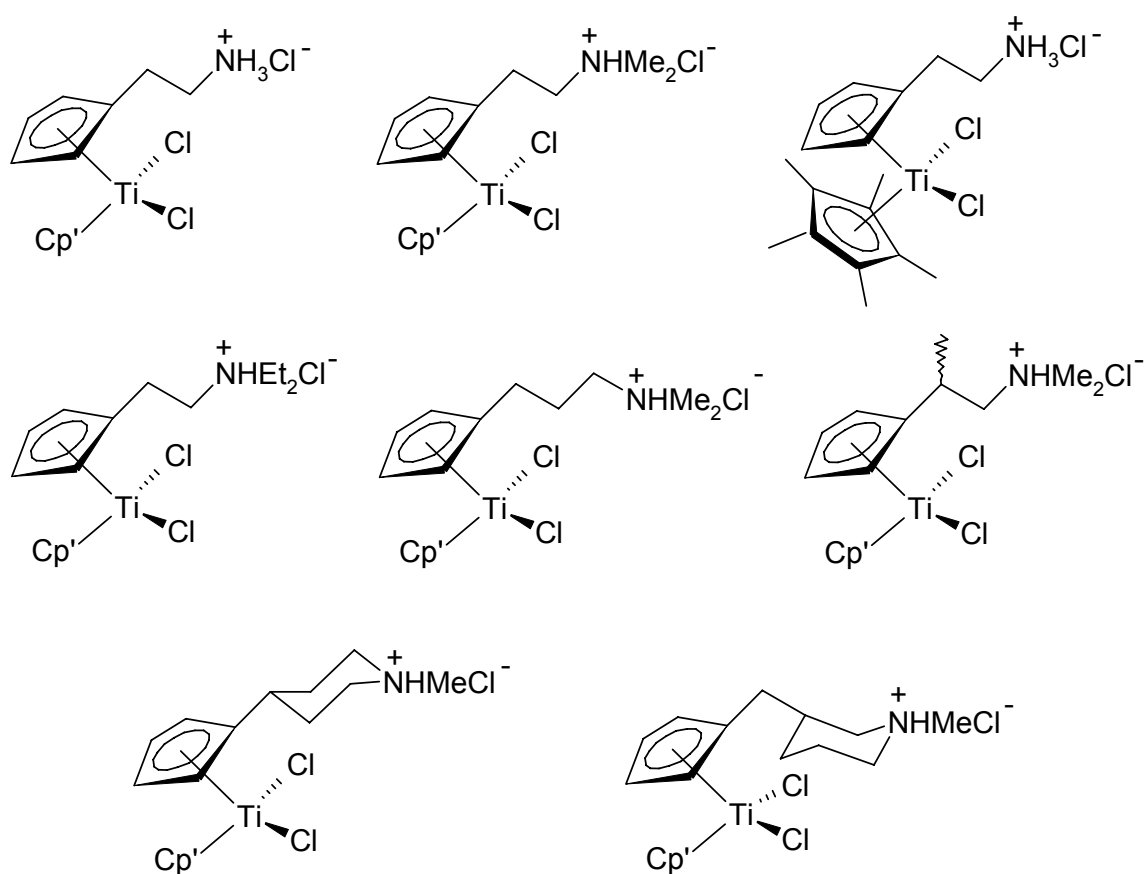


Figure 22 A library of monocationic and dicationic TDC derivatives prepared by Baird and coworkers. Cp' represents either $\eta^5\text{-C}_5\text{H}_5$ or $\eta^5\text{-C}_5\text{H}_4\text{R}$ where R is the corresponding alkylammonium.⁴⁸

lines H209 and A2780, H209/CP and A780/CP.⁴⁸

As a general trend, it was found that the dicationic complexes demonstrated significantly higher potencies than the monocationic analogues. The simple, linear alkylammonium derivatives displayed very little if any cytotoxicity against any of the cell lines. The most active analogues proved to be those bearing cyclic alkylammonium groups or the species containing a chiral centre as shown in Figure 23. Considering that the analogue containing a stereocentre is actually made up of a mixture of three stereoisomers (R,R, S,S and R,S), it is unknown which of the three, or if all of the isomers, are actually the cytotoxic species. Attempts at separating the three stereoisomers were unsuccessful. These derivatives were significantly more potent than was TDC, but still an order of magnitude less potent than cisplatin.

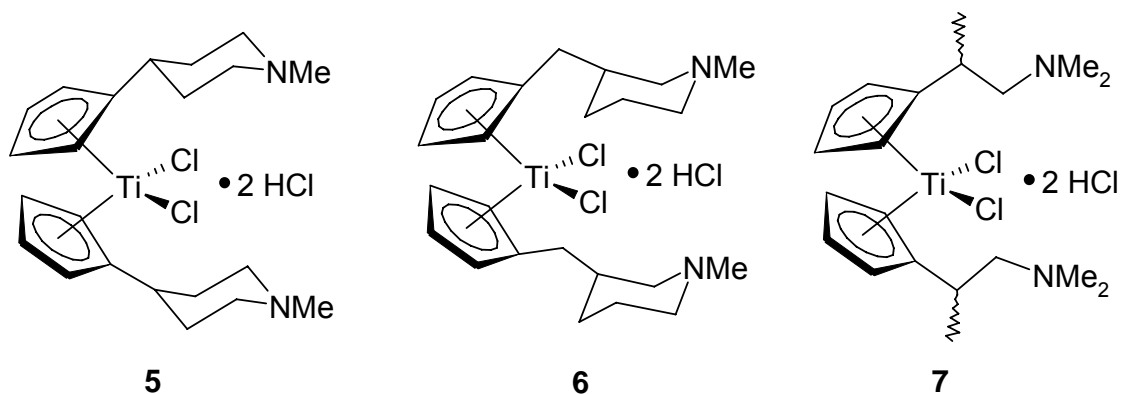


Figure 23 The most cytotoxic TDC derivatives prepared by Baird and coworkers.⁴⁸

Other TDC derivatives were prepared using a different synthetic strategy. Tacke and coworkers treated functionalized fulvenes with titanium dichloride to

synthesize highly substituted *ansa*-titanocenes containing a carbon-carbon bridge as shown in Figure 24 (**8**).^{97,98} This particular *ansa* analogue is actually a mixture of approximately a 1:1 ratio of the *cis* and *trans* stereoisomers. They also had success at preparing non-*ansa*-titanocene analogues such as those shown in Figure 24 (**9** and **10**).⁹⁹⁻¹⁰² The *ansa* derivative and the anisole substituted analogue shown in Figure 24 were tested for cytotoxicities against 36 different cancer cell lines and in four explanted human tumours.^{100,103-105} The *in vitro* and *ex vivo* experiments showed that these titanocene analogues were quite effective against prostate, cervical and renal cancer cell lines. The *N*-methylpyrrole substituted titanocene (Figure 24, **10**) was recently prepared and shown to have the most potent antitumour activity of all TDC derivatives prepared thus far with an IC₅₀ of 5.5 μM against the pig kidney cell line (LLC-PK) compared to that of cisplatin (IC₅₀ = 3.3 μM). This titanocene derivative actually consists of 3 stereoisomers (1:2:1 ratio of R,R, R,S and S,S) and it is unknown if all or one of the isomers are the active species.

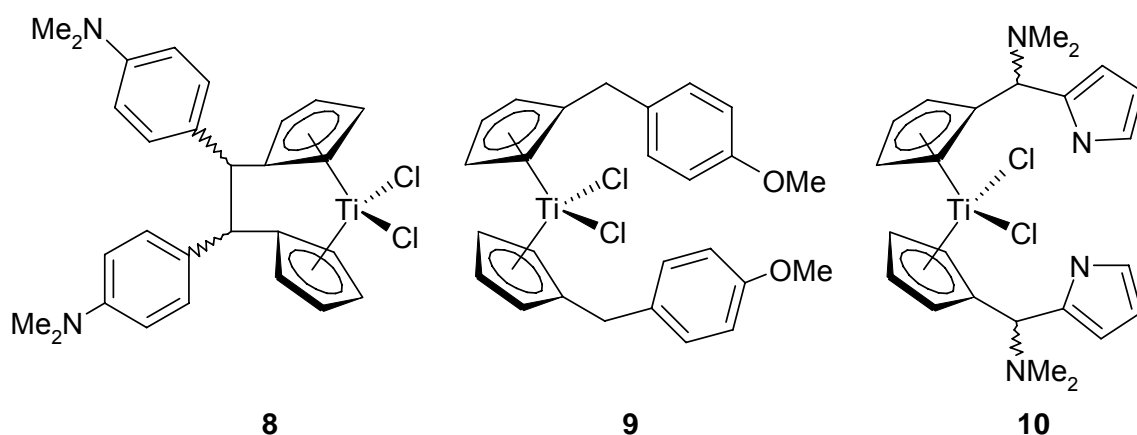


Figure 24 TDC analogues prepared by Tacke and coworkers.¹⁰⁰

To date, there is very little understood as to why the modification of the Cp ligands produces such extreme differences in cytotoxic activities. NMR studies of titanium-transferrin interactions have indicated that the Cp ligands are completely displaced after 30 min when TDC is reacted with apotransferrin. This is much faster than the rate that Cp ligands are hydrolyzed by water alone and therefore it seems likely that transferrin is facilitating this displacement. It had been suggested that the displaced cyclopentadiene or its Diels-Alder dimer may in fact be the cytotoxic species, but *in vivo* experiments have shown that neither one exhibits any anti-tumour activity.¹⁰⁶ Therefore, it appears that the Cp ligands have no actual role in the cytotoxic activity, but may rather act to stabilize the Ti(IV) ion from rapid hydrolysis when TDC is dissolved until it is coordinated to transferrin. If that is the case, it is unclear why there is such a pronounced difference in potency between TDC and its analogues. Another possibility that might explain this result is that the TDC derivatives are actually acting by a different mechanism of action than TDC itself.

1.12 Preparation of TDC derivatives containing alkylammonium groups

The above mentioned TDC analogues bearing alkylammonium substituents prepared by the Baird and McGowan groups were synthesized following the series of reactions outlined in Figure 25. This linear synthetic methodology always began with the reaction of sodium cyclopentadienide and a haloalkylamine. The example shown in Figure 25 is the reaction of NaCp with 2-(N,N-dimethylamino)chloroethane. The cyclopentadienide anion behaves like a nucleophile and is able to undergo typical S_N2 reactions with the electrophilic

carbon bearing an appropriate leaving group. This produces a mixture of 3 possible cyclopentadiene stereoisomers bearing the alkylamine substituent.

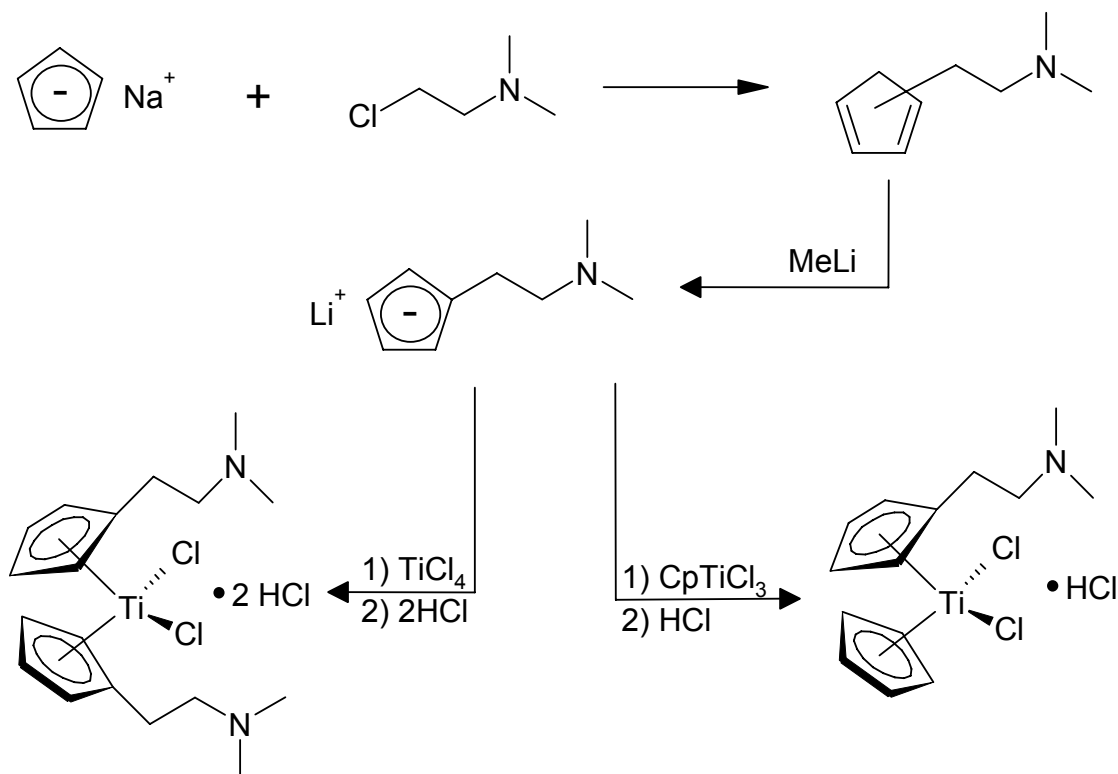


Figure 25 Synthetic scheme of the preparation of TDC derivatives bearing alkylammonium groups.

The substituted cyclopentadienes are susceptible to Diels-Alder dimerization reactions however; immediate deprotonation of the ring using a strong base such as methyl lithium will prevent this. The monosubstituted titanocene analogues are prepared by reacting one equivalent of the substituted lithium cyclopentadienide salts with (η^5 -cyclopentadienyl)trichlorotitanium. Similarly, the generation of the disubstituted titanocene derivatives results from the reaction of two equivalents of the substituted lithium cyclopentadienide salts

with titanium tetrachloride. Both the mono- and di-substituted complexes can then be converted to the corresponding hydrochloride salts upon reaction with an excess of hydrochloric acid (Figure 25).

1.13 Different methodology in preparing titanocene dichloride derivatives

The above mentioned linear synthetic strategy has some significant disadvantages such as the exclusion of protic functional groups (ie: alcohols), and the large number of synthetic steps necessary to prepare a library of complexes. It would be useful if instead there were some method that could directly functionalize TDC, allowing for an easy method to generate a large number of candidates with minimal cost/effort.

Gansäuer and coworkers¹⁰⁷ addressed this exact problem by preparing a TDC building block that allows for facile functionalization. Their strategy involved preparing a TDC derivative bearing a functional group that would be more reactive towards nucleophiles than the TiCl_2 fragment. This strategy was realized by attaching the highly electrophilic carboxylic acid chloride functional group to the Cp ligand in titanocene (Figure 26). The resulting TDC analogues could be prepared quantitatively in large scale batches.

The acid chloride substituted TDC (**11**) was then treated with a series of diverse amines in order to test its ability to act as a useful building block (Figure 26). These amines included natural amino acids, diamines as well as fluorescence-labeled amines. In each of the reactions, the corresponding

Moreover, this methodology was also successful with incorporating protic, polar groups such as alcohols. Reaction of the building block **11** with alcohols resulted in the corresponding esters with excellent yields. An example of one of the esters is shown in Figure 28. By incorporating biomolecules such as the steroid illustrated below, the targeting specificity of titanocene derivatives may be improved. This acid chloride TDC building block (**11**) may provide quick and

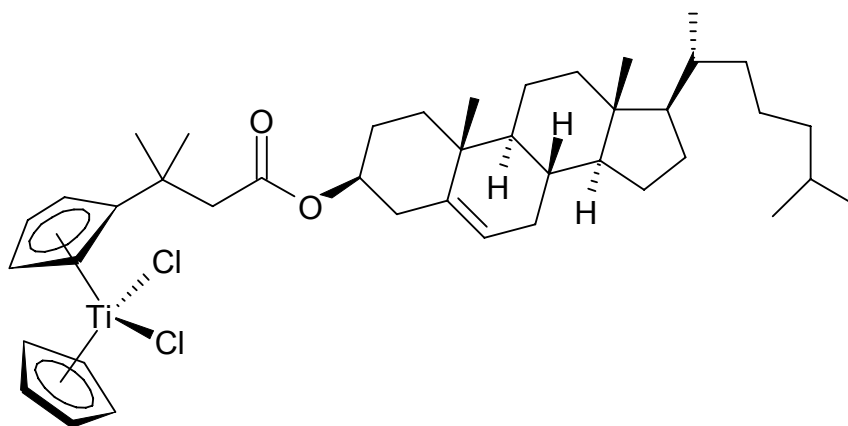


Figure 28 An example of a steroid substituted TDC prepared from the reaction of the acid chloride building block with the corresponding alcohol.¹⁰⁷

easy access to a wide range of functionalized TDC derivatives which may prove useful in both catalysis (polymer chemistry) and medicinal chemistry.

1.14 Research Objectives

The objectives of this research were to build upon the previous successes that this research group has had regarding the preparation of cytotoxic TDC derivatives. Structure-activity studies suggested that the more potent TDC analogues contained cyclic alkylammonium groups or substituents containing

stereocentres. This research expanded upon these results by preparing more cyclic and chiral analogues in an effort to establish better structure-activity

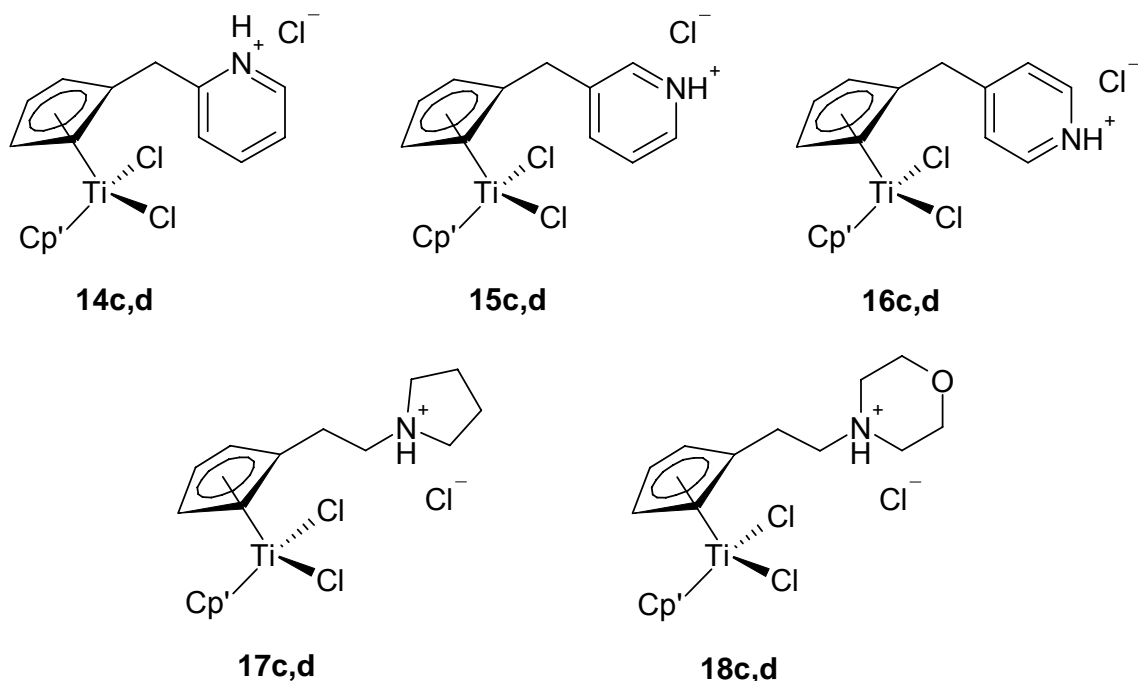


Figure 29 A small library of dicationic and monocationic TDC derivatives containing cyclic alkylammonium groups. Cp' represents either η^5 -C₅H₅ or η^5 -C₅H₄R where R is the corresponding alkylammonium.

relationships. A series of dicationic and monocationic TDC derivatives bearing cyclic alkylammonium groups was prepared with the structures shown in Figure 29. The analogues were made up of pyrrolidine, morpholine or picolyl (with the nitrogen at varying positions) substituents.

In addition, a small library of TDC derivatives containing chiral centres was also prepared (Figure 30). Two of the analogues contain the ephedrine group (Figure 30, **19c,d**) and the others were prepared from the enantiomerically

pure starting materials S-alaninol and R-alaninol (Figure 30, **20c,d**). The latter titanocene complexes are composed of enantiomerically pure isomers, providing the first opportunity to study individually both enantiomers of a TDC derivative. Following their syntheses, each compound was fully characterized by ^1H , ^{13}C NMR spectroscopy, mass spectrometry and elemental analysis. When possible, molecular structures were also determined by x-ray diffraction.

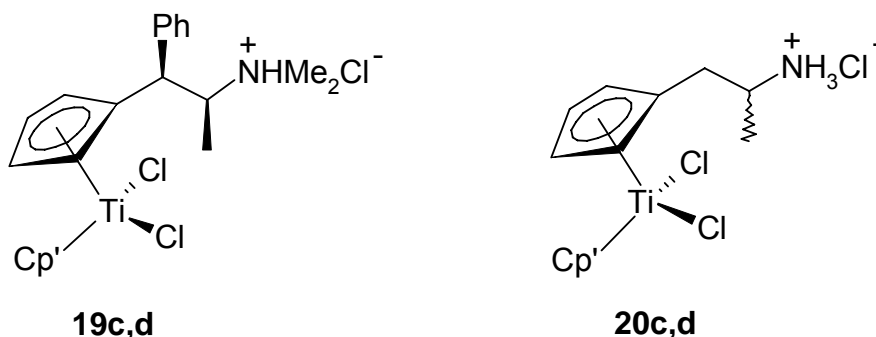


Figure 30 TDC derivatives containing chiral centres. Cp' represents either $\eta^5\text{-C}_5\text{H}_5$ or $\eta^5\text{-C}_5\text{H}_4\text{R}$ where R is the corresponding alkylammonium.

Determination of the cytotoxicities of these titanocene based complexes was accomplished through the use of MTT *in vitro* assays.^{108,109} All complexes were initially screened against the benchmark human non-small cell lung cancer cell line A549. The cell line A549 is used as a preliminary screening test because it is particularly robust. If the complexes showed promising cytotoxicity against A549 cells, they were further tested against human small cell lung cancers H69 and H209, cervical cancer HeLa, ovarian cancer A2780 and its cisplatin resistant variant A2780/CP. These cell lines were chosen due to the urgent need for improved chemotherapy against these solid tumour types.

Ultimately, the primary goal of this research was the development of more effective TDC derivatives that maybe useful in anticancer therapy.

Chapter 2: Experimental

2.1 General

All synthetic procedures were carried out under an inert atmosphere of oxygen-free argon, from Praxair, which was further purified by passing through a column of BASF catalyst heated to 140 °C and a column of 5 Å molecular sieves from Aldrich. Manipulation of air-sensitive materials employed standard Schlenk line techniques and an MBraun Labmaster glovebox. Solvents were taken directly from anhydrous and deoxygenated grade solvents from Aldrich after passing through activated alumina columns (Innovative Technology, Inc.). All chemicals were purchased from Aldrich and Ivy Fine Chemicals and were purified as appropriate before use. NMR solvents were received from Cambridge Isotope Labs.

All ^1H , ^{13}C and 2D NMR spectra were run by the author on a Bruker Avance 300 MHz (300.1 MHz, ^1H) or Bruker Avance 600 MHz (600.0 MHz, ^1H) NMR spectrometer with the residual proton resonances of the deuterated solvents serving as internal references for ^1H spectra. In the case of ^{13}C spectra, the carbon resonances of the solvents or a small amount of methanol were used as internal references. All chemical shifts are reported on the δ (ppm) scale with the following information listed in brackets: splitting pattern, number of protons represented by the signal, coupling constants if any, and position number. All 1D spectra were processed using Bruker XWIN-NMR or MestRe-C (version 2.3a) software, while 2D spectra were processed using Bruker XWIN-NMR software.

Mass spectra were obtained by the author on a Quatro Fisons Pro Quadrupole mass spectrometer in ES+ mode with a solution of nitromethane or dichloromethane and 5% methanol used as a solvent. Where reported [M] represents the unprotonated TDC derivative. Canadian Microanalytical Services of Delta, B.C., performed elemental analyses. All FT-IR spectra were obtained on a Perkin Elmer Spectrum One FT-IR spectrometer by the author and were processed using Spectrum v5.01 software; all solid samples were prepared with mineral oil. IR spectra were only obtained to determine if water is present in the TDC analogues. Optical rotations were determined by the author using a Rudolph Research Analytical Autopol V polarimeter. The samples were placed in a Temptrol polarimeter tube with a 1 dm path cell length and the rotations were measured at $\lambda = 633$ nm, an absorption minimum.

2.2 X-Ray Crystal Structure Determination

The x-ray crystallographic structure determination was carried out by Dr. Ruiyao Wang using a Bruker SMART CCD 1000 X-ray diffractometer with graphite-monochromated Mo $K\alpha$ radiation ($\lambda = 0.71073$ Å) controlled with Crysostream Controller 700. Typically, a crystal was mounted on a glass fibre with epoxy glue. No significant decay was observed during data collection. Data were processed on a Pentium PC using the Bruker AXS Windows NT SHELXTL software package (version 5.10). The raw intensity data were converted (including corrections for scan speed, background, and Lorentz and polarization effects) to structure amplitudes and their esds using the program SAINT, which

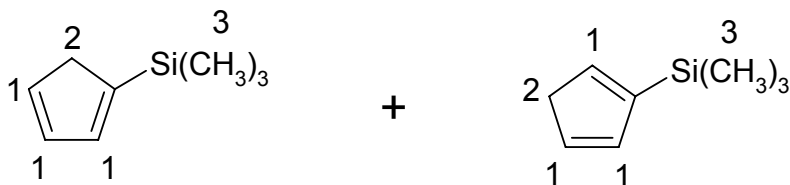
corrects for Lp and decay. Absorption corrections were applied using the program SADABS. All non-hydrogen atoms were refined anisotropically. The positions for all hydrogen atoms were calculated, and their contributions were included in the structure factor calculations.

2.3 Preparation and Characterization of Compounds

Synthesis of sodium cyclopentadienide (NaCp)¹¹⁰

NaCp was synthesized following a method by Roesky *et al.*¹¹⁰ 10.2 g of freshly cut sodium (0.442 mol) was added to a 500 mL round bottom flask containing 350 mL of dicyclopentadiene. On heating, the solution turned dark brown in colour (around 40 °C). The reaction mixture was allowed to reflux at 160 °C for 8 h. Over the course of the reaction a white precipitate formed along with the evolution of gas. Hydrogen no longer evolved once all of the sodium was consumed. The reaction mixture was heated for a further 30 min after gas evolution ended to ensure all of the sodium had reacted. The reaction mixture was then filtered hot and the precipitate was washed three times with 50 mL portions of hexanes. The resulting light brown precipitate was dried in vacuo yielding the desired product (34.7 g, 89%). The ¹H NMR data matches data in the literature.¹¹⁰ ¹H NMR (300 MHz, *d*₆-DMSO): δ 5.37 ppm.

Synthesis of (trimethylsilyl)cyclopentadiene¹¹¹



Sodium cyclopentadienide (48.7 g, 0.552 mol) was put into a 500 mL, round bottom flask along with 300 mL of anhydrous THF and kept in an ice/water bath. Chlorotrimethylsilane (70 mL, 0.55 mol) was slowly added dropwise causing the reaction mixture to turn yellow. After complete addition the reaction mixture was left to stir for 1 h and then the solvent was removed *in vacuo*. The residue was treated with 100 mL of water and extracted with diethyl ether (3 x 75 mL). The organic layers were collected, dried with MgSO₄ and the solvent was removed under vacuum yielding a red oil. Vacuum distillation at 10 torr yielded a slightly yellow oil with a boiling point of 40 - 50°C. The ¹H NMR data matched the data presented in the literature.¹¹¹ Yield: 37.6 g, 49%. ¹H NMR (300 MHz, CDCl₃): δ 6.74-6.53 (m, 6H, 1), 0.22 and 0.20 (2 x s, 4H, 2), 0.01 and 0.01 (2 x s, 18H, 3) ppm.

Synthesis of (η⁵-cyclopentadienyl)trichlorotitanium¹¹²

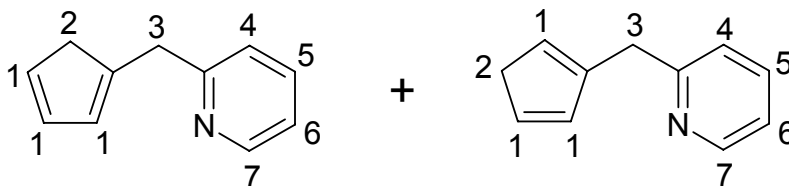
Titanium tetrachloride (29.5 mL, 0.268 mol) was put into a 500 mL round bottom flask along with 200 mL of anhydrous toluene and kept in an ice/water bath. (Trimethylsilyl)cyclopentene (37.1 g, 0.268 mol) was slowly added dropwise causing the reaction mixture to turn black with the formation of a yellow precipitate. After complete addition, half of the toluene was removed *in vacuo*

and the resulting mixture was passed through a Schlenk frit isolating a yellow precipitate. The precipitate was washed 3 times with cold toluene (25 mL) and dried overnight under vacuum. Vacuum sublimation of the product at 0.02 torr yielded yellow-orange crystals at 120 °C. The ^1H NMR spectrum matched the data present in the literature.¹¹² Yield: 42.5 g, 72.3%. ^1H NMR (300 MHz, CDCl_3): δ 7.06 ppm.

Clinical Formulation of MKT-4⁵⁶

The preparation of MKT-4 was performed following the procedure outlined in the patent by Müller *et al.*⁵⁶ TDC (240 mg, 0.96 mmol) was added to 60 mL of an aqueous solution containing *d*-mannitol (1.2 g, 6.6 mmol) and sodium chloride (1.08 g, 18.5 mmol). The resulting mixture was stirred and heated to near boiling. The reaction mixture turned a light, peach colour and became opaque. Once all of the TDC was dissolved, the mixture was filtered and the filtrate was frozen to -50 °C and dried overnight under vacuum yielding a light, orange powder. Yield: ~2g.

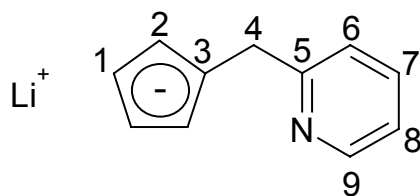
Synthesis of (2-picolyl)cyclopentadiene (14a).¹¹³



The synthesis of this compound has been previously shown in the literature.¹¹³ 2-Picolyl chloride hydrochloride (25.5 g, 0.156 mol) was added to an

aqueous solution of NaOH (8.6 g, 0.22 mol). The solution was extracted three times with toluene (50 mL), and the organic layers were combined and dried with MgSO₄ and then slowly added dropwise to a solution of NaCp in THF (2 M, 85 mL, 0.17 mol) at 0 °C. An off white precipitate formed during the addition and the reaction mixture turned brown. After allowing the mixture to stir overnight an excess of H₂O was added. The layers were separated and the organic layer was dried with MgSO₄. Removal of the solvent gave a dark, golden oil which was purified by vacuum distillation (boiling point: 80-84 °C, 0.54 mm Hg) to give a clear, colourless oil consisting of a mixture of isomers. Yield: 13.2 g, 54%. ¹H NMR (300 MHz, CDCl₃): δ 8.53 (m, 2H, 7), 7.57 (m, 2H, 5), 7.14 (m, 2H, 4), 7.09 (m, 2H, 6), 6.5-6.0 (m, 6H, 1), 3.93, 3.90 (2 x s, 4H, 3), 2.98, 2.91 (2 x s, 4H, 2) ppm.

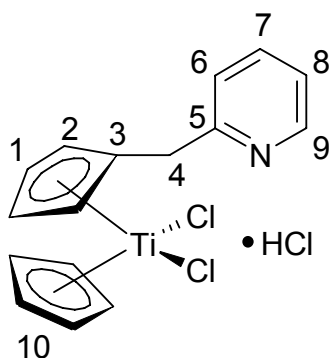
Synthesis of Lithium (2-picolyl)cyclopentadienide (14b).



The synthesis of this compound has been previously accomplished in the literature.¹¹³ Freshly distilled (2-picolyl)cyclopentadiene (2.32 g, 14.8 mmol) was dissolved in hexanes (100 mL) and kept in an ice/water bath. A solution of methyllithium (1.6 M, 15 mmol) in ethyl ether was added drop-wise to give immediately an orange precipitate. The reaction mixture was stirred for thirty minutes and the product was collected with a Schlenk filter. After washing the

precipitate with cold hexanes (2 x 50 mL), the product was dried overnight under vacuum. Yield: 2.03 g, 84%. ^1H NMR (600 MHz, $\text{DMSO-}d_6$): δ 8.30 (d, 1H, $^3J = 4.8$ Hz, 9), 7.51 (m, 1H, 7), 7.28 (d, 1H, $^3J = 7.8$ Hz, 6), 6.99 (m, 1H, 8), 5.20 (m, 4H, 1 and 2), 3.83 (s, 2H, 4) ppm. ^{13}C NMR (151 MHz, $\text{DMSO-}d_6$): δ 166.4 (5), 147.5 (9), 135.0 (7), 123.1 (6), 119.4 (8), 114.6 (3), 103.6 (2), 102.8 (1), 40.9 (4) ppm.

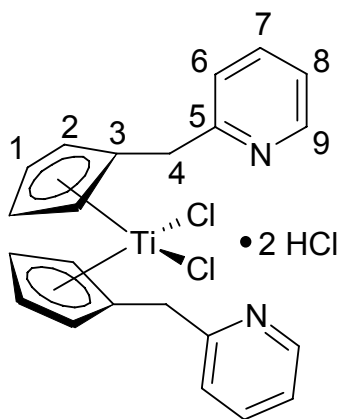
Synthesis of 14c.



Lithium (2-picolyl)cyclopentadienide (0.932 g, 5.72 mmol) was dissolved in THF (50 mL) and the solution was added slowly to a solution of (η^5 -Cp)trichlorotitanium (1.30 g, 5.93 mmol) in THF (100 mL) at 0 °C. The reaction mixture turned dark red and formed a light brown precipitate during the addition. The mixture was stirred for 2 h and then filtered, and the resulting dark red filtrate was treated with an excess of HCl in ether (5 mL, 2 M) to give an orange precipitate. The red supernatant was discarded and the product was dissolved in ethanol (10 mL) and added dropwise to diethyl ether (250 mL), resulting in precipitation of a red powder. The product was filtered and dried overnight *in vacuo*. The compound was dissolved in ethanol and recrystallized by slow

evaporation, giving dark red crystals suitable for elemental analysis. Yield: 1.60 g, 74%. ^1H NMR (600 MHz, DMSO-d_6): δ 8.77 (d, 1H, $^3J = 4.2$ Hz, 9), 8.40 (m, 1H, 7), 7.87 (d, 1H, $^3J = 7.2$ Hz, 6), 7.82 (m, 1H, 8), 6.79 (m, 2H, 1), 6.75 (s, 5H, 10), 6.65 (m, 2H, 2), 4.38 (s, 2H, 4) ppm. ^{13}C NMR (151 MHz, DMSO-d_6): δ 155.0 (5), 145.1 (7), 142.5 (9), 130.7 (3), 126.8 (6), 124.6 (8), 123.9 (2), 120.7 (10), 116.5 (1), 34.5 (4) ppm. Mass Spectra (ES, m/z (%)): 340 (1) $[\text{M}+\text{H}]$, 304 (100) $[\text{M}-\text{Cl}]$, 285 (30), 220 (10), 158 (50). Analysis calculated for **14c**: C, 51.04; H, 4.28; N, 3.72. Found: C, 50.60; H, 4.42; N, 3.61.

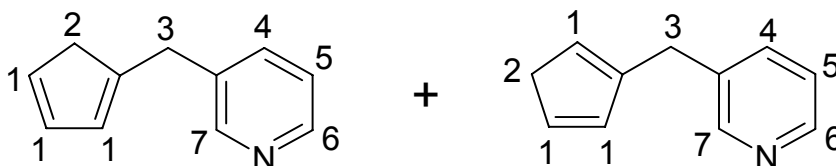
Synthesis of **14d**.



Lithium (2-picolyl)cyclopentadienide (0.837 g, 5.13 mmol) was dissolved in THF (100 mL), and titanium tetrachloride (1 M, 2.6 mmol) solution in toluene was slowly added dropwise at 0 °C. During the addition the reaction mixture turned dark red with the formation of a brown precipitate. After complete addition, the reaction mixture was stirred for 2 h and then filtered. The resulting dark red filtrate was treated with an excess of HCl in ether (4 mL, 2 M) resulting in the immediate formation of an orange precipitate. The light red supernatant was

discarded and the solid was dissolved in ethanol (15 mL). Red crystals immediately began to form that were suitable for elemental and x-ray crystallographic analyses. The supernatant was added dropwise to diethyl ether (400 mL) and a dark orange powder precipitated. The orange powder was isolated by filtration and dried overnight under vacuum. Yield: 1.02 g, 78%. ^1H NMR (600 MHz, DMSO- d_6): δ 8.79 (d, 2H, $^3J = 4.8$ Hz, 9), 8.45 (m, 2H, 7), 7.93 (d, 2H, $^3J = 7.8$ Hz, 6), 7.87 (m, 2H, 8), 6.84 (m, 4H, 1), 6.73 (m, 4H, 2), 4.42 (s, 4H, 4) ppm. ^{13}C NMR (151 MHz, DMSO- d_6): δ 154.7 (5), 145.5 (7), 142.3 (9), 130.9 (3), 127.0 (6), 125.0 (8), 123.6 (2), 117.2 (1), 34.4 (4) ppm. Mass Spectra (ES, m/z (%)): 429 (5) [M-Cl+MeOH], 395 (100) [M-Cl], 239 (12), 216.5 (100) [M+H] $^{+2}$, 198 (80), 157 (50). Analysis calculated for **14d**: C, 52.42; H, 4.40; N, 5.56. Found: C, 52.19; H, 4.46; N, 5.34.

Synthesis of (3-picolyl)cyclopentadiene (15a).



3-Picolyl chloride hydrochloride (25.35 g, 0.154 mol) was added to an aqueous solution of NaOH (7.6 g, 0.19 mol). The solution was extracted four times with toluene (40 mL), and the toluene layers were combined and dried with Na_2SO_4 and then added drop-wise to a solution of NaCp in THF (2 M, 80 mL, 0.16 mol) at 0 °C. An off-white precipitate formed during the addition and the reaction mixture turned orange-brown. After the reaction mixture had stirred

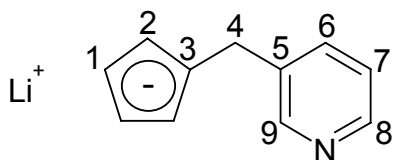
overnight, H₂O (50 mL) was added. The layers were separated and the organic layer was dried with Na₂SO₄. Removal of the solvent gave a yellow-brown oil which was purified by vacuum distillation (boiling point: 60-65 °C at 0.04 mm Hg) to give a clear, slightly yellow oil consisting of a mixture of isomers. Yield: 11.4 g, 47%. ¹H NMR (600 MHz, CDCl₃): δ 8.48 (2 × s, 2H, 7), 8.44 (2 × m, 2H, 6), 7.48 (2 × m, 2H, 4), 7.18 (2 × m, 2H, 5), 6.5-5.9 (m, 6H, 1), 3.71, 3.67 (2 × s, 4H, 3), 2.96, 2.83 (2 × s, 4H, 2) ppm.

Synthesis of (3-picolyl)cyclopentadiene hydrochloride (15e).



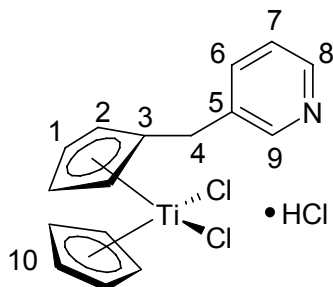
(3-Picolyl)cyclopentadiene (2.35 g, 0.0150 mol) was dissolved in diethyl ether (100 mL) and treated with an excess of HCl in diethyl ether (10 mL, 2 M). During the addition a fine, white precipitate formed which was then filtered and washed with cold ether (3 x 50 mL). Yield: 2.42 g, 83%. ¹H NMR (500 MHz, D₂O): δ 8.49-8.54 (m, 4H, 6 and 7), 7.53 (m, 2H, 4), 7.24 (m, 2H, 5), 6.01-6.47 (m, 6H, 1), 3.77, 3.73 (2 x s, 4H, 3), 3.02, 2.89 (2 x s, 4H, 2) ppm.

Synthesis of lithium (3-picolyl)cyclopentadienide (15b).



Freshly distilled (3-picolyl)cyclopentadiene (5.00 g, 31.8 mmol) was dissolved in hexanes (200 mL) and kept in an ice/water bath. A solution of methyllithium (1.6 M, 32 mmol) in ethyl ether was added drop-wise to give immediately an off white precipitate. The reaction mixture was stirred for thirty minutes and the product was collected with a Schlenk filter. After washing the precipitate with cold hexanes (2 x 50 mL), the product was dried overnight under vacuum. Yield: 3.96 g, 76%. ^1H NMR (600 MHz, $\text{DMSO-}d_6$): δ 8.37 (s, 1H, 9), 8.22 (d, 1H, $^3J = 4.2$ Hz, 8), 7.54 (d, 1H, $^3J = 7.2$ Hz, 6), 7.15 (d of d, 1H, 7), 5.19 (m, 2H, 1), 5.16 (m, 2H, 2), 3.71 (s, 2H, 4) ppm. ^{13}C NMR (151 MHz, $\text{DMSO-}d_6$): δ 149.7 (9), 145.2 (8), 141.9 (5), 135.7 (6), 122.6 (7), 115.7 (3), 103.1 (2), 102.8 (1), 35.2 (4) ppm.

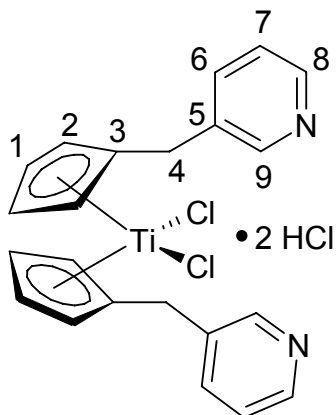
Synthesis of 15c.



Lithium (3-picolyl)cyclopentadienide (0.796 g, 4.88 mmol) was dissolved in THF (60 mL) and the solution was added slowly to a solution of $(\eta^5-$

Cp)trichlorotitanium (1.51 g, 6.84 mmol) in THF (100 mL) at 0 °C. The reaction mixture turned dark red and formed a light brown precipitate during the addition. The mixture was stirred for 2 h and then filtered, and the resulting dark red filtrate was treated with an excess of HCl in ether (4 mL, 2 M) to give an orange precipitate. The red supernatant was discarded and the product was dissolved in methanol (15 mL) and added dropwise to diethyl ether (400 mL), resulting in precipitation of an orange powder. The product was filtered and dried overnight *in vacuo*. The compound was recrystallized in dichloromethane by layering with benzene, giving dark red crystals suitable for elemental analysis. Yield: 1.56 g, 85%. ¹H NMR (600 MHz, D₂O): δ 8.68 (d, 1H, ³J = 6.0 Hz, 8), 8.62 (s, 1H, 9), 8.45 (d, 1H, ³J = 7.8 Hz, 6), 8.02 (d of d, 1H, 7), 6.66 (s and m, 7H, 1, 10), 6.54 (s, 2H, 2), 4.09 (s, 2H, 4) ppm. ¹³C NMR (151 MHz, D₂O): δ 148.2 (6), 141.4 (9), 140.5 (5), 140.1 (8), 136.9 (3), 127.9 (7), 119.7 (10), 119.2 (1), 117.6 (2), 32.6 (4) ppm. Mass spectra (ES, m/z (%)) = 340 (90) [M+H], 304 (20) [M-Cl], 158 (15), 99 (15). Analysis calculated for **15c**: C, 51.04; H, 4.28; N, 3.72. Found: C, 50.90; H, 4.29; N, 3.71.

Synthesis of 15d.



Lithium (3-picolyl)cyclopentadienide (0.538 g, 3.30 mmol) was dissolved in THF (60 mL), and titanium tetrachloride (1 M, 1.8 mmol) solution in toluene was slowly added dropwise at 0 °C. During the addition the reaction mixture turned dark red with the formation of a brown precipitate. After complete addition, the reaction mixture was stirred for 2 h and then filtered. The resulting dark red filtrate was treated with an excess of HCl in ether (3 mL, 2 M) resulting in the immediate formation of an orange precipitate. The light red supernatant was discarded and the solid was dissolved in ethanol (15 mL). The solution was added dropwise to diethyl ether (400 mL) and a dark orange powder precipitated. The hygroscopic product was isolated by filtration and dried overnight under vacuum. The compound was recrystallized in dichloromethane by layering with benzene to give dark red crystals suitable for elemental analysis. Yield: 0.756 g, 83%. ¹H NMR (600 MHz, D₂O): δ 8.69 (d, 2H, ³J = 6.0 Hz, 8), 8.65 (s, 2H, 9), 8.47 (d, 2H, ³J = 8.4 Hz, 6), 8.03 (d of d, 2H, 7), 6.64 (m, 4H, 1), 6.56 (m, 4H, 2), 4.12 (s, 4H, 4) ppm. ¹³C NMR (151 MHz, D₂O): δ 148.0 (6), 141.4 (9), 140.5 (5), 140.0 (8), 135.8 (3), 127.9 (7), 118.7 (1), 117.7 (2), 32.6 (4) ppm. Mass spectra

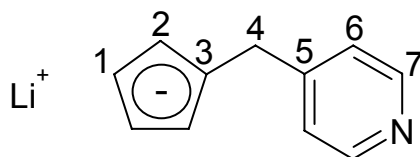
(ES, m/z (%)) = 431 (50) [M+H], 427 (20) [M-Cl+MeOH], 395 (25) [M-Cl], 313 (30), 239 (10), 158 (100). Analysis calculated for **15d**: C, 52.42; H, 4.40; N, 5.56. Found: C, 51.72; H, 4.34; N, 5.51.

Synthesis of (4-picolyl)cyclopentadiene (16a).



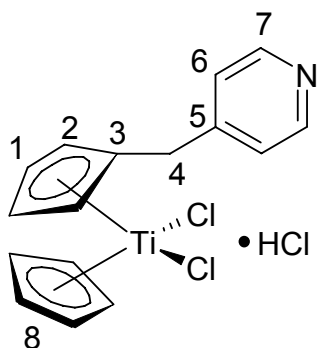
4-Picolyl bromide hydrobromide (25.3 g, 0.100 mol) was added to an aqueous solution of NaOH (4.1 g, 0.10 mol). The solution was extracted three times with diethyl ether (50 mL), and the organic layers were combined and dried with Na₂SO₄ and then added drop-wise to a solution of NaCp in THF (2M, 51 mL, 0.10 mol) at 0 °C. An off white precipitate formed during the addition and the reaction mixture turned orange-brown. After the reaction mixture had stirred for 2 h, H₂O (50 mL) was added. The layers were separated and the organic layer was dried with Na₂SO₄. Removal of the solvent gave a brown oil which was purified by vacuum distillation (boiling point: 80-85 °C at 0.5 mm Hg) to give a clear, slightly yellow oil consisting of a mixture of isomers. Yield: 9.53 g, 61%. ¹H NMR (300 MHz, CDCl₃): δ 8.49 (m, 4H, 5), 7.11 (m, 4H, 4), 6.5-6.0 (m, 6H, 1), 3.71, 3.68 (2 x s, 4H, 3), 2.98, 2.83 (2 x s, 4H, 2) ppm.

Synthesis of lithium (4-picolyl)cyclopentadienide (16b).



Freshly distilled (4-picolyl)cyclopentadiene (4.10 g, 0.0260 mol) was dissolved in hexanes (100 mL) and kept in an ice/water bath. A solution of methyllithium (1.6 M, 26.4 mmol) in ethyl ether was added drop-wise to give immediately a light orange precipitate. The reaction mixture was stirred for thirty minutes and the product was collected with a Schlenk filter. After washing the precipitate with cold hexanes (2 x 50 mL), the product was dried overnight under vacuum. Yield: 4.05 g, 95%. ^1H NMR (600 MHz, $\text{DMSO-}d_6$): δ 8.29 (d, 2H, $^3J = 6.0$ Hz, 7), 7.17 (d, 2H, $^3J = 6.0$ Hz, 6), 5.20 (m, 2H, 1), 5.17 (m, 2H, 2), 3.67 (s, 2H, 4) ppm. ^{13}C NMR (151 MHz, $\text{DMSO-}d_6$): δ 155.5 (5), 148.5 (7), 124.1 (6), 114.4 (3), 103.2 (2), 102.9 (1), 37.3 (4) ppm.

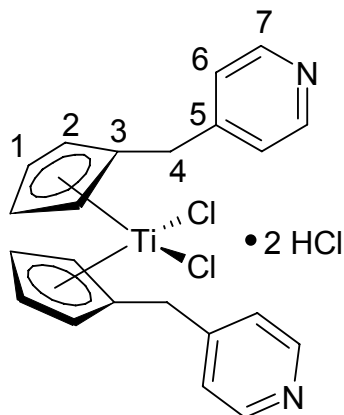
Synthesis of 16c.



Lithium (4-picolyl)cyclopentadienide (0.787 g, 4.82 mmol) was dissolved in THF (15 mL) and the solution was added slowly to a solution of $(\eta^5-$

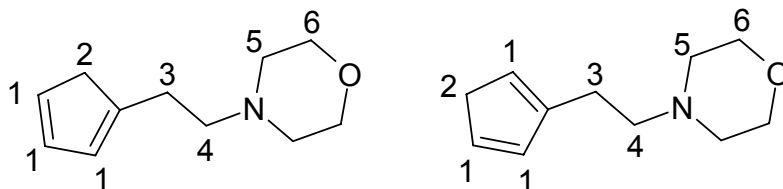
Cp)trichlorotitanium (1.32 g, 6.04 mmol) in THF (150 mL) at 0 °C. The reaction mixture turned dark red and formed a brown precipitate during the addition. The mixture was stirred for 2 h and then filtered, and the resulting dark red filtrate was treated with an excess of HCl in ether (4 mL, 2 M) to give an orange precipitate. The red supernatant was layered with 40 mL of diethyl ether causing the formation of crystals that were suitable for elemental and x-ray crystallographic analyses. The orange precipitate was dissolved in methanol (10 mL) and added dropwise to diethyl ether (400 mL), resulting in precipitation of an orange powder. The product was filtered and dried overnight in vacuo. Yield: 1.36 g, 75%. ¹H NMR (600 MHz, DMSO-*d*₆): δ 8.82 (d, 2H, ³*J* = 6.6 Hz, 7), 7.92 (d, 2H, ³*J* = 6.6 Hz, 6), 6.80 (m, 2H, 1), 6.72 (s, 5H, 8), 6.51 (m, 2H, 2), 4.26 (s, 2H, 4) ppm. ¹³C NMR (151 MHz, DMSO-*d*₆): δ 159.7 (5), 141.7 (7), 132.1 (3), 127.1 (6), 123.8 (2), 120.5 (8), 116.5 (1), 36.2 (4) ppm. Mass Spectra (ES, *m/z* (%)): 340 (30) [M+H], 304 (100) [M-Cl], 171 (10) [M+H]²⁺, 157 (35). Analysis calculated for **16c**: C, 51.04; H, 4.28; N, 3.72. Found: C, 50.94; H, 4.43; N, 3.80.

Synthesis of 16d.



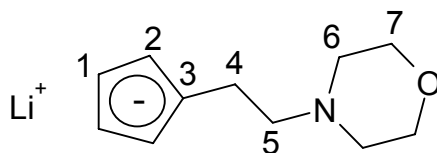
Lithium (4-picolyl)cyclopentadienide (0.828 g, 5.08 mmol) was dissolved in THF (15 mL) and the solution was added slowly to a solution of titanium tetrachloride (1M, 2.55 mmol) in THF (150 mL) at 0 °C. The reaction mixture turned dark red and formed a significant amount of brown precipitate during the addition. The brown precipitate was isolated by filtration and then dissolved in methanol and treated with HCl in ether (4 mL, 2M) resulting in a dark red solution. This was added to an excess of diethyl ether causing the formation of an orange precipitate. The product was filtered and dried overnight *in vacuo*. The compound was recrystallized in dichloromethane by layering with hexanes to yield suitable crystals for elemental analysis. Yield: 1.13 g, 88%. ^1H NMR (600 MHz, DMSO- d_6): δ 8.86 (d, 4H, $^3J = 6.0$ Hz, 7), 7.97 (d, 4H, $^3J = 6.0$ Hz, 6), 6.83 (m, 4H, 1), 6.58 (m, 4H, 2), 4.28 (m, 4H, 4) ppm. ^{13}C NMR (151 MHz, DMSO- d_6): δ 160.0 (5), 141.3 (7), 132.1 (3), 127.3 (6), 123.5 (2), 116.9 (1), 36.2 (4) ppm. Mass Spectra (ES, m/z (%)): 431 (20) [M+H], 429 (40) [M-Cl+MeOH], 395 (40) [M-Cl], 313 (25), 270 (8), 239 (10). Analysis calculated for **16d**: C, 52.42; H, 4.40; N, 5.56. Found: C, 51.66; H, 4.30; N, 5.39.

Synthesis of [2-(1-morpholinyl)ethyl]cyclopentadiene (17a).



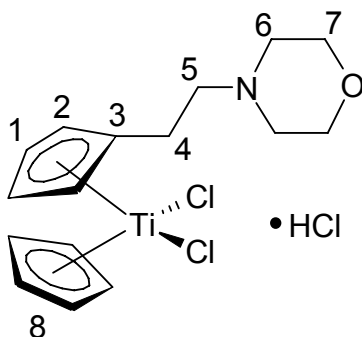
A THF solution of NaCp (2M, 0.112 mol, 2 equivalents) was slowly added dropwise to a suspension of 4-(2-chloroethyl)morpholine hydrochloride (10.2 g, 0.0551 mol) in THF at 0 °C. During addition, the reaction mixture turned dark pink with the formation of a white precipitate. After complete addition the reaction mixture was refluxed for 8 h. The solvent was then removed *in vacuo* and the resulting purple solid was treated with dilute HCl (0.075 mol) in water. The aqueous layer was separated and added directly to a mixture of NaOH/H₂O (pH=13) and diethyl ether. The ether solution of the free amine was separated and the basic solution was further extracted with diethyl ether. The combined organic extracts were dried over Na₂SO₄, filtered and the solvent removed *in vacuo* to yield an amber oil consisting of a mixture of isomers. Subsequent vacuum distillation gave a clear, colourless oil containing a mixture of two isomers (boiling point: 55-57 °C at 0.1 mm Hg). Yield: 7.27 g, 74%. ¹H NMR (300 MHz, CDCl₃): δ 6.4-5.9 (m, 6H, 1), 3.66 (m, 8H, 6), 2.89, 2.85 (2 x s, 4H, 2), 2.56 (m, 4H, 4), 2.49 (m, 4H, 3), 2.38 (m, 8H, 5) ppm.

Synthesis of lithium [2-(1-morpholinyl)ethyl]cyclopentadienide (17b).



A solution of [2-(1-morpholinyl)ethyl]cyclopentadiene (6.69 g, 0.0373 mol) in hexanes was cooled to 0 °C. A diethyl ether solution of methyllithium (1.6 M, 0.0373 mol) was slowly added dropwise over thirty minutes causing the immediate formation of an off-white precipitate. After complete addition the reaction mixture was left to stir at 0 °C for 1 h. The precipitate was collected using a Schlenk filter and washed with cold diethyl ether. The precipitate was dried overnight under vacuum. Yield: 4.94 g, 72%. ^1H NMR (600 MHz, $\text{C}_5\text{D}_5\text{N}$): δ 6.34 (m, 2H, 1), 6.26 (m, 2H, 2), 3.69 (m, 4H, 7), 3.02 (t, $^3J = 7.5$ Hz, 2H, 4), 2.80 (t, $^3J = 7.5$ Hz, 5), 2.46 (m, 4H, 6) ppm. ^{13}C NMR (151 MHz, $\text{C}_5\text{D}_5\text{N}$): δ 118.1 (3), 104.2 (2), 104.1 (1), 67.6 (7), 63.6 (4), 54.8, (6), 28.9 (5) ppm.

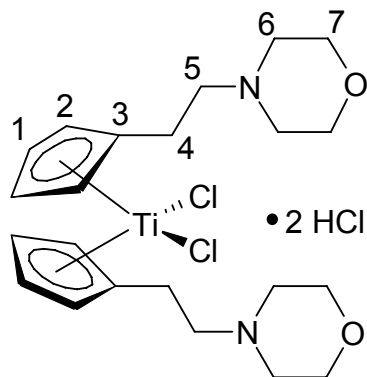
Synthesis of 17c.



A solution containing lithium [2-(1-morpholinyl)ethyl]cyclopentadienide (0.603 g, 3.26 mmol) in THF was slowly added dropwise to a solution of (η^5 -

Cp)trichlorotitanium (0.955 g, 4.35 mmol) in THF at 0 °C. During the addition the reaction mixture turned dark red and formed a light brown precipitate. The mixture was stirred for 2 h and then filtered isolating a dark red filtrate. The filtrate was treated with an excess of HCl in ether (3 mL, 2 M) immediately generating an orange precipitate. The yellow supernatant was discarded and the compound was dissolved in methanol. The resulting solution was added dropwise to diethyl ether inducing the precipitation of an orange powder. The compound was dried overnight under vacuum. Recrystallization of the product by slow evaporation of hexanes into a dichloromethane solution produced crystals that were suitable for elemental analysis. Yield: 0.816 g, 63%. ¹H NMR (600 MHz, D₂O): δ 6.66 (2 x s, 7H, 1 and 8), 6.50 (m, 2H, 2), 4.12, 3.81 (2 x m, 4H, 7), 3.54, 3.21 (2 x m, 4H, 6), 3.41 (t, ³J = 7.2 Hz, 5), 2.96 (t, ³J = 7.2 Hz, 4) ppm. ¹³C NMR (151 MHz, D₂O): δ 135.9 (3), 119.5 (8), 118.3 (1), 117.5 (2), 64.4 (7), 56.6 (5), 52.5 (6), 24.3 (4) ppm. Mass Spectra (ES, m/z (%)) = 362 (25) [M+H], 344 (90), 326 (100) [M-Cl], 308 (15), 264 (12). Analysis calculated for **17c** •H₂O: C, 46.13; H, 5.81; N, 3.36. Found: C, 45.78; H, 5.52; N, 3.71. IR (nujol mull): ν (cm⁻¹) 3320 (H₂O).

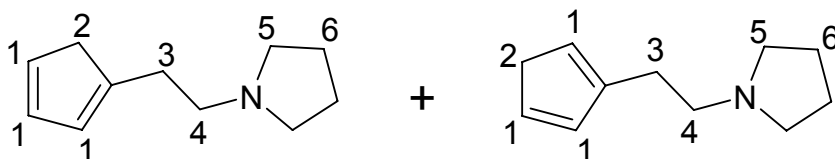
Synthesis of 17d.



A solution of lithium [2-(4-morpholinyl)ethyl]cyclopentadienide (0.856 g, 4.62×10^{-3} mol) in anhydrous THF was cooled to 0 °C. A solution containing TiCl_4 in toluene (1 M, 2.32×10^{-3} mol) was slowly added dropwise over thirty minutes causing the reaction mixture to turn dark red. After complete addition the reaction mixture was left to stir at 0 °C for 1 h and at room temperature for an additional hour. The reaction mixture was vacuum filtered removing a white precipitate. The resulting dark red filtrate was treated with an excess of HCl in ether (4 mL, 2M) in diethyl ether causing the immediate formation of an orange precipitate. The product was isolated by filtration and washed with THF and toluene. Recrystallization from methanol and diethyl ether yielded an orange-red precipitate. Yield: 1.22 g, 95.6%. ^1H NMR (600 MHz, D_2O): δ 6.41 (s, 4H, 1), 6.32 (s, 4H, 2), 3.89, 3.59 (2 x m, 8H, 7), 3.33, 3.00 (2 x m, 8H, 6), 3.19 (t, $^3J = 7.8$ Hz, 5), 2.73 (t, $^3J = 7.8$ Hz, 4) ppm. ^{13}C NMR (151 MHz, D_2O): δ 134.0 (3), 117.4 (1), 116.3 (2), 63.4 (7), 56.0 (5), 51.5 (6), 23.4 (4) ppm. Mass Spectra (ES, m/z (%)) = 475 (100) $[\text{M}+\text{H}]$, 471 (40) $[\text{M}-\text{Cl}+\text{MeOH}]$, 457 (70), 324 (12), 292 (25),

288 (40), 238 (15) [M]⁺2. Analysis calculated for **17d**•2H₂O: C, 45.23; H, 6.56; N, 4.79. Found: C, 44.37; H, 6.31; N, 4.78. IR (nujol mull): ν (cm⁻¹) 3368 (H₂O).

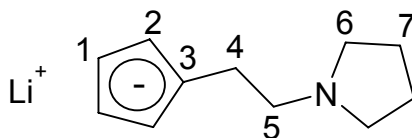
Synthesis of [2-(1-pyrrolidyl)ethyl]cyclopentadiene (18a).¹¹⁴



The synthesis of the compound has been previously described in the literature.¹¹⁴ 1-(2-Chloroethyl)pyrrolidine hydrochloride (10.38 g, 61.0 mmol) was dissolved in THF (250 mL) and a solution of NaCp (2.0 M, 0.134 mol, 2 equivalents) in THF was slowly added dropwise at 0 °C. During the addition the reaction mixture turned dark pink with the formation of a white precipitate. The reaction mixture was refluxed for 12 h and the solvent was then removed *in vacuo*. The resulting residue was treated with a dilute solution of HCl (1 equivalent). The aqueous layer was separated and then treated with a NaOH/H₂O solution (pH = 13) and diethyl ether. The ether solution of the free amine was separated and the aqueous layer was extracted twice more with diethyl ether (2 × 50 mL). The combined organic extracts were dried with Na₂SO₄ and the solvent was removed to give a golden oil. Vacuum distillation of the crude product yielded a clear, colourless oil containing a mixture of two isomers (boiling point: 48-55 °C at 0.1 mm Hg). The ¹H NMR spectrum of this compound closely matches the reported data.¹¹⁴ Yield: 6.56 g, 66%. ¹H NMR (300 MHz,

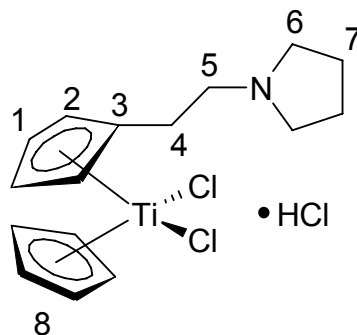
CDCl₃): δ 6.5-6.0 (m, 6H, 1), 2.91, 2.87 (2 \times s, 4H, 2), 2.60 (s, 4H, 4), 2.51 (s, 4H, 3), 2.49 (m, 8H,5), 1.76 (m, 8H, 6) ppm.

Synthesis of lithium [2-(1-pyrrolidyl)ethyl]cyclopentadienide (18b).



Freshly distilled [2-(1-pyrrolidyl)ethyl]cyclopentadiene (6.56 g, 40.2 mmol) was dissolved in hexanes (100 mL), and a solution of methyllithium (1.6 M, 40.2 mmol) in diethyl ether was added by syringe at 0 °C. During the addition, an off white precipitate formed with the evolution of gas. After complete addition, the reaction mixture was stirred for 30 min and the solid was filtered, washed with cold diethyl ether and dried *in vacuo*. Yield: 4.58 g, 67%. ¹H NMR (600 MHz, C₅D₅N): δ 6.32 (m, 2H, 1), 6.24 (m, 2H, 2), 3.02 (t, 2H, ³J = 7.2 Hz, 4), 2.79 (t, 2H, ³J = 7.2 Hz, 5), 2.45 (m, 4H, 6), 1.45 (m, 4H, 7) ppm. ¹³C NMR (151 MHz, C₅D₅N): δ 117.9 (3), 104.7 (1), 103.6 (2), 61.6 (4), 54.7 (6), 30.9 (5), 24.1 (7) ppm.

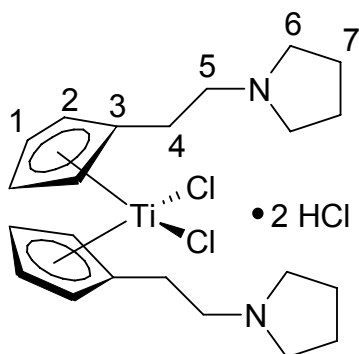
Synthesis of 18c



Lithium [2-(1-pyrrolyl)ethyl]cyclopentadienide (0.498 g, 2.95 mmol) was suspended in 50 mL of toluene and a solution of (η^5 -Cp)trichlorotitanium (0.647 g, 2.95 mmol) in toluene (20 mL) was slowly added by syringe at 0 °C. A dark red colour and a brown precipitate formed immediately, and the reaction mixture was stirred for 2 h. The mixture was filtered to give a dark red filtrate which was treated with an excess of HCl in ether (3 mL, 2 M) to give an orange precipitate. The precipitate was collected and washed with diethyl ether (2 x 50 mL) and then dissolved in methanol (15 mL). The resulting solution was slowly added to diethyl ether (300 mL) to induce precipitation. The red powder was isolated and dried overnight *in vacuo*. The product was recrystallized from dichloromethane by slow diffusion with hexanes to give dark red crystals suitable for elemental analysis. Yield: 0.844 g, 72%. ^1H NMR (600 MHz, D_2O): δ 6.63 (2 x s, 7H, 1 and 8), 6.50 (s, 2H, 2), 3.61, 3.06 (2 x m, 4H, 6), 3.40 (t, 2H, $^3J = 7.2$ Hz, 5), 2.90 (t, 2H, $^3J = 7.2$ Hz, 4), 2.11, 1.96 (2 x m, 4H, 7) ppm. ^{13}C (151 MHz, D_2O): δ 135.1 (3), 118.7 (8), 117.8 (1), 116.7 (2), 54.3 (6), 54.0 (5), 25.8 (4), 22.6 (7) ppm. Mass spectra (ES, m/z (%)) = 346 (80) [M+H], 344 (10) [M-Cl+MeOH], 311 (10) [M-Cl], 84

(100). Analysis calculated for **18c**: C, 50.23; H, 6.06; N, 3.66. Found: C, 50.55; H, 5.57; N, 4.40.

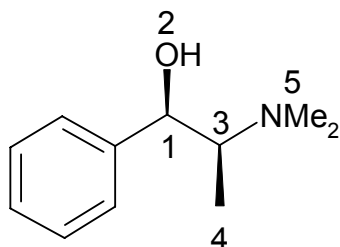
Synthesis of **18d**.



Lithium [2-(1-pyrrolidyl)ethyl]cyclopentadienide (0.929 g, 5.50 mmol) was suspended in toluene (75 mL), and a solution of titanium tetrachloride (1 M, 2.75 mmol) in toluene was slowly added by syringe at 0 °C. The reaction mixture turned dark red during the addition with the formation of a brown precipitate. The reaction mixture was stirred for 2 h, and then filtered to give a dark red filtrate. The filtrate was treated with an excess of HCl in ether (4 mL, 2 M) in diethyl ether, resulting in the immediate formation of an orange precipitate. The solid was filtered, washed with toluene (2 x 50 mL) and dissolved in methanol (10 mL). This solution was added dropwise to diethyl ether (300 mL) to give a red precipitate which was isolated and dried overnight *in vacuo*. The compound was recrystallized by layering a dichloromethane solution with benzene to give dark red crystals suitable for elemental and x-ray crystallographic analyses. Yield: 0.693 g, 49%. ¹H NMR (600 MHz, D₂O): δ 6.65 (s, 4H, 1), 6.56 (s, 4H, 2), 3.66, 3.11 (2 × m, 8H, 6), 3.45 (t, 4H, ³J = 7.5 Hz, 5), 2.94 (t, 4H, ³J = 7.5 Hz, 4), 2.16,

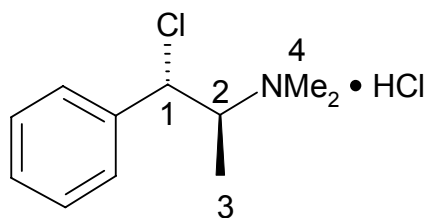
2.01 (2 × m, 8H, 7) ppm. ^{13}C (151 MHz, D_2O): δ 134.2 (3), 117.8 (1), 117.0 (2), 54.4 (2 × s, 5 and 6), 25.9 (4), 22.7 (7) ppm. Mass spectra (ES, m/z (%)) = 443 (40) $[\text{M}+\text{H}]$, 407 (90) $[\text{M}-\text{Cl}]$, 280 (8), 262 (8), 180 (40), 163 (80). Analysis calculated for **18d**• H_2O : C, 49.46; H, 6.79; N, 5.24. Found: C, 48.87; H, 6.76; N, 5.36. IR (nujol mull): ν (cm^{-1}) 3321 (H_2O).

Synthesis of (1R, 2S)-N-methylephedrine.¹¹⁵



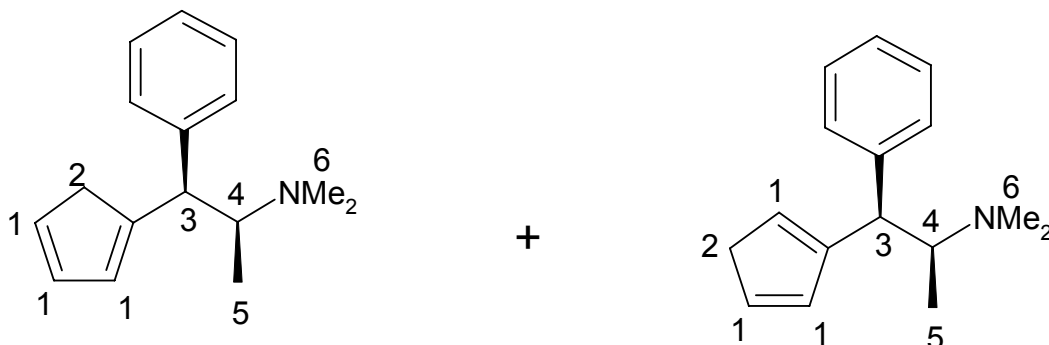
Ephedrine (5.09 g, 30.8 mmol) was put into a 100 mL round bottom flask along with 30 mL of formalin (37% by weight formaldehyde in water, 13 eq) and 30 mL of formic acid (25 eq). The reaction mixture was refluxed for 3 h. The solvents were then removed *in vacuo* and the resulting paste was basified to a pH = 11 using a 1 M NaOH solution. The aqueous phase was extracted with ether (3 x 50 mL) and the combined extracts were dried with Na_2SO_4 and the solvent was removed yielding a clear, yellow oil. The ^1H NMR spectrum matches previously reported data.¹¹⁵ Yield: 5.48 g, 99%. ^1H NMR (300 MHz, CDCl_3): δ 7.36-7.25 (m, 5H, Ph), 4.96 (d, 1H, $^3J = 3.6$ Hz, 1), 3.58 (s, 1H, 2), 2.54 (dq, 1H, $^3J = 3.6, 6.9$ Hz, 3), 2.37 (s, 6H, 5), 0.83 (d, 3H, $^3J = 6.9$ Hz, 4) ppm.

Synthesis of (1S, 2S)-1-chloro-2-(N,N-dimethylamino)-1-phenylpropane hydrochloride (19).¹¹⁶



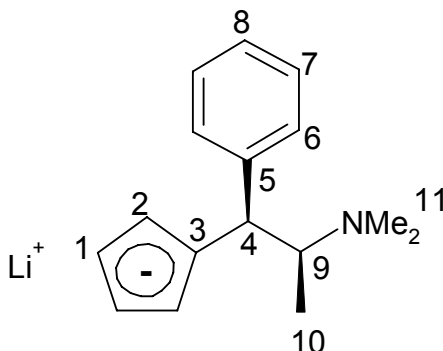
(1R, 2S)-*N*-methylephedrine (39.05 g, 218.0 mmol) was dissolved in 200 mL of anhydrous chloroform and put into a 500 mL round bottom flask. The solution was kept at 0 °C in an ice water bath. Thionyl chloride (20.0 mL, 1.25 eq) was slowly added dropwise over 30 minutes and the solution turned dark red. The reaction mixture was left to stir for 12 h and the solvent was then removed *in vacuo* leaving a sticky, red solid. The product was crystallized in a 3:1 mixture of diethyl ether: ethanol at -72 °C. The ¹H NMR spectrum matches previously reported data.¹¹⁶ Yield: 31.87 g, 62%. ¹H NMR (600 MHz, CD₃OD): δ 7.54-7.43 (m, 5H, Ph), 5.32 (d, 1H, ³J = 10.8 Hz, 1), 4.15 (dq, 1H ³J = 10.8, 6.6 Hz, 2), 3.04 and 2.93 (2 x s, 6H, 4), 1.10 (d, 3H, ³J = 6.6 Hz, 3) ppm.

Synthesis of (1R, 2S)-1-cyclopentadienyl-2-N,N-dimethylamino-1-phenylpropane (19a).¹¹⁷



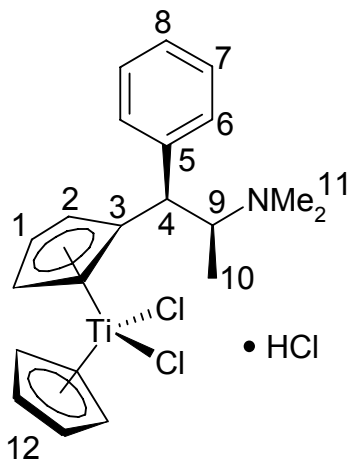
A mixture of (1S, 2S)-1-chloro-2-(N,N-dimethylamino)-1-phenylpropane hydrochloride (19.11 g, 81.6 mmol) in THF (200 mL) was prepared in a 500 mL round bottom flask. To this mixture, a freshly prepared NaCp (36.4 g, 5 eq) in 200 mL of THF was slowly added dropwise at room temperature. The reaction mixture was left to stir for 16 h and then treated with water (30 mL). All of the volatiles were removed *in vacuo* and the residue was treated with diethyl ether (300 mL). The organic layer was separated and dried with Na₂SO₄. Removal of the solvent yielded a brown oil consisting of a mixture of isomers. The ¹H NMR spectrum matches previously reported data.¹¹⁷ Yield: 14.8 g, 80%. ¹H NMR (300 MHz, CDCl₃): δ 7.33-7.15 (m, 10H, Ph), 6.62-6.17 (m, 6H, 1), 3.80, 3.77 (2 x d, 2H, ³J = 6.4 Hz, 3), 3.31 (m, 2H, 4), 2.99 (m, 4H, 2), 2.31 and 2.30 (2 x s, 12H, 6), 0.78 and 0.76 (2 x d, 6H, ³J = 3.0 Hz, 5) ppm.

Synthesis of lithium [(1R, 2S)(2-dimethylamino-1-phenyl)propyl]cyclopentadienide (19b).¹¹⁸



A solution of (1R, 2S)1-Cp-2-dimethylamino-1-phenylpropane (11.31 g, 49.7 mmol) in anhydrous hexanes (200 mL) was stirred in a 250 mL round bottom flask. The solution was cooled to 0 °C and slowly treated with a solution of methyl lithium in diethyl ether (1.6 M, 1 eq). A tan coloured precipitate formed during the reaction and, after complete addition, the reaction mixture was left to stir for 1 h. The precipitate was isolated by filtration, washed with hexanes (3 x 50 mL) and left to dry overnight under vacuum. The NMR spectra of this complex match previously reported data.¹¹⁸ Yield: 10.5 g, 91%. ¹H NMR (600 MHz, DMSO-*d*₆): δ 7.31 (d, 2H, ³J = 7.2 Hz, 6), 7.14 (t, 2H, ³J = 7.2 Hz, 7), 7.00 (t, 1H, ³J = 7.2 Hz, 8), 5.36 (s, 2H, 2), 5.29 (s, 2H, 1), 3.76 (d, 1H, ³J = 9.0 Hz, 4), 3.02 (m, 1H, 9), 2.08 (s, 6H, 11), 0.72 (d, 3H, ³J = 6.6 Hz, 10) ppm. ¹³C (151 MHz, DMSO-*d*₆): δ 148.2 (5), 128.8 (6), 127.1 (7), 124.1 (8), 120.7 (3), 102.4 (1), 101.6 (2), 64.4 (9), 51.8 (4), 40.7 (11), 11.2 (10) ppm.

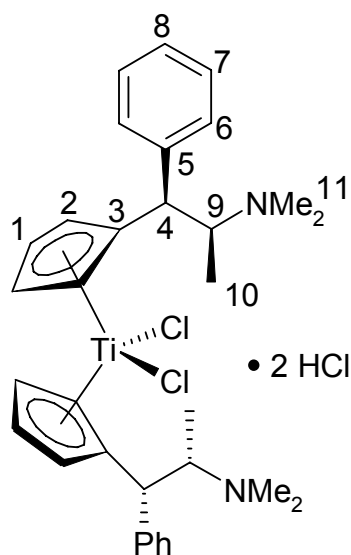
Synthesis of 19c.



Lithium [(1R, 2S)(2-dimethylamino-1-phenyl)propyl]cyclopentadienide (0.764 g, 3.27 mmol) was suspended in 100 mL of toluene in a 200 mL Schlenk flask and a solution of (η^5 -Cp)trichlorotitanium (0.806 g, 3.67 mmol) in toluene (20 mL) was slowly added by syringe while in a dry ice/isopropanol bath (-72 °C). The resulting solution turned dark red and, once addition was complete, the reaction mixture was left to stir and slowly warm to room temperature for 3 h. The mixture was subsequently filtered and the filtrate was treated with an excess of hydrochloric acid in ether (3 mL, 2M). This resulted in the formation of an orange precipitate which was isolated by filtration, washed with ether (3 x 50 mL) and dried overnight under vacuum. Yield: 1.06 g, 72%. The product was recrystallized by layering a solution of **19c** in dichloromethane with hexanes which produced crystals that were suitable for X-ray and elemental analyses. ^1H NMR (600 MHz, D_2O): δ 7.42 (t, 2H, $^3J = 7.2$ Hz, 7), 7.38 (t, 1H, $^3J = 7.2$ Hz, 8), 7.21 (d, 2H, $^3J = 7.2$ Hz, 6), 6.88 and 6.66 (2 x s, 2H, 1), 6.74 and 6.38 (2 x s, 2H, 2), 6.53 (s, 5H, 12), 4.29 (d, 1H, $^3J = 10.2$ Hz, 4), 4.24 (m, 1H, 9), 2.95 and

2.75 (2 x s, 6H, 11), 1.05 (d, 3H, $^3J = 6.0$ Hz, 10) ppm. ^{13}C (151 MHz, D_2O): δ 139.4 (5), 138.9 (3), 129.2 (7), 129.0 (6), 128.1 (8), 119.7 and 117.7 (2), 118.9 and 114.4 (1), 118.9 (12), 63.9 (9), 47.1 (4), 42.6 and 36.4 (11), 10.7 (10) ppm. Mass spectra (ES, m/z (%)) = 410 (100) [M+H], 374 (10) [M-Cl], 345 (8) [M-Cp], 329 (80) [M-N(CH₃)₂NHCl], 227 (20) [Ligand], 181 (20) [M-Ligand]. Analysis calculated for **19c**•H₂O: C, 54.28; H, 6.07; N, 3.03. Found: C, 54.29; H, 5.93; N, 2.95. IR (nujol mull): ν (cm⁻¹) 3412 (H₂O).

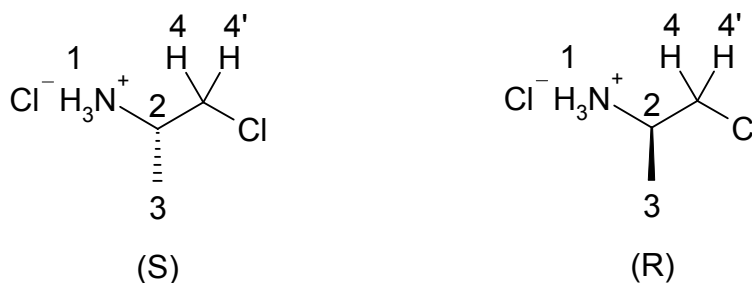
Synthesis of 19d.



Lithium [(1R, 2S)(2-dimethylamino-1-phenyl)propyl]cyclopentadienide (0.971 g, 4.16 mmol) was suspended in 100 mL of anhydrous toluene and cooled in a dry ice/isopropanol bath (-72 °C). The resulting suspension was treated with titanium tetrachloride in toluene (1M, 2.08 mL, 2.08 mmol) which caused the reaction mixture to turn dark red with the formation of a brown precipitate. After complete addition the reaction mixture was left to slowly warm to room

temperature and was stirred for 4 h. The mixture was subsequently filtered and the dark red filtrate was treated with an excess of hydrochloric acid in ether (4 mL, 2 M). This caused the formation of an orange precipitate that was isolated by filtration, washed with ether (3 x 50 mL) and dried overnight under vacuum. Yield: 0.857 g, 64%. Suitable crystals for elemental analysis were formed by layering a dichloromethane solution of **19d** with hexanes. ^1H NMR (600 MHz, D_2O): δ 7.43 (t, 4H, $^3J = 7.8$ Hz, 7), 7.39 (t, 2H, $^3J = 7.2$ Hz, 8), 7.23 (d, 4H, $^3J = 7.2$ Hz, 6), 6.52 and 6.39 (2 x s, 4H, 2), 6.43 and 5.95 (2 x s, 4H, 1), 4.30 (d, 2H, $^3J = 9.6$ Hz, 4), 4.07 (m, 2H, 9), 2.92 and 2.75 (2 x s, 12H, 11), 1.04 (d, 6H, $^3J = 6.6$ Hz, 10) ppm. ^{13}C (151 MHz, D_2O): δ 138.3 (5), 135.6 (3), 129.3 (6), 129.1 (7), 128.5 (8), 121.9 and 114.0 (1), 120.5 and 118.6 (2), 64.8 (9), 47.0 (4), 43.0 and 36.6 (11), 10.6 (10) ppm. Mass spectra (ES, m/z (%)) = 571 (60) [M+H], 555 (10) [M-CH₃], 535 (50) [M-Cl], 517 (1), 500 (15), 464 (100), 408 (10) [M-Ligand], 345 (30), 286 (5) [M]²⁺, 264 (20). Analysis calculated for **19d**•H₂O: C, 56.49; H, 6.81; N, 4.12. Found: C, 56.63; H, 6.67; N, 4.01. IR (nujol mull): ν (cm⁻¹) 3388 (H₂O).

Synthesis of (S and R)-1-chloropropyl-2-ammonium chloride (S)-20 and (R)-20.¹¹⁹

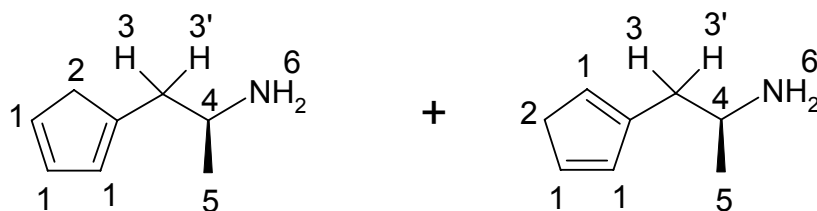


The synthesis of these compounds have been previously described in the literature.¹¹⁹ (S)-alaninol (22.2 g, 0.296 mol) was dissolved in 250 mL of anhydrous chloroform. The resulting solution was cooled in an ice water bath and slowly treated with thionyl chloride (54 g, 1.5 equivalents) while being vigorously stirred. This resulted in the immediate formation of a thick precipitate. After complete addition, 1 mL of DMF was added and the reaction mixture was stirred at 50 °C. The precipitate slowly dissolved and gas evolved from the reaction mixture. The mixture was left to stir for 12 h at 50 °C and then put in the freezer at -30 °C which caused the formation of white, transparent crystals. The product was isolated by filtration and washed with cold chloroform. Yield: 34.3 g, 89%. Characterization data are reported below.

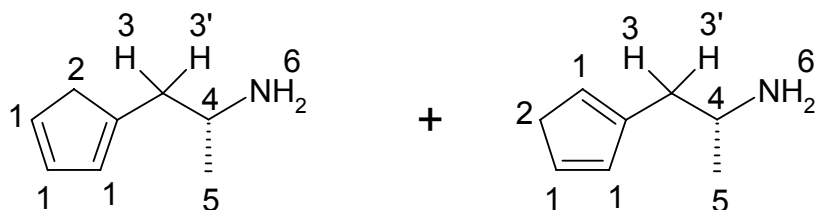
(R)-alaninol (13.6 g, 0.182 mmol) was dissolved in 200 mL of anhydrous chloroform and cooled to 0 °C in an ice water bath. The resulting solution was slowly treated with thionyl chloride (32.8 g, 1.5 equivalents) which caused the immediate formation of a thick precipitate. The reaction mixture was then treated with 1.5 mL of DMF and heated to 50 °C. The precipitate slowly dissolved and a

gas evolved from the reaction mixture. The mixture was left to stir for 12 h at 50 °C and then cooled in the freezer at -30 °C which caused the formation of colourless, transparent crystals. The product was isolated by filtration and washed with cold chloroform. Yield: 21.4 g, 91%. ¹H NMR (600 MHz, DMSO): δ 8.52 (s, 3H, 1), 3.86 (dd, 1H, ²J = 11.4 Hz, ³J = 4.8 Hz, 4), 3.82 (dd, 1H, ²J = 11.4 Hz, ³J = 4.8 Hz, 4'), 3.49 (m, 1H, 2), 1.27 (d, 3H, ³J = 6.6 Hz, 3) ppm. Mass spectra (ES, m/z (%)) = 93 (100) [M+H], 76 (80) [M-NH₂], 57 (10) [M-HCl].

Synthesis of (S and R)-(2-aminopropyl)cyclopentadiene (S)-20a and (R)-20a.



A freshly prepared solution of sodium cyclopentadienide (0.79 mol) in THF (300 mL) was slowly added to a suspension of (S)-1-chloropropyl-2-ammonium chloride (34.3 g, 0.264 mol) in THF (100 mL). The mixture was stirred at 50 °C for two h and then at room temperature for 12 h. The solvent was removed *in vacuo* and the residue was treated with water (100 mL) and extracted five times with diethyl ether (100 mL each). The organic layers were collected and dried with Na₂SO₄, and the solvent was removed yielding a brown oil. Vacuum distillation yielded a clear, yellow oil with a boiling point of 50 °C (at 3.7 torr). Yield: 21.8 g, 67%. Characterization data are reported below.



A freshly prepared solution of sodium cyclopentadienide (0.49 mol) in THF (250 mL) was slowly added dropwise to a heterogeneous mixture of (R)-1-chloropropyl-2-ammonium chloride (21.4 g, 0.165 mol) in THF (100 mL). After complete addition the reaction mixture was heated and stirred at 50 °C for 2 h after which it was left to stir for 12 h at room temperature. The solvent was then removed *in vacuo* leaving an orange solid behind. The residue was treated with 100 mL of water and then extracted with diethyl ether (8 x 50 mL). The organic layers were collected, dried with Na₂SO₄ and the solvent was removed. The resulting brown oil was vacuum distilled yielding a clear, colourless oil with a boiling point of 57 °C (at 5 torr). Yield: 10.9 g, 54%. ¹H NMR (600 MHz, CDCl₃): δ 6.43-6.08 (m, 6H, 1), 3.13 and 3.08 (2 x m, 2H, 4), 2.92 (m, 4H, 2), 2.46 (2 x dd, 2H, ²J = 15.0 Hz, ³J = 5.4 Hz, 3), 2.33 (2 x dd, 2H, ²J = 15.0 Hz, ³J = 7.8 Hz, 3'), 1.31 (s, 2H, 6), 1.10 (2 x d, ³J = 6.0 Hz, 5) ppm.

Synthesis of lithium (S and R)-(2-aminopropyl)cyclopentadienide (S)-20b (R)-20b.

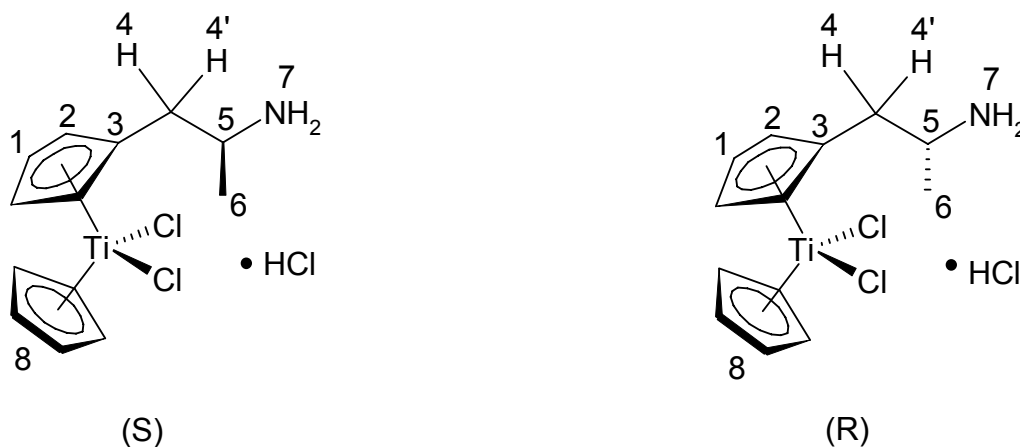


A solution of (S)-(2-aminopropyl)cyclopentadiene (15.2 g, 124 mmol) in 200 mL of anhydrous hexanes was prepared in a 250 mL round bottom flask. The resulting solution was cooled to 0 °C in an ice/water bath and one equivalent of methyllithium in diethyl ether (1.6 M, 77.5 mL, 124 mmol) was slowly added dropwise. This resulted in the immediate formation of a white precipitate. After complete addition the reaction mixture was left to stir at 0 °C for 2 h. The precipitate was then isolated by filtration, washed with cold hexanes (3 x 50 mL) and dried overnight *in vacuo*. Yield: 14.8 g, 93%. Characterization data are reported below.

10.9 g of (R)-(2-aminopropyl)cyclopentadiene (88.6 mmol) was put into a 250 mL round bottom flask along with 180 mL of anhydrous hexanes. The resulting solution was cooled to 0 °C in an ice/water bath and then slowly treated with one equivalent of methyllithium in diethyl ether (1.6 M, 55.4 mL, 88.6 mmol). A white precipitate immediately formed, and after complete addition, the reaction mixture was left to stir for 2 h at 0 °C. The precipitate was isolated by filtration, washed with cold hexanes (3 x 50 mL) and dried overnight under vacuum. Yield:

10.1 g, 88 %. ^1H NMR (600 MHz, DMSO): δ 5.20 (m, 2H, 1), 5.18 (m, 2H, 2), 2.65 (m, 1H, 5), 2.46 (dd, 1H, $^2J = 13.2$ Hz, $^3J = 4.2$ Hz, 4), 2.06 (dd, 1H, $^2J = 13.2$ Hz, $^3J = 8.4$ Hz, 4'), 0.93 (d, 3H, $^3J = 6.6$ Hz, 6) ppm. ^{13}C (151 MHz, DMSO): δ 115.5 (3), 103.4 (2), 102.4 (1), 49.2 (5), 43.1 (4), 23.9 (6) ppm.

Synthesis of (S)-20c and (R)-20c.



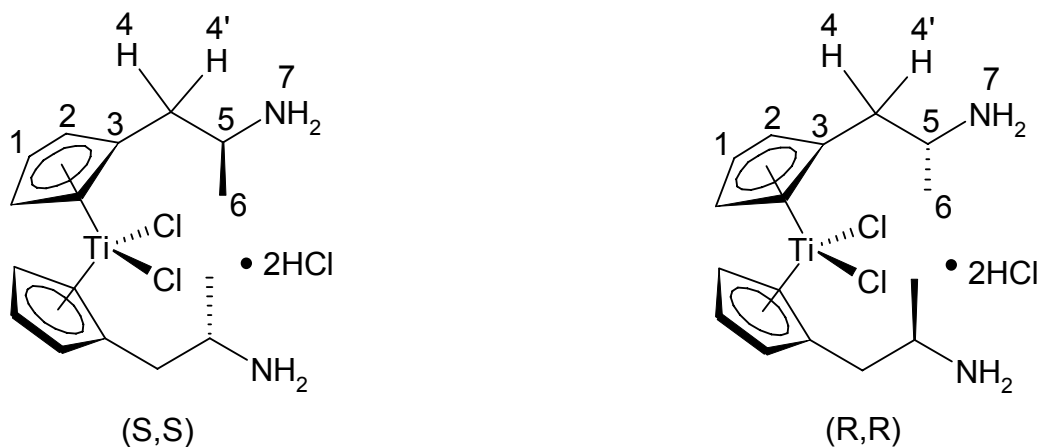
A solution of freshly sublimed (η^5 -Cp)trichlorotitanium (1.73 g, 6.48 mmol) in anhydrous THF (100 mL) was prepared and kept in an ice/water bath. This was slowly treated with a solution of lithium (S)-(2-aminopropyl)cyclopentadienide (0.837 g, 6.48 mmol) in 20 mL of THF which caused the reaction mixture to turn dark orange and then red. After complete addition the reaction mixture was left to slowly warm while stirring to room temperature for 3 h. The mixture was then filtered and the dark, red filtrate was treated with an excess of hydrochloric acid in diethyl ether (5 mL, 2M) causing the formation of a bright, red precipitate. The precipitate was isolated by filtration, washed with diethyl ether (3 x 50 mL) and dried overnight under vacuum. A solution of the product in 40% methanol/dichloromethane was layered with hexanes which yielded crystals that

were suitable for elemental analysis. Yield: 1.76 g, 79%. Characterization data are reported below.

Freshly sublimed (η^5 -Cp)trichlorotitanium (1.85 g, 8.45 mmol) was added to 100 mL of anhydrous THF and kept in an ice/water bath. A solution of lithium (R)-(2-aminopropyl)cyclopentadienide (0.866 g, 6.70 mmol) in a minimal amount of THF was slowly added dropwise causing the reaction mixture to turn light orange. The reaction mixture turned dark red as it was left to stir and slowly warm to room temperature for 2 h. The mixture was then filtered and the filtrate was treated with an excess of hydrochloric acid in diethyl ether (6 mL, 2 M) causing the immediate formation of an orange precipitate. The precipitate was isolated by filtration, washed 3 times with cold diethyl ether (50 mL) and dried overnight under vacuum. A solution of the product in 25% DMSO in dichloromethane was layered with benzene which yielded crystals that were suitable for elemental analysis. Yield: 1.15 g, 84%. ^1H NMR (600 MHz, DMSO): δ 8.19 (s, 3H, 7), 6.80 and 6.78 (2 x m, 2H, 1), 6.68 (s, 5H, 8), 6.43 (m, 2H, 2), 3.37 (m, 1H, 5), 3.05 (dd, 1H, $^2J = 13.8$ Hz, $^3J = 5.4$ Hz, 4), 2.77 (dd, 1H, $^2J = 13.8$ Hz, $^3J = 8.7$ Hz, 4'), 1.14 (d, 3H, $^3J = 6.6$ Hz, 6) ppm. ^{13}C (151 MHz, DMSO): δ 131.1 (3), 125.1 and 124.8 (2), 120.2 (8), 115.9 and 115.8 (1), 47.4 (5), 35.6 (4), 18.0 (6) ppm. Mass spectra (ES, m/z (%)) = 306 (10) [M+H], 270 (12) [M-Cl], 235 (5) [M-2Cl], 164 (100). The specific rotations found at $\lambda = 633$ nm, 25 °C in DMSO for (S)-**20c** and (R)-**20c** are -29.1° and $+28.4^\circ$, respectively. Analysis calculated for **20c**• $\frac{1}{2}$ H₂O: C, 44.42; H, 5.16; N, 3.98. Found (S)-**20c**: C, 44.18; H,

5.01; N, 4.35. Found (R)-**20c**: C, 44.59; H, 5.33; N, 4.11. IR (nujol mull): ν (cm^{-1}) (S)-**20c** 3295 (H_2O), (R)-**20c** 3336 (H_2O).

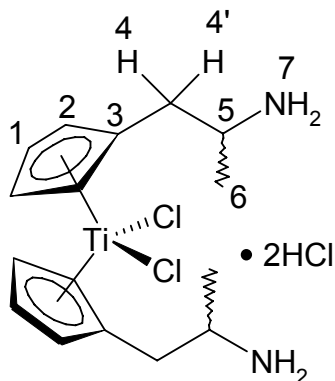
Synthesis of (S,S)-**20d** and (R,R)-**20d**



A solution of lithium (S)-(2-aminopropyl)cyclopentadienide (0.993 g, 7.69 mmol, 2 equivalents) in 100 mL of anhydrous THF was prepared and kept in an ice/water bath. A solution of titanium tetrachloride in toluene (1M, 3.8 mL, 1 equivalent) was slowly added dropwise causing the reaction mixture to turn dark red with the formation of a light brown precipitate. After complete addition the reaction mixture was left to stir and slowly warm to room temperature for 2 h. The mixture was then filtered and the filtrate was treated with an excess of hydrochloric acid in diethyl ether (5 mL, 2 M) which caused the immediate formation of a red precipitate. The precipitate was isolated by filtration, washed with cold diethyl ether (50 mL) and dried overnight under vacuum. Crystals suitable for elemental analysis were grown by layering a 25% methanol/dichloromethane solution with hexanes. Yield: 1.16 g, 70%.

A solution containing lithium (R)-(2-aminopropyl)cyclopentadienide (1.08 g, 8.38 mmol, 2 equivalents) in 100 mL of anhydrous THF was prepared and kept in an ice/water bath. Titanium tetrachloride in toluene (1M, 4.19 mL, 1 equivalent) was slowly added dropwise causing the reaction mixture to turn dark red with the formation of a light brown precipitate. After complete addition the reaction mixture was left to stir and slowly warm to room temperature over a 2 h period. The mixture was then filtered and the dark red filtrate was treated with an excess of hydrochloric in diethyl ether (5 mL, 2 M) causing the immediate formation of an orange precipitate. The precipitate was isolated by filtration, washed 3 times with cold diethyl ether (50 mL) and dried overnight under vacuum. Crystals suitable for elemental analysis were grown by slow diffusion of hexanes into a 25% methanol/dichloromethane solution. Yield: 1.23 g, 67%. ^1H NMR (600 MHz, DMSO): δ 8.29 (s, 6H, 7), 6.79 and 6.77 (2 x m, 4H, 1), 6.46 (m, 4H, 2), 3.37 (m, 2H, 5), 3.04 (dd, 2H, $^2J = 13.8$ Hz, $^3J = 5.1$ Hz, 4), 2.76 (dd, 2H, $^2J = 13.8$ Hz, $^3J = 8.4$ Hz, 4'), 1.15 (d, 6H, $^3J = 6.0$ Hz, 6) ppm. ^{13}C (151 MHz, DMSO): δ 131.0 (3), 124.5 and 124.2 (2), 116.1 and 116.1 (1), 47.4 (5), 35.6 (4), 17.9 (6) ppm. Mass spectra, sample dissolved in methanol (ES, m/z (%)) = 323 (95) [M-2Cl+MeO], 292 (100) [M-2Cl], 236 (10), 169 (10), 141 (20). The specific rotations found at $\lambda = 633$ nm, 25 °C for (S,S)-**20d** and (R,R)-**20d** are -39.4° and +39.2°, respectively. Analysis calculated for **20d**•2½H₂O: C, 39.94; H, 6.49; N, 5.82. Found (S,S)-**20d**: C, 39.93; H, 6.11; N, 5.50. Found (R,R)-**20d**: C, 39.41; H, 5.85; N, 5.39. IR (nujol mull): ν (cm⁻¹) (S,S)-**20d** 3425 (H₂O), (R,R)-**20d** 3355 (H₂O).

Synthesis of a mixture of (S,S)-20d, (R,R)-20d and (R,S)-20d.



A solution containing both lithium (S)-(2-aminopropyl)cyclopentadienide (0.404 g, 3.12 mmol) and lithium (R)-(2-aminopropyl)cyclopentadienide (0.410 g, 3.17 mmol) in 100 mL of anhydrous THF was prepared and kept in an ice/water bath. The resulting solution was slowly treated with one equivalent of titanium tetrachloride in toluene (1M, 3.1 mL, 3.1 mmol) causing the reaction mixture to turn dark red with the formation of a brown precipitate. After complete addition, the reaction mixture was left to stir and slowly warm to room temperature for 2 h. The mixture was filtered and the dark red filtrate was treated with an excess of hydrochloric acid in diethyl ether (5 mL, 2M). This caused the immediate formation of an orange-red precipitate which was isolated by filtration, washed 3 times with cold diethyl ether (50 mL) and dried overnight under vacuum. Yield: 1.22 g, 89.7%. ¹H NMR (600 MHz, DMSO): δ 8.34 (s, 6H, 8), 6.80 and 6.77 (2 x m, 4H, 1), 6.46 (m, 4H, 2), 3.36 (m, 2H, 5), 3.04 (dd, ²J = 14.1 Hz, ³J = 5.1 Hz, 2H, 4), 2.76 (dd, 2H, ²J = 13.8 Hz, ³J = 8.4 Hz, 4'), **2.75 (dd, 2H, ²J = 13.8, ³J = 9 Hz, 4')**, 1.15 (d, ³J = 6.6 Hz, 6). ¹³C (151 MHz, DMSO): δ 131.10 and **131.08** (3), 124.5 **124.4** 124.1 **124.0** (2), **116.6 116.3** 116.2 116.1 (1), 47.4 (5), 35.6 (4), 17.9

(6). Bolded values are tentatively assigned to (R,S)-**20d** and their assignment will be explained in the results and discussion.

2.4 MTT Assay

Dr. S.P.C. Cole of Division of Cancer Biology and Genetics at the Queen's University Cancer Research Institute provided A549, H209, H209/CP, H69, HeLa, A2780 and A2780/CP cell lines. Kathy Sparks from Dr. Cole's lab performed the majority of the MTT assays, while Marina Chan (Ph.D. student, Department of Pharmacology and Toxicology) performed a minority.

Cell culture and chemosensitivity testing.

The H69, H209, H209/CP, A549 lung tumour cell lines and the HeLa cervical carcinoma cell line were cultured in RPMI 1640 medium containing 5% calf serum while the A2780 and A2780/CP ovarian tumour cell lines were cultured in DMEM medium with 7.5% fetal bovine serum. All cells were cultured at 37 °C in a humidified atmosphere of 5% CO₂ and 95% air.

The cytotoxic potencies of the various compounds were determined using the colorimetric 3-(4,5-dimethylthiazol-2-yl)-2,5-diphenyl tetrazolium bromide (MTT) assay as developed by Mosmann¹²⁰ and adapted for chemosensitivity testing of human tumour cells.^{108,109} Cells (>90% viable as determined by trypan blue exclusion test) were suspended in culture medium and dispensed into 96-well microtitre plates in a volume of 100 µL. H69 cells were plated at 2.5 x 10⁴ cells per well, the A549 cells at 1.0 x 10⁴ cells per well and the A2780 cells at 0.5

$\times 10^4$ cells per well, based on preliminary experiments indicating these to be optimal cell densities for the MTT assay conditions chosen. After incubation of the cells for 24 h, compounds were added in a volume of 100 μL to bring the total volume of culture medium in the wells to 200 μL .

All solutions and dilutions of the titanocene derivatives were prepared immediately before addition to the cultured cells to limit the possibility of precipitation upon standing. The compounds were first dissolved in approximately 5 mL of medium and the volume was adjusted such that the final drug concentration was 2 mM. The stock solutions were then diluted as required and added to the wells. Final drug concentrations typically ranged from 0.1 to 200 μM in the assays. Each drug concentration was added to four replicate wells. Cisplatin (Sigma P4394) was frequently tested in each set of assays as a positive control.

After addition of the drugs, the microtitre plates were returned to the 37 °C incubator for 4 days. Three hours before completion of the incubation time, 100 μL of medium was removed from each well, and 25 μL of MTT (Sigma M2128) solution (2 mg/mL in phosphate buffered saline) was added. The plates were then returned to the 37 °C incubator for 3 h to allow for the reduction of the tetrazolium salt to formazan by viable cells. Subsequently, 100 μL of 1 M HCl/isopropanol (1:24) was added to each well followed by vigorous mixing with a multichannel micropipette to dissolve the dark blue formazan crystals formed by MTT reduction. Absorbance values at 570 nm were then measured using a UV spectrophotometer. Controls consisted of wells with untreated cells and

provided the baseline absorbance. Mean values (\pm SD) of the quadruplicate determinations were calculated and results expressed as a percentage of the baseline absorbance at 570 nm. Using GraphPAD Prism (version 3.02) software, IC₅₀ values (defined as the drug concentration that reduced the absorbance to 50% of control values) were obtained from the best fit of the data to a sigmoidal curve.

Chapter 3: Results and Discussion

For the purpose of this thesis, the following labeling scheme outlined in Figure 31 is used to simplify notation and keep complexes derived from the same alkylammonia substituents together. Neutral, substituted Cp ligands are labeled as **a**, whereas the deprotonated lithium salts are labeled as **b**. The monocationic TDC derivatives are labeled as **c** and the dicationic derivatives are **d**.

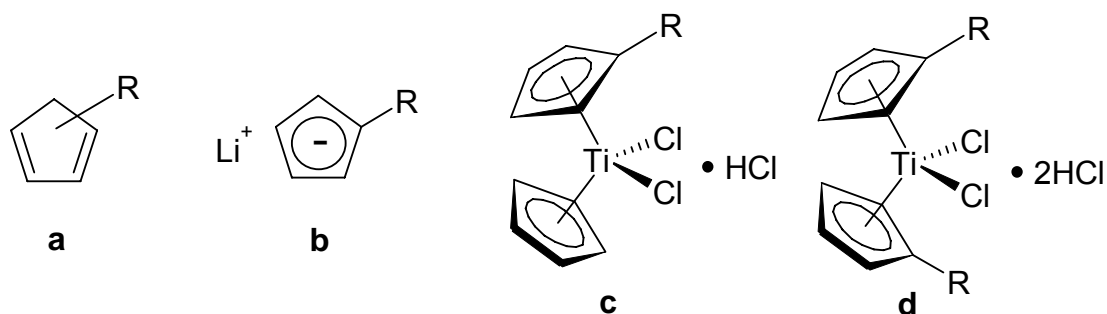


Figure 31 Labeling scheme for the molecules used in this research. R represents varying alkylammonia groups.

3.1 Synthesis of (1R, 2S)-N-Methylephedrine

Ephedrine is a controlled substance that is commercially available from Aldrich after much paperwork. The methylation of ephedrine was accomplished following the well established *Eschweiler-Clarke* method which has been previously described in the literature (Figure 32).¹¹⁵ A solution of (1R, 2S)-ephedrine in formalin (37% wgt formaldehyde in water, 13 molar equivalents) was treated with 25 molar equivalents of formic acid. The resulting solution was heated to reflux for 3 h. The resulting solution was cooled to room temperature

and basified using a solution of NaOH to pH=11. Isolation of the product was achieved through extraction using diethyl ether and subsequent solvent removal under reduced pressure. This reaction was performed several times and the product was always attained cleanly and in high yield (>98%). The identity of the product was confirmed by comparing its ^1H NMR spectrum (in CDCl_3) with literature data.¹²¹

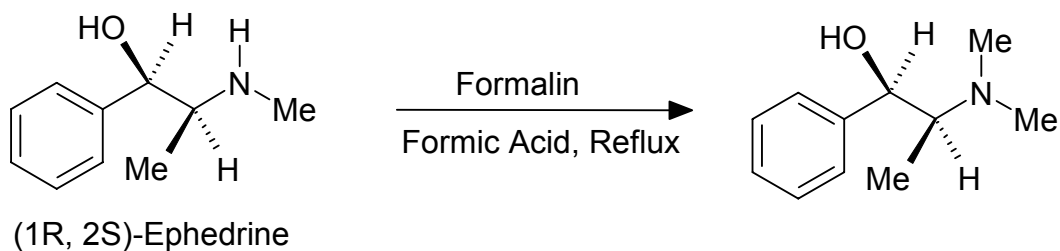


Figure 32 Preparation of (1R, 2S)-*N*-methylephedrine using formalin (37% wgt formaldehyde in water) and formic acid.

3.2 Chlorination of (1R, 2S)-*N*-Methylephedrine and Alaninol

The chlorination of (1R,2S)-*N*-methylephedrine was achieved following the method outlined in literature. Thionyl chloride (1.25 molar equivalents) was slowly added to a cold (0 °C) solution of (1R, 2S)-*N*-methylephedrine in anhydrous chloroform. The reaction mixture turned dark red while being left to stir for 12 hours. The solvent was removed *in vacuo* and the crude product was analyzed by ^1H NMR spectroscopy. The crude ^1H NMR spectrum showed that the product mixture consisted of two diastereomers (Figure 33) which is consistent with the literature.¹¹⁶ The (1S, 2S)-product was easily separated by recrystallization in a 3:1 mixture of diethylether: ethanol at -72 °C, giving an

isolated yield of 62%. The identity of the product was confirmed by comparing its ^1H NMR spectrum with data from the literature.^{116,117} The ^1H NMR data for **19** is shown in Table 1.

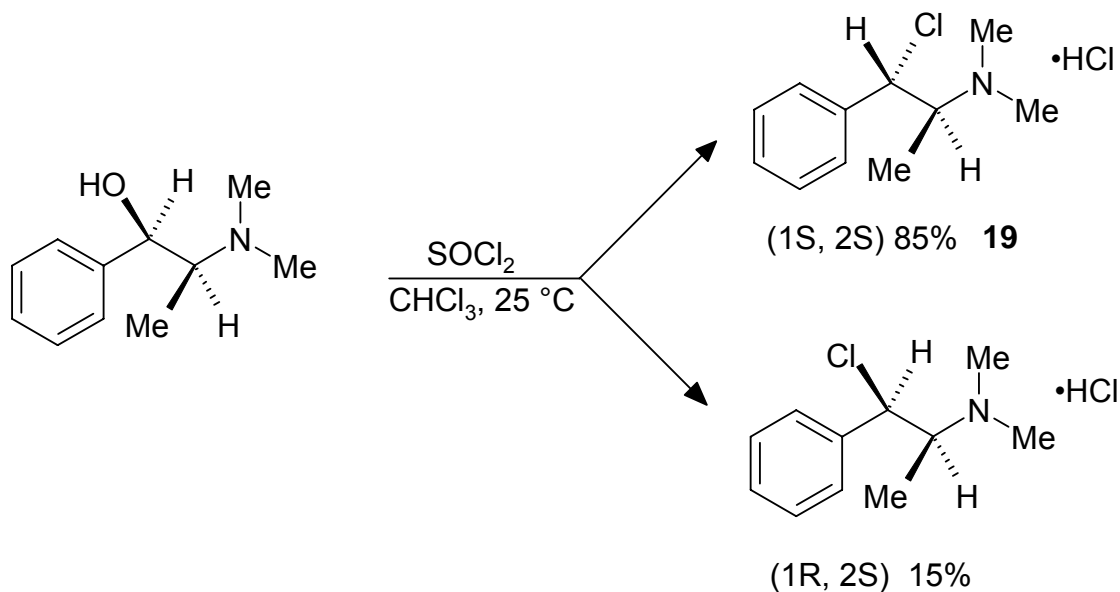


Figure 33 The chlorination of (1R, 2S)-*N*-methylephedrine using thionyl chloride resulted in the formation of the (1S, 2S) and (1R, 2S) diastereomers in a ratio of 85:15, respectively.

(R) and (S)-Alaninol were purchased from Ivy Fine Chemicals with an enantiomeric excess of >98% each. The chlorination of these alcohols was accomplished using a similar procedure to the one that was applied to *N*-methylephedrine.¹¹⁹ Thionyl chloride (1.5 equivalents) was added to a solution of (R) or (S)-alaninol in 250 mL of anhydrous chloroform (Figure 34). A catalytic amount of *N,N*-dimethylformamide was then added and the reaction mixture was slowly heated to $50\text{ }^\circ\text{C}$ and left to stir for 12 hours. The resulting solution was then put in a freezer at $-30\text{ }^\circ\text{C}$ which caused the immediate formation of a white

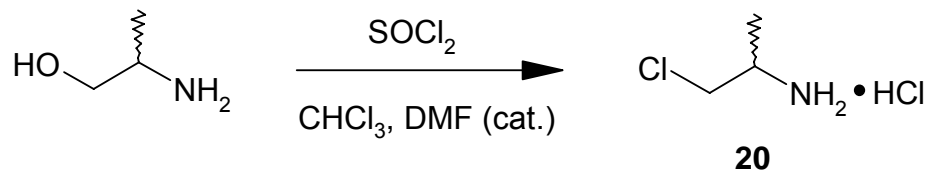


Figure 34 Chlorination of (S) and (R)-Alaninol.

precipitate. Isolation of the product by filtration gave yields of 89% and 91% for the (S) and (R) species, respectively. The identity of the products was confirmed by mass spectrometric analysis. The mass of the molecular ion (93), along with the 3:1 isotopic distribution pattern (M:M+2) is consistent with the (S and R)-1-chloropropyl-2-ammonium chloride (**20**). The ^1H NMR data for (S and R)-**20** is shown in Table 1.

Table 1 ^1H NMR data (δ), assignments for the hydrochloride salts **19**, **20**.

Product	^1H NMR Assignment/(ppm)
	7.54-7.43 (m, 5H, Ph), 5.32 (d, 1H, $^3J = 10.8$ Hz, 1), 4.15 (dq, 1H, $^3J = 10.8, 6.6$ Hz, 2), 3.04 and 2.93 (2 x s, 6H, 4), 1.10 (d, 3H, $^3J = 6.6$ Hz, 3)
	8.52 (s, 3H, 1), 3.86 (dd, 1H, $^2J = 11.4$ Hz, $^3J = 4.8$ Hz, 4), 3.82 (dd, 1H, $^2J = 11.4$ Hz, $^3J = 4.8$ Hz, 4'), 3.49 (m, 1H, 2), 1.27 (d, 3H, $^3J = 6.6$ Hz, 3)

3.2 Syntheses of Cyclic Aminoalkylcyclopentadienes (14a – 20a)

The general procedure to prepare the cyclic aminoalkylcyclopentadienes initially involved the conversion of cyclopentadiene to its conjugate base. In this form, sodium cyclopentadienide can readily react to form carbon-carbon bonds by nucleophilic substitution. Consequently, the treatment of sodium cyclopentadienide with a series of cyclic aminoalkyl chlorides resulted in the conversion to the desired ligands. A representative reaction scheme is outlined in Figure 35, and the substrates used are listed in Table 2.

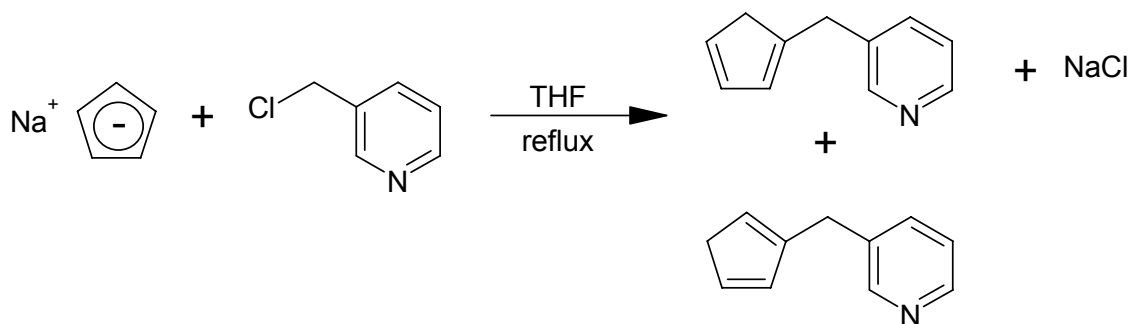
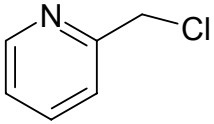
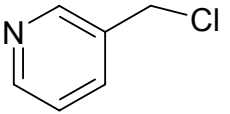
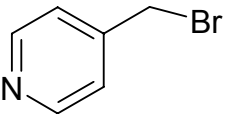
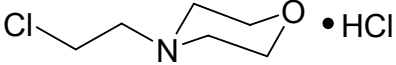
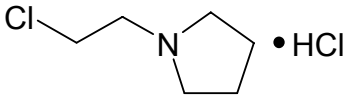
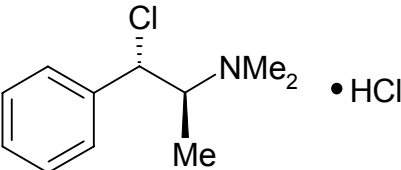
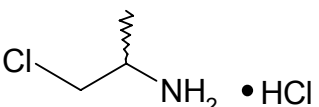


Figure 35 Representative reaction scheme for the synthesis of the cyclic aminoalkylcyclopentadiene, **15a**.

The picolyl chloride reactants (**14** – **16**) were received as hydrochloride salts and were initially converted to their free bases by treatment with one molar equivalent of sodium hydroxide in water. The aqueous solutions were then extracted with diethyl ether isolating the free bases. The isolated free bases were then slowly added to one molar equivalent of sodium cyclopentadienide in THF while stirring. After complete addition, the reaction mixtures were refluxed for 2 - 16 h. The reaction in THF generates the picolyl substituted

Table 2 Summary of reaction conditions used in the preparation of cyclic aminoalkyl-substituted cyclopentadienes (**14a – 20a**).

Product	Aminoalkane	NaCp	Reaction time	Yield
14a	 19.9 g, 156 mmol	2 M, 85.0 mL	16 h	13.2 g, 54.0%
15a	 19.6 g, 154 mmol	2 M, 80.0 mL	16 h	11.4 g, 46.8%
16a	 17.2 g, 100 mmol	2 M, 51.0 mL	2 h	9.53 g, 60.6%
17a	 10.2 g, 55.1 mmol	2 M, 55.1 mL	8 h	7.27 g, 73.6%
18a	 10.38 g, 61.0 mmol	2 M, 67.0 mL	12 h	6.56 g, 65.8%
19a	 19.11 g, 81.6 mmol	2.1 M, 200 mL	16h	14.8 g, 79.7%
(S)-20a (R)-20a	 (S) 34.3 g, 0.264 mol (R) 21.4 g, 0.165 mol	2.6 M, 300 mL 2.0 M, 250 mL	14h 14h	21.82 g, 67.1% 10.9 g, 53.7%

cyclopentadiene monomer and insoluble sodium chloride. Subsequent workup and isolation typically yielded the crude, picolyl substituted cyclopentadienes as amber coloured oils. Purification by vacuum distillation generated clear, colourless oils that were characterized by ^1H NMR spectroscopy.

In the preparation of the aminoalkyl substituted cyclopentadienes (**17a** – **18a**, (S) and (R)-**20a**), the hydrochloride salts of the aminoalkyl chlorides were used directly. This necessitated the use of two molar equivalents of sodium cyclopentadienide. All other reaction conditions and subsequent workups were similar to those mentioned above. The preparation of the ephedrine substituted cyclopentadiene (**19a**) followed a procedure outlined in the literature.¹¹⁷ A five fold excess of sodium cyclopentadienide was added to a mixture of **19** in anhydrous THF. The reaction mixture was left to stir for 16 hours at room temperature. Workup and isolation of the product yielded a brown oil which was used as is in subsequent reactions. Optimized reaction conditions and times for the preparation of all aminoalkylcyclopentadienes are summarized in Table 2.

Reaction between sodium cyclopentadienide and the aminoalkyl chlorides creates a new carbon-carbon bond and causes the once equivalent carbons in the cyclopentadienide anion to become non-equivalent. The initial cyclopentadiene regioisomer formed is the 1-substituted-2,4-cyclopentadiene (**A**), as illustrated in Figure 36. The regioisomer **A**, has been shown to undergo hydride rearrangements via 1,2-shift or 1,3-shifts to generate the 1-substituted-1,3-cyclopentadiene or 2-substituted-1,3-cyclopentadiene isomers, respectively.^{122,123} This equilibrium is common with cyclopentadiene derivatives

and the relative abundances of the different regioisomers have been shown to be temperature dependent.¹²³ Consequently, the preparation of the aminoalkyl-substituted cyclopentadienes always resulted in the formation of a mixture of isomers. A summary of the ¹H NMR data and assignments for the aminoalkylcyclopentadienes are shown in Table 3.

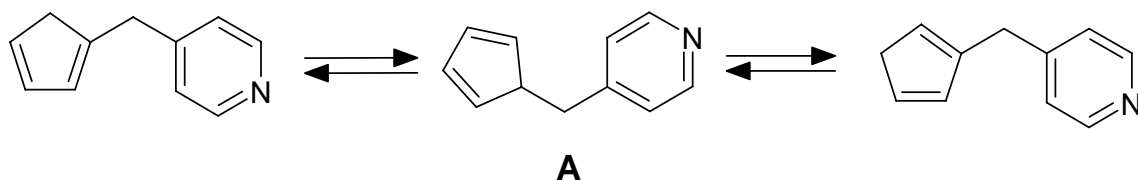


Figure 36 Equilibrium of the regioisomers of **17a**.

After purifying the cyclopentadiene derivatives by vacuum distillation, the resulting clear, colourless oils were analyzed using ¹H NMR spectroscopy and showed the presence of a mixture of regioisomers. Each of the synthesized cyclopentadiene derivatives (**14a** – **20a**) showed a distinctive resonance pattern in the olefinic region of the ¹H NMR spectrum, as shown as region **1** in Figure 37. The broad singlets, labeled as **2**, represent the saturated protons present within the cyclopentadiene ring. These singlets are another distinctive feature that is observed with each cyclopentadiene derivative that was prepared. The 4-picolyly substituted cyclopentadienes illustrated in Figure 37 have all the proton signals labeled and assigned. The protons ortho to the nitrogen (**5**) are represented by two doublets which are at a higher frequency than the meta protons (**4**) that are

also a pair of doublets. This is consistent with what has been previously reported for other para substituted pyridines.¹²⁴ The methylene protons (**3**) are observed

Table 3 Summary of ¹H NMR data (δ) for compounds **14a** – **20a**.

Product	¹ H NMR Assignment/(ppm)
	8.53 (m, 2H, 7), 7.57 (m, 2H, 5), 7.14 (m, 2H, 4), 7.09 (m, 2H, 6), 6.5-6.0 (m, 6H, 1), 3.93, 3.90 (2 x s, 4H, 3), 2.98, 2.91 (2 x s, 4H, 2)
	8.48 (2 x s, 2H, 7), 8.44 (2 x m, 2H, 6), 7.48 (2 x m, 2H, 4), 7.18 (2 x m, 2H, 5), 6.5-5.9 (m, 6H, 1), 3.71, 3.67 (2 x s, 4H, 3), 2.96, 2.83 (2 x s, 4H, 2)
	8.49 (m, 4H, 5), 7.11 (m, 4H, 4), 6.5-6.0 (m, 6H, 1), 3.71, 3.68 (2 x s, 4H, 3), 2.98, 2.83 (2 x s, 4H, 2)
	6.4-5.9 (m, 6H, 1), 3.66 (m, 8H, 6), 2.89, 2.85 (2 x s, 4H, 2), 2.56 (m, 4H, 4), 2.49 (m, 4H, 3), 2.38 (m, 8H, 5)
	6.5-6.0 (m, 6H, 1), 2.91, 2.87 (2 x s, 4H, 2), 2.60 (s, 4H, 4), 2.51 (s, 4H, 3), 2.49 (m, 8H, 5), 1.76 (m, 8H, 6)
	7.33-7.15 (m, 10H, Ph), 6.62-6.17 (m, 6H, 1), 3.80, 3.77 (2 x d, 2H, ³ J = 6.4 Hz, 3), 3.31 (m, 2H, 4), 2.99 (m, 4H, 2), 2.31 and 2.30 (2 x s, 12H, 6), 0.78 and 0.76 (2 x d, 6H, ³ J = 3.0 Hz, 5)
	6.43-6.08 (m, 6H, 1), 3.13 and 3.08 (2 x m, 2H, 4), 2.92 (m, 4H, 2), 2.46 (2 x dd, 2H, ² J = 15.0 Hz, ³ J = 5.4 Hz, 3), 2.33 (2 x dd, 2H, ² J = 15.0 Hz, ³ J = 7.8 Hz, 3'), 1.31 (s, 2H, 6), 1.10 (2 x d, ³ J = 6.0 Hz, 5)

as a pair of singlets. The overall yields of these reactions range from 46 – 74% where the majority of the product loss was from the purification by vacuum distillation. Because these cyclopentadiene derivatives may slowly undergo dimerization to form dicyclopentadienes, the derivatives were either used immediately or kept in the freezer.

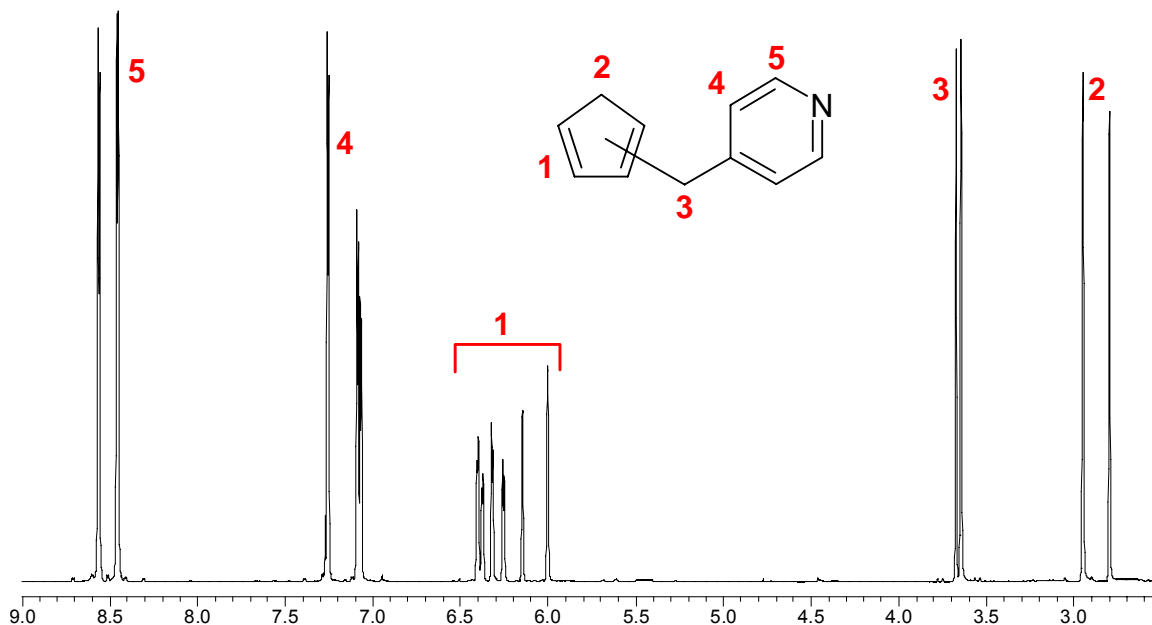


Figure 37 ¹H NMR spectrum of a picolyl-substituted cyclopentadiene (**17a**) in CDCl₃. The pattern between δ 6.5 – 5.9 ppm is characteristic for all aminoalkyl-cyclopentadienes in this series (**14a** – **20a**).

3.3 Results from the syntheses of Lithium Cyclic Aminoalkylcyclopentadienide salts (**14b** – **20b**)

The fact that there is a mixture of regioisomers from the preceding alkylation reaction is irrelevant because of the subsequent deprotonation reaction. Cyclopentadiene and its substituted derivatives have a pK_a ~ 16 and can be easily converted to the aromatic cyclopentadienide anions by using a

strong base.¹²⁵ Each of the purified aminoalkylcyclopentadienes were dissolved in cold hexanes and treated with methyllithium at 0 °C as shown in Figure 38. Methyllithium is a convenient base for this reaction since the byproduct methane bubbles out of the reaction mixture. This synthesis resulted in the formation of precipitates varying in colour from off-white to orange that were isolated by vacuum filtration and stored under an inert atmosphere in the glove box. Although air-sensitive, these lithium salts may be stored for months in an inert atmosphere with little to no apparent decomposition. The yields for this reaction were generally high, with some greater than 84%. A summary of the reaction conditions, yields as well as the ¹H and ¹³C NMR data for all of the lithium cyclic aminoalkylcyclopentadienides are shown in Table 4 and the lithium chiral aminoalkylcyclopentadienides are shown in Table 5.

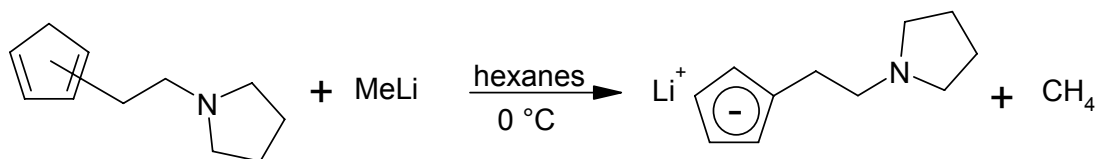


Figure 38 Representative reaction between methyllithium and a cyclic aminoalkylcyclopentadiene (**18a**) in hexanes at 0 °C which affords the air and water sensitive lithium salt **18b**.

The air and moisture sensitive lithium cyclic aminoalkylcyclopentadienide salts were dissolved in DMSO-*d*₆ or pyridine-*d*₅ for analysis by ¹H, ¹³C and 2-D NMR (COSY, HSQC and HMBC). All compounds (**14b** – **20b**) displayed signals between 6.50–5.10 ppm representing the four aromatic protons on the Cp ring. The signals representing protons 1 and 2 were resolved

Table 4 Summary of reaction conditions, yields and ^1H , ^{13}C NMR Data (δ) for the lithiated salts **14b** – **18b**.

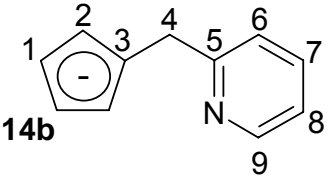
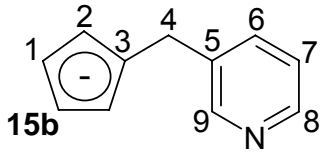
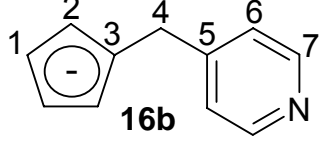
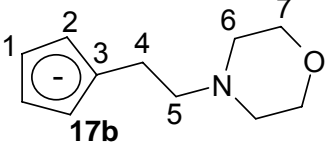
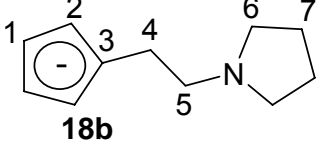
Product	Reagent, Base	Yield	^1H NMR Assignment/(ppm)	^{13}C NMR Assignment/(ppm)
 <p>14b</p>	<p>14a (2.32 g, 14.8 mmol), MeLi (1.6 M, 9.4 mL, 15.0 mmol)</p>	<p>2.03 g, 84.2%</p>	<p>8.30 (d, 1H, $^3J = 4.8$ Hz, 9), 7.51 (m, 1H, 7), 7.28 (d, 1H, $^3J = 7.8$ Hz, 6), 6.99 (m, 1H, 8), 5.20 (m, 4H, 1 and 2), 3.83 (s, 2H, 4)</p>	<p>166.4 (5), 147.5 (9), 135.0 (7), 123.1 (6), 119.4 (8), 114.6 (3), 103.6 (2), 102.8 (1), 40.9 (4)</p>
 <p>15b</p>	<p>15a (5.00 g, 31.8 mmol), MeLi (1.6 M, 20.0 mL, 32.0 mmol)</p>	<p>3.96 g, 76.2%</p>	<p>8.37 (s, 1H, 9), 8.22 (d, 1H, $^3J = 4.2$ Hz, 8), 7.54 (d, 1H, $^3J = 7.2$ Hz, 6), 7.15 (d of d, 1H, 7), 5.19 (m, 2H, 1), 5.16 (m, 2H, 2), 3.71 (s, 2H, 4)</p>	<p>149.7 (9), 145.2 (8), 141.9 (5), 135.7 (6), 122.6 (7), 115.7 (3), 103.1 (2), 102.8 (1), 35.2 (4)</p>
 <p>16b</p>	<p>16a (4.10 g, 26.0 mmol), MeLi (1.6 M, 16.5 mL, 26.4 mmol)</p>	<p>4.05 g, 95.4%</p>	<p>8.29 (d, 2H, $^3J = 6.0$ Hz, 7), 7.17 (d, 2H, $^3J = 6.0$ Hz, 6), 5.20 (m, 2H, 1), 5.17 (m, 2H, 2), 3.67 (s, 2H, 4)</p>	<p>155.5 (5), 148.5 (7), 124.1 (6), 114.4 (3), 103.2 (2), 102.9 (1), 37.3 (4)</p>
 <p>17b</p>	<p>17a (6.69 g, 37.3 mmol), MeLi (1.6 M, 23.3 mL, 37.3 mmol)</p>	<p>4.94 g, 71.6%</p>	<p>6.34 (m, 2H, 1), 6.26 (m, 2H, 2), 3.69 (m, 4H, 7), 3.02 (t, $^3J = 7.5$ Hz, 2H, 4), 2.80 (t, $^3J = 7.5$ Hz, 5), 2.46 (m, 4H, 6)</p>	<p>118.1 (3), 104.2 (2), 104.1 (1), 67.6 (7), 63.6 (4), 54.8 (6), 28.9 (5)</p>
 <p>18b</p>	<p>18a (6.56 g, 40.2 mmol), MeLi (1.6 M, 25.1 mL, 40.2 mmol)</p>	<p>4.58 g, 67.3%</p>	<p>6.32 (m, 2H, 1), 6.24 (m, 2H, 2), 3.02 (t, 2H, $^3J = 7.2$ Hz, 4), 2.79 (t, 2H, $^3J = 7.2$ Hz, 5), 2.45 (m, 4H, 6), 1.45 (m, 4H, 7)</p>	<p>117.9 (3), 104.7 (1), 103.6 (2), 61.6 (4), 54.7 (6), 30.9 (5), 24.1 (7)</p>

Table 5 Summary of reaction conditions, yields, and ^1H , ^{13}C NMR Data (δ) for the lithiated salts **19b** – **20b**.

Product	Reagent, Base	Yield	^1H NMR Assignment/(ppm)	^{13}C NMR Assignment/(ppm)
<p>19b</p>	<p>19a (11.31 g, 49.7 mmol), MeLi (1.6 M, 31.1 mL, 49.8 mmol)</p>	<p>10.53 g, 90.8%</p>	<p>7.313 (d, 2H, $^3J = 7.2$ Hz, 6), 7.142 (t, 2H, $^3J = 7.2$ Hz, 7), 7.005 (t, 1H, $^3J = 7.2$ Hz, 8), 5.355 (s, 2H, 2), 5.289 (s, 2H, 1), 3.762 (d, 1H, $^3J = 9.0$ Hz, 4), 3.022 (m, 1H, 9), 2.075 (s, 6H, 11), 0.718 (d, 3H, $^3J = 6.6$ Hz, 10)</p>	<p>148.2 (5), 128.8 (6), 127.1 (7), 124.1 (8), 120.7 (3), 102.4 (1), 101.6 (2), 64.4 (9), 51.8 (4), 40.7 (11), 11.2 (10)</p>
<p>(S)-20b, (R)-20b</p>	<p>(S)-20a (15.24 g, 123.7 mmol), MeLi (1.6 M, 77.5 mL, 124 mmol);</p> <p>(R)-20a (10.91 g, 88.6 mmol) MeLi (1.6 M, 55.4 mL, 88.6 mmol)</p>	<p>(S)-20b 14.80 g, 92.6%;</p> <p>(R)-20b 10.09 g, 88.2 %</p>	<p>5.200 (m, 2H, 1), 5.175 (m, 2H, 2), 2.650 (m, 1H, 5), 2.456 (dd, 1H, $^2J = -13.2$ Hz, $^3J = 4.2$ Hz, 4), 2.065 (dd, 1H, $^2J = -13.2$ Hz, $^3J = 8.4$ Hz, 4'), 0.934 (d, 3H, $^3J = 6.6$ Hz, 6)</p>	<p>115.5 (3), 103.4 (2), 102.4 (1), 49.2 (5), 43.1 (4), 23.9 (6)</p>

into two distinct multiplets in all of the salts except for **14b** which was represented as a single multiplet. These signals are typically seen as multiplets resulting from an AA'BB' spin system. However, it has been previously shown that trace amounts of water in the deuterated solvents can broaden the proton resonances of the Cp ring.¹¹⁸

A representative ¹H NMR spectrum of the lithiated salt **18b** dissolved in pyridine-*d*₅ is shown in Figure 39. The integrations of all of the signals accurately match the number of protons represented in each signal. The methylene protons **3** and **4** are clearly identified in the spectrum as triplets between 3.2 and 2.7 ppm, displaying a “roofing effect” towards each other. The identification of which triplet belonging to each methylene was accomplished using a ¹H – ¹H COSY

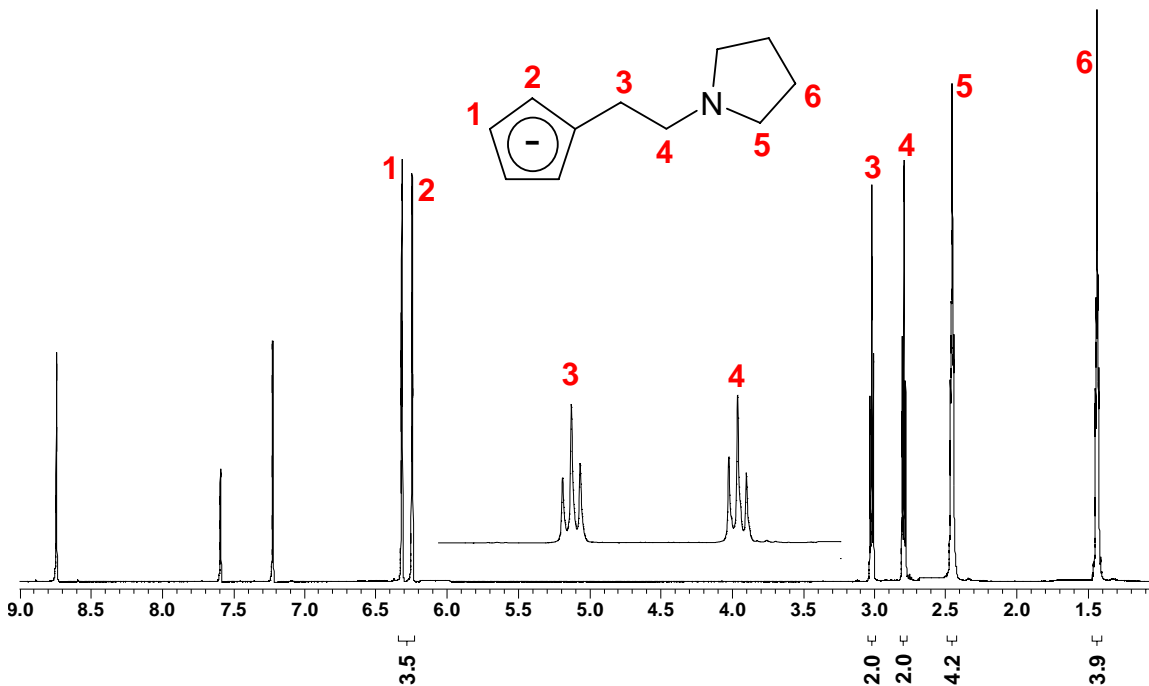


Figure 39 ¹H NMR spectrum of the lithiated salt **18b** in pyridine-*d*₅. The region between δ 3.1 – 2.7 is expanded to show the triplet splitting pattern.

experiment, where a correlation between protons **3** and **2** was observed. This correlation also clearly helped identify both protons **1** and **2**. An HMBC experiment illustrated a correlation between carbon **2** and protons **3**, providing further evidence for this assignment. The methylene groups within the pyrrolidine ring were observed as multiplets at 2.45 and 1.45 ppm with the methylenes adjacent to the nitrogen resonating at a higher frequency. All ^{13}C NMR chemical shift assignments were accomplished using the 2D correlation experiments HSQC and HMBC.

3.4 Results from the syntheses of monocationic titanocene dichloride analogues (14c – 20c)

In general, the synthesis of the monosubstituted TDC derivatives was achieved by the reaction of ($\eta^5\text{-Cp}$)titanium trichloride with the corresponding lithium aminoalkylsubstituted cyclopentadienide salt (**14b** – **20b**) in either THF or toluene as shown in Figure 40. One molar equivalent of a lithium salt was either dissolved in a polar, aprotic solvent such as THF or suspended in a non-polar solvent like toluene. Originally, a literature preparation was followed requiring the use of a non-polar solvent such as toluene to suspend the lithium salts.⁴⁸ However, the suspensions in toluene were only shown to be successful in the preparation of complexes **16c** and **19c**. Solubility problems in toluene appeared to hinder the reaction in preparing the other complexes, so a polar, aprotic solvent (THF) was used instead.

The synthesis of the monocationic complexes is a somewhat exothermic reaction and therefore was done in an ice bath to improve the reaction yields. Drop-wise addition of a 1.3 molar excess of (η^5 -Cp)titanium trichloride caused the clear, colourless solutions to turn dark red. Generally, a small amount of an off-white precipitate would form as the reaction proceeded. Monitoring the progress of the reaction using traditional methods such as thin layer chromatography (TLC) or NMR spectroscopy was impractical due to the highly reactive species in solution. Therefore, the reaction was usually left to stir for 1 h at 0 °C and allowed to warm to room temperature and stir for several hours after no further precipitate was formed to ensure completion. The reaction mixture was subsequently filtered to remove any precipitated lithium chloride.

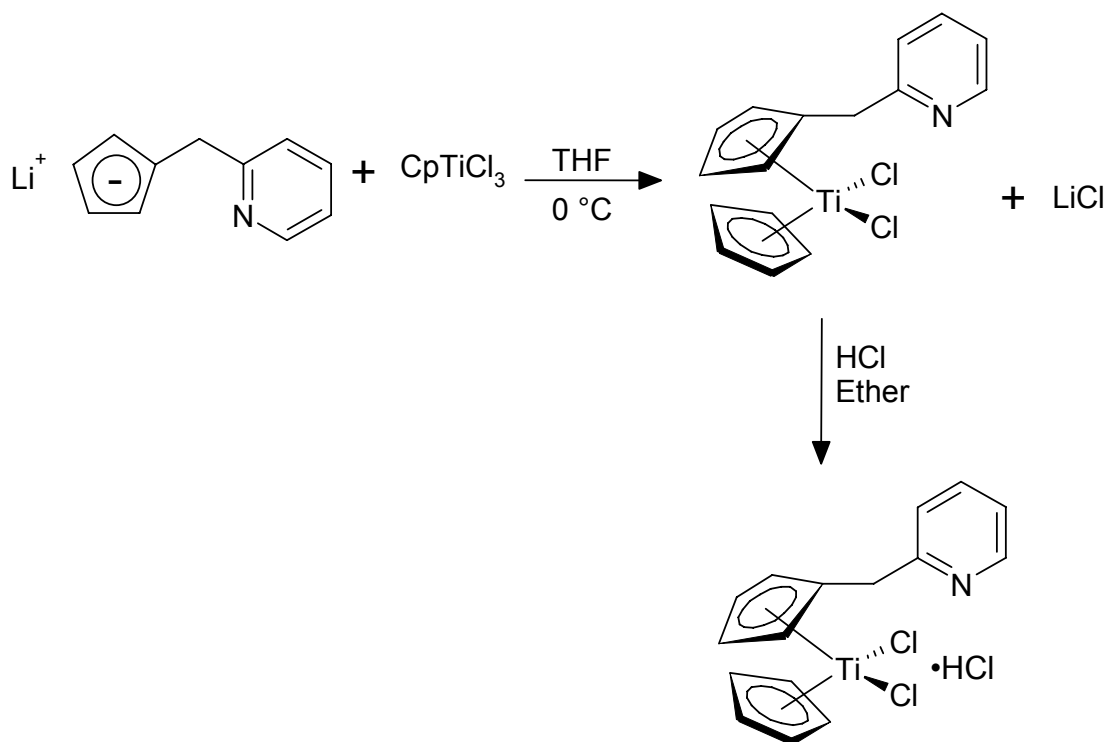


Figure 40 Representative reaction scheme for the synthesis of **14c**.

The TDC derivatives were not isolated in their “base” forms since these complexes have been shown to be highly reactive.^{126,127} The pendant amino-containing groups have been shown to undergo undesirable side reactions when left exposed to air. It has been suggested that the pendant amino group facilitates hydrolysis by enhancing the concentration of an attacking hydroxyl anion and by trapping hydrogen chloride.¹²⁸ Analogous complexes of this type have been used as novel catalysts in the polymerization of olefins and the amino groups have been shown to reversibly coordinate to the titanium centre.¹²⁹ Addition of hydrochloric acid would result in the protonation of the pendant nitrogen which would inhibit unwanted side reactions and dramatically change the physical properties of the complexes. Consequently, an excess of hydrochloric acid (2 M) in diethyl ether was added at room temperature to the complexes causing the immediate formation of dark red precipitates. Acid addition was continued until no further precipitate was formed. The precipitate was isolated by vacuum filtration and the colour of the supernatant was reflective of the amount of complex remaining in solution. In one particular case (**16c**), the supernatant led to the formation of crystals that were suitable for analysis by x-ray crystallography.

The complexes were further washed with non-polar solvents (diethyl ether) and handled under air. The crude products were then dissolved in a minimal amount of methanol, ethanol, or a combination of both. The red alcohol solutions were then reprecipitated in an excess of diethyl ether resulting in the formation of bright red powders. All products were dried under reduced pressure

in a drying pistol or an oven. A summary of all of the reaction conditions and yields is shown in Table 6. Overall, the reaction between (η^5 -Cp)titanium trichloride and a lithium aminoalkyl cyclopentadienide

Table 6 Summary of reaction conditions and yields for the generation of monocationic TDC complexes **14c** – **20c**.

Product	LiCp'/(g,mmol)	TiCpCl ₃	Yield
TiCp(C ₅ H ₄ CH ₂ C ₅ H ₃ N)Cl ₂ •HCl 14c	14b (0.932, 5.72)	1.30 g, 5.93 mmol	1.60 g, 74.4%
TiCp(C ₅ H ₄ CH ₂ C ₅ H ₃ N)Cl ₂ •HCl 15c	15b (0.796, 4.88)	1.51 g, 6.84 mmol	1.56 g, 84.9%
TiCp(C ₅ H ₄ CH ₂ C ₅ H ₃ N)Cl ₂ •HCl 16c	16b (0.787, 4.82)	1.32 g, 6.04 mmol	1.36 g, 74.7%
TiCp(C ₅ H ₄ CH ₂ CH ₂ N(CH ₂) ₄ O)Cl ₂ •HCl 17c	17b (0.603, 3.26)	0.955 g, 4.35 mmol	0.816 g, 62.9%
TiCp(C ₅ H ₄ CH ₂ CH ₂ N(CH ₂) ₄)Cl ₂ •HCl 18c	18b (0.498, 2.95)	0.647 g, 2.95 mmol	0.844 g, 71.8%
TiCp(C ₅ H ₄ CH(Ph)CH(CH ₃)NMe ₂)•HCl 19c	19b (0.764, 3.27)	0.806 g, 3.67 mmol	1.06 g, 72.4%
(S)-TiCp(C ₅ H ₄ CH ₂ CH(CH ₃)NH ₂)•HCl (S)- 20c	(S)- 20b (0.837, 6.48)	1.73 g, 6.48 mmol	1.76 g, 79.3%
(R)-TiCp(C ₅ H ₄ CH ₂ CH(CH ₃)NH ₂)•HCl (R)- 20c	(R)- 20b (0.866, 6.70)	1.85 g, 8.45 mmol	1.15 g, 84.4%

salt was straight forward resulting in respectable yields ranging from 72 – 85% with one particular yield being somewhat poor (63% for **17c**). The reaction

conditions were found to be optimal in THF as opposed to toluene. However, the use of a polar, aprotic solvent caused some reduction in yield as the final products were somewhat soluble in THF. Overall, this two step reaction was found to efficiently produce the corresponding monocationic TDC derivatives. The specific rotations of (S)-**20c** and (R)-**20c** were measured in DMSO at $\lambda = 633$ nm and found to be -29.1° and $+28.4^\circ$, respectively. These values confirm that they are in fact, enantiomers of each other. All of the structures of the prepared monocationic derivatives are shown in Figure 41. The characterization of the monocationic complexes using ^1H and ^{13}C NMR spectroscopy, mass spectrometry, elemental analysis and X-ray crystallography will be discussed below.

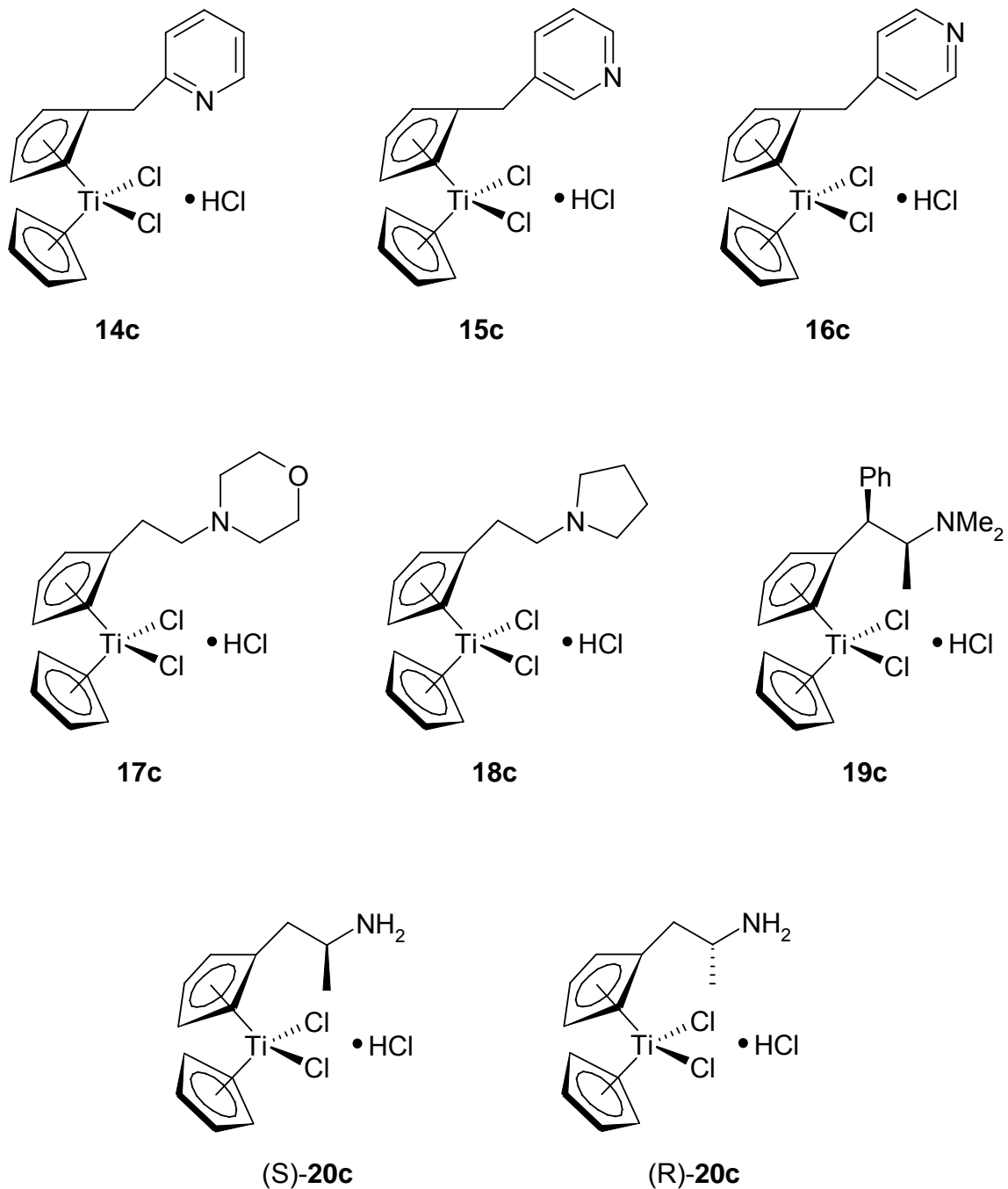


Figure 41 Structures of the monocationic aminoalkylsubstituted TDC derivatives (**14c – 20c**)

3.5 Results for the syntheses of the dicationic titanocene dichloride analogues (14d – 20d)

The preparation of the dicationic TDC derivatives followed an analogous procedure as the one employed for the monocationic derivatives and is illustrated in Figure 42. Two molar equivalents of the appropriate lithium aminoalkylcyclopentadienide salt was dissolved in THF or suspended in toluene at 0 °C. One molar equivalent of titanium tetrachloride (as a 1 M solution in toluene) was then slowly added dropwise causing the colour of the reaction mixture to turn dark red. The preparation of the complexes **14d**, **15d** and **17d – 20d** proceeded with the appearance of a small amount of an off-white precipitate (LiCl) over the next 2 – 4 hours of stirring. The reaction mixture was then filtered to remove the lithium chloride. The resulting dark red solution was then treated with an excess of hydrochloric acid in diethyl ether (2 M) causing the formation of a dark red precipitate. The precipitate was isolated by vacuum filtration and washed with diethyl ether. The crude products were dissolved in methanol, ethanol, or a mixture of both and reprecipitated in an excess of diethyl ether. The resulting bright red powders could now be handled under air and were dried under reduced pressure in a drying pistol or oven.

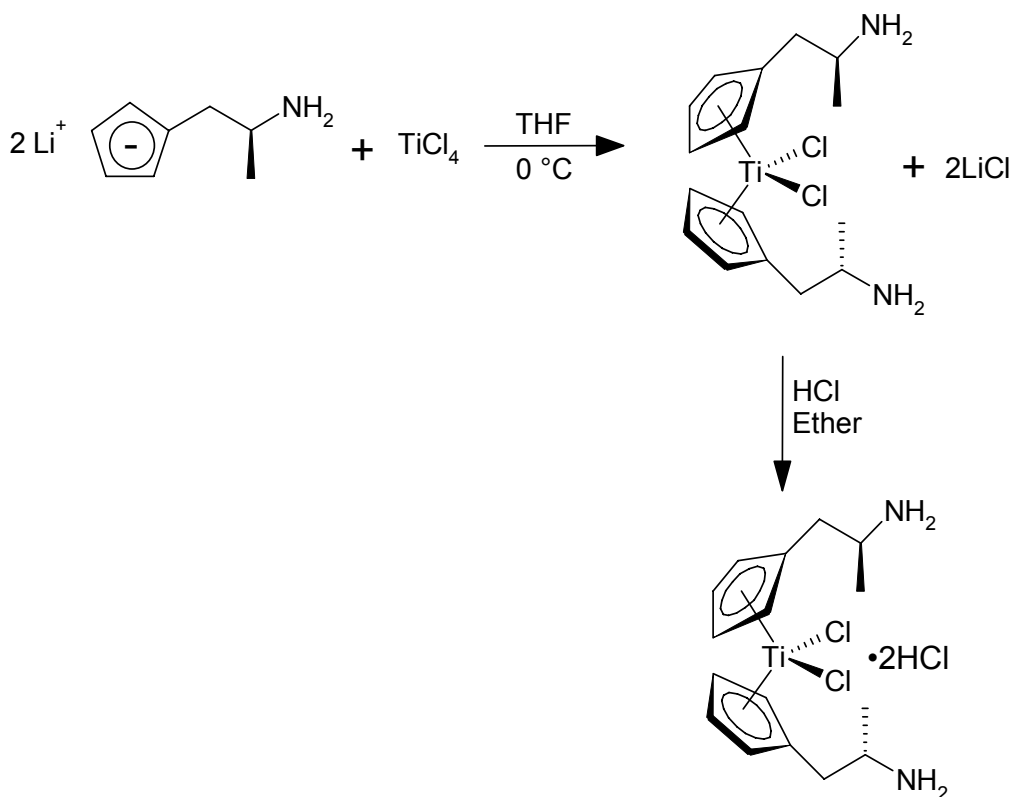


Figure 42 Representative reaction scheme for the preparation of (S,S)-**20d**.

The complex Mix-**20d** is composed of a mixture of stereoisomers consisting of equal amounts of (S,S), (R,S), (S,R) and (R,R)-**20d** as shown in Figure 43. The enantiomeric pair, (S,S)-**20d** and (R,R)-**20d**, exhibit identical physical properties while (S,R)-**20d** and (R,S)-**20d** are identical since the complex is meso. The synthesis of Mix-**20d** [containing 1:2:1 of (S,S):(R,S):(R,R)-**20d**] was accomplished by initially preparing a solution of one molar equivalents of (S)-**20b** and (R)-**20b** in THF at 0°C. The resulting solution was then treated with one molar equivalent of titanium tetrachloride and all subsequent handling followed the method outlined above.

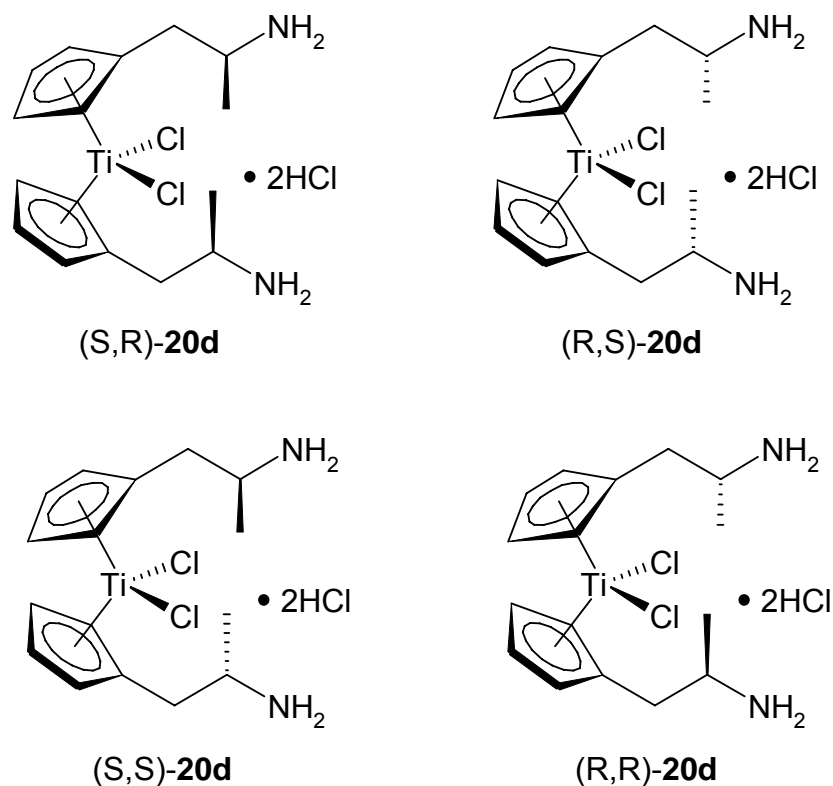


Figure 43 The four possible stereoisomers of complex **20d** present in (Mix)-**20d**.

The synthesis of the dicationic complex **16d** deviated significantly from the other complexes. A dark brown precipitate formed upon the addition of titanium tetrachloride to the lithium aminoalkylcyclopentadienide salt **16b**. The reaction mixture had a pale orange colour when it was left to settle, indicating very little to no product dissolved in THF. The mixture was filtered, isolating the brown precipitate which was then analyzed by ^1H NMR spectroscopy identifying the product as the “base form” of the titanocene derivative **16d**. This precipitate is most likely the result of a coordination polymer which is consistent with what has been observed in other titanocene analogues of this type.⁹³ The complex was

dissolved in methanol and treated with an excess of hydrochloric acid in diethyl ether (2M) to ensure complete conversion to the hydrochloride salt **16d**. The resulting dark red methanol solution was added to an excess of diethyl ether causing the formation of a bright red precipitate that was isolated and dried. The structures of all of the prepared dicationic TDC derivatives are shown in Appendix A.

The syntheses of the dicationic TDC analogues were relatively straightforward except in the preparation of **16d**. The majority of the syntheses of the dicationic complexes were very successful with yields ranging from 64 – 96 %. One noted exception was in the preparation of **18d** which resulted in a yield of 49%. This particular poor yield is attributed to the solubility problems associated with doing the reaction in toluene. All of the abovementioned monocationic and dicationic complexes were recrystallized in an effort to fully characterize the derivatives by X-ray crystallography and elemental analyses. Only two monocationic and two dicationic complexes generated crystals that were suitable for crystallographic analyses, although all complexes provided crystals that were suitable for elemental analyses.

The complexes (S,S)-**20d**, (R,R)-**20d** and Mix-**20d** were prepared in order to study the effect of chirality on cytotoxic activity. Therefore, it was important to measure the specific rotations of these complexes to demonstrate that they were enantiomers of each other. Enantiomeric compounds rotate the plane of polarized light by exactly the same amount, but in opposite directions. The specific rotations of (S,S)-**20d** and (R,R)-**20d** were measured in DMSO at $\lambda =$

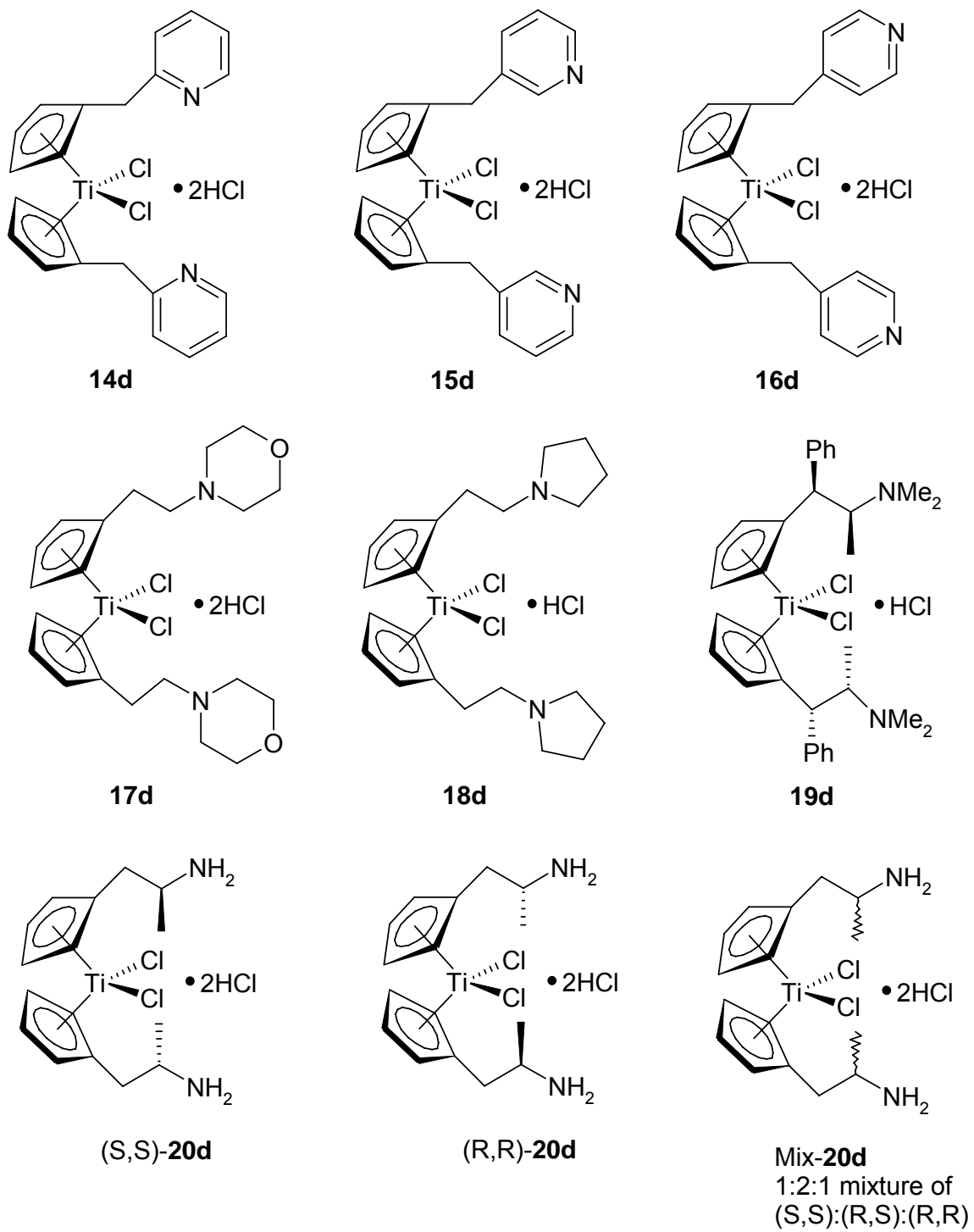


Figure 44 Structures of the dicationic aminoalkylsubstituted TDC derivatives (14d – 20d).

633 nm and found to be -39.4° and $+39.2^\circ$, respectively; confirming that they were indeed enantiomers of each other. The product **Mix-20d** was expected to be a statistical mixture of (S,S):(R,S):(R,R) in a ratio of 1:2:1. The specific rotation of this mixture was expected to be 0° considering there is an equal molar amount of the enantiomers (S,S) and (R,R), effectively canceling each other out. Moreover, the (R,S) isomer is a meso compound and would not display any optical activity. After isolation, the specific rotation of the product (**Mix-20d**) was measured in DMSO at $\lambda = 633$ nm and found to be 0° confirming the ratio of stereoisomers present. A summary of the reaction conditions and yields for the syntheses of the dicationic TDC complexes is outlined in Table 7. Characterization of the dicationic complexes using ^1H and ^{13}C NMR spectroscopy, mass spectrometry, elemental analysis and X-ray crystallography will be discussed below.

Table 7 Summary of reaction conditions and yields for the generation of dicationic TDC complexes **14d** – **20d**.

Product	LiCp'/(g, mmol)	TiCl ₄	Yield
Ti(C ₅ H ₄ CH ₂ C ₅ H ₃ N) ₂ Cl ₂ •2HCl 14d	14b (0.837, 5.13)	1 M, 2.6 mmol	1.02 g, 78.1%
Ti (C ₅ H ₄ CH ₂ C ₅ H ₃ N) ₂ Cl ₂ •2HCl 15d	15b (0.538, 3.30)	1 M, 1.8 mmol	0.756 g, 83.3%
Ti (C ₅ H ₄ CH ₂ C ₅ H ₃ N) ₂ Cl ₂ •2HCl 16d	16b (0.828, 5.08)	1M, 2.6 mmol	1.13 g, 88.2%
Ti(C ₅ H ₄ CH ₂ CH ₂ N(CH ₂) ₄ O) ₂ Cl ₂ •2HCl 17d	17b (0.856, 4.62)	1 M, 2.3 mmol	1.22 g, 95.6%
Ti(C ₅ H ₄ CH ₂ CH ₂ N(CH ₂) ₄) ₂ Cl ₂ •2HCl 18d	18b (0.929, 5.50)	1 M, 2.8 mmol	0.693 g, 48.8%
Ti(C ₅ H ₄ CH(Ph)CH(CH ₃)NMe ₂) ₂ •2HCl 19d	19b (0.971, 4.16)	1 M, 2.1 mmol	0.857 g, 63.9%
(S,S)-Ti(C ₅ H ₄ CH ₂ CH(CH ₃)NH ₂) ₂ •2HCl (S,S)- 20d	(S)- 20b (0.993, 7.69)	1 M, 3.8 mmol	1.16 g, 70.0%
(R,R)-Ti(C ₅ H ₄ CH ₂ CH(CH ₃)NH ₂) ₂ •2HCl (R,R)- 20d	(R)- 20b (1.08, 8.38)	1 M, 4.2 mmol	1.23 g, 67.1%
Mix-Ti(C ₅ H ₄ CH ₂ CH(CH ₃)NH ₂) ₂ •2HCl 1:2:1 of (S,S):(R,S):(R,R)- 20d	(R)- 20b (0.404, 3.12) (S)- 20b (0.410, 3.17)	1 M, 3.1 mmol	1.22 g, 89.7%

3.6 Characterization by NMR Spectroscopy of the monocationic titanocene dichloride complexes **14c** – **20c**.

This library of TDC salts shows remarkable solubility in polar solvents. They were dissolved in deuterated water or deuterated dimethylsulfoxide for analysis by ^1H , ^{13}C and 2-D (COSY, HSQC and HMBC) NMR spectroscopy. The majority of the analyses were performed in $\text{DMSO-}d_6$ since this solvent was shown to give the sharpest peaks. The proton NMR spectra for all of the complexes displayed a clear singlet that has been assigned to the resonances on the unsubstituted Cp ring. In all cases, the singlet appeared between 6.75 – 6.53 ppm and integrated to approximately 5 protons. This range of values is consistent with those that have been reported for similar complexes.^{48,49}

As with the lithium cyclopentadienide salts, the proton resonances of the substituted Cp ring are expected to be a pair of multiplets integrating to two protons each between δ 6.3 – 7 ppm. A representative ^1H NMR spectrum of the monocationic titanocene derivative **16c** dissolved in $\text{DMSO-}d_6$ is illustrated in Figure 45. The integrations of all of the signals accurately match the number of protons represented in each signal. Protons **1** and **2** on the substituted Cp ligand are represented by the triplets shown in the inset between 6.4 – 6.9 ppm. A correlation between protons **2** and **4** was observed using $^1\text{H} - ^1\text{H}$ COSY spectroscopy. This correlation helped identify which triplet belonged to which proton. The unsubstituted Cp ligand is represented by the singlet **8**, integrating to five protons. Protons **6** and **7** on the pyridine ring are represented by two

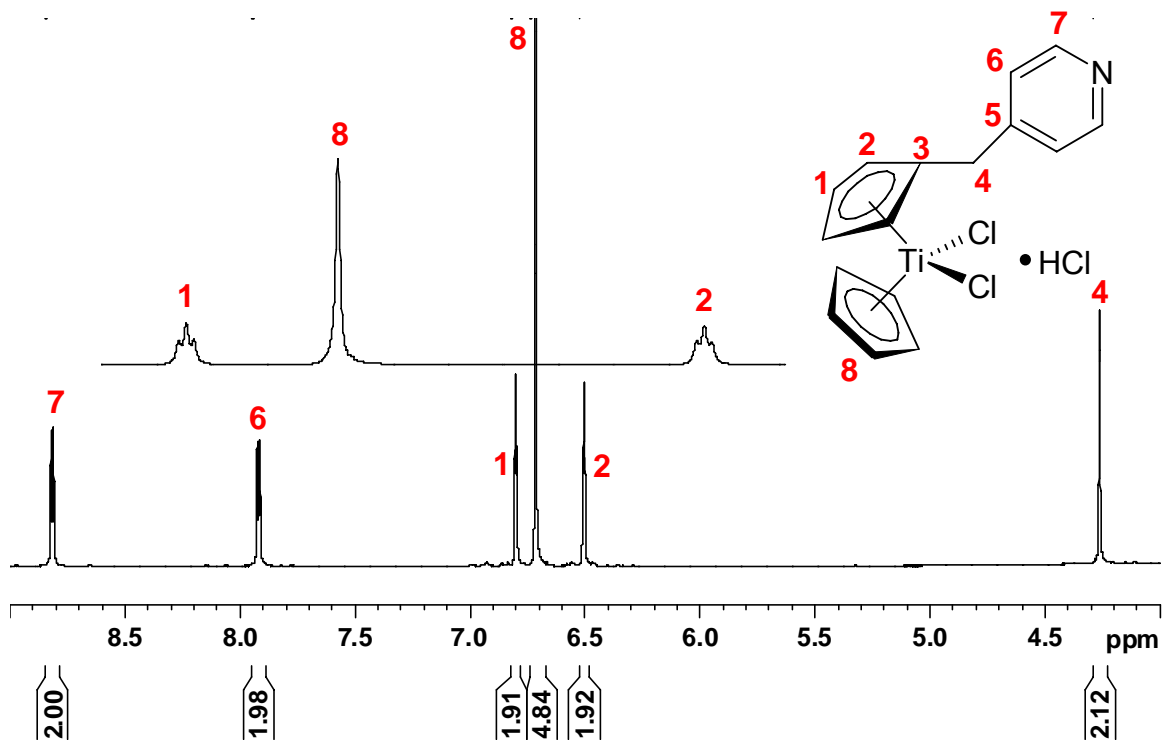


Figure 45 ^1H NMR spectrum of the titanocene derivative **16c** in $\text{DMSO-}d_6$. The region between δ 6.4 – 6.9 ppm is expanded to show the triplets on the substituted Cp ring.

doublets between 7.8 – 9 ppm with the protons adjacent to the nitrogen resonating at a higher frequency. The ^1H and ^{13}C assignment of all of the cyclic monocationic analogues (**14c** – **18c**) was relatively straightforward aided by the correlation experiments, HSQC and HMBC. A summary of the ^1H and ^{13}C NMR data and assignments for the cyclic titanocene derivatives is shown in Table 8.

Table 8 ^1H and ^{13}C NMR Data (δ) for titanocene derivatives (**14c** – **18c**).

Product	^1H NMR Assignment/(ppm)	^{13}C NMR Assignment/(ppm)
<p>14c</p>	<p>8.77 (d, 1H, $^3J = 4.2$ Hz, 9), 8.40 (m, 1H, 7), 7.87 (d, 1H, $^3J = 7.2$ Hz, 6), 7.82 (m, 1H, 8), 6.79 (m, 2H, 1), 6.75 (s, 5H, 10), 6.65 (m, 2H, 2), 4.38 (s, 2H, 4)</p>	<p>155.0 (5), 145.1 (7), 142.5 (9), 130.7 (3), 126.8 (6), 124.6 (8), 123.9 (2), 120.7 (10), 116.5 (1), 34.5 (4)</p>
<p>15c</p>	<p>8.68 (d, 1H, $^3J = 6.0$ Hz, 8), 8.62 (s, 1H, 9), 8.45 (d, 1H, $^3J = 7.8$ Hz, 6), 8.02 (d of d, 1H, 7), 6.66 (s and m, 7H, 1, 10), 6.54 (s, 2H, 2), 4.09 (s, 2H, 4)</p>	<p>148.2 (6), 141.4 (9), 140.5 (5), 140.1 (8), 136.9 (3), 127.9 (7), 119.7 (10), 119.2 (1), 117.6 (2), 32.6 (4)</p>
<p>16c</p>	<p>8.82 (d, 2H, $^3J = 6.6$ Hz, 7), 7.92 (d, 2H, $^3J = 6.6$ Hz, 6), 6.80 (m, 2H, 1), 6.72 (s, 5H, 8), 6.51 (m, 2H, 2), 4.26 (s, 2H, 4)</p>	<p>159.7 (5), 141.7 (7), 132.1 (3), 127.1 (6), 123.8 (2), 120.5 (8), 116.5 (1), 36.2 (4)</p>
<p>17c</p>	<p>6.66 (2 x s, 7H, 1 and 8), 6.50 (m, 2H, 2), 4.12, 3.81 (2 x m, 4H, 7), 3.54, 3.21 (2 x m, 4H, 6), 3.41 (t, $^3J = 7.2$ Hz, 5), 2.96 (t, $^3J = 7.2$ Hz, 4)</p>	<p>135.9 (3), 119.5 (8), 118.3 (1), 117.5 (2), 64.4 (7), 56.6 (5), 52.5 (6), 24.3 (4)</p>
<p>18c</p>	<p>6.63 (2 x s, 7H, 1 and 8), 6.50 (s, 2H, 2), 3.61, 3.06 (2 x m, 4H, 6), 3.40 (t, 2H, $^3J = 7.2$ Hz, 5), 2.90 (t, 2H, $^3J = 7.2$ Hz, 4), 2.11, 1.96 (2 x m, 4H, 7)</p>	<p>135.1 (3), 118.7 (8), 117.8 (1), 116.7 (2), 54.3 (6), 54.0 (5), 25.8 (4), 22.6 (7)</p>

Complexes **19c**, (S)-**20c** and (R)-**20c** contain chiral centres in the pendant alkylammonium side chain. These particular complexes generate some very interesting NMR spectra. The chiral centres in **19c** cause the methyl groups of the protonated N-(CH₃)₂ to be diastereotopic (non-equivalent) as shown in Figure 46. Protonation of the nitrogen prevents free exchange from occurring which causes the methyls to be diastereotopic. Furthermore, since there is a chiral

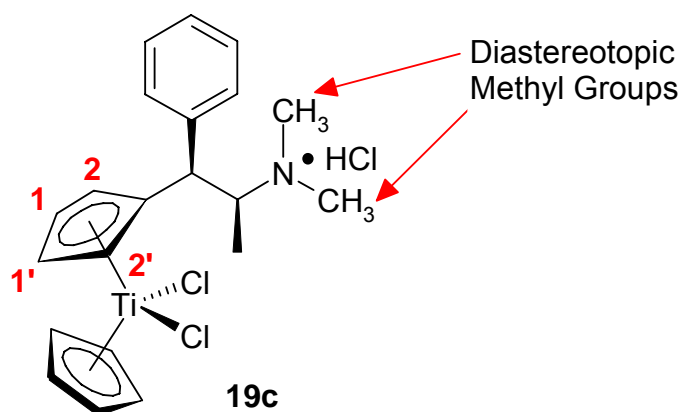


Figure 46 Structure of the chiral complex **19c** showing the diastereotopic N,N-methyls and diastereotopic methines on the substituted Cp ring.

centre α to the Cp ring, all of the methines on the Cp ring also are non-equivalent. This resulted in the appearance of four separate signals representing protons **1** and **2**. The ¹H NMR spectrum of **19c** in D₂O is shown in Figure 47 with all of the signals assigned. All the integrations of the signals accurately represent the corresponding number of protons that they represent. The diastereotopic methyls bonded to the nitrogen (**11**) were represented by a pair of singlet resonances at δ 2.95 and 2.75 ppm. The resonances for the diastereotopic methyls were separated by 0.20 ppm; this is quite a bit different to

the reported separation for diastereotopic methyls (0.03 ppm) of the previously reported chiral TDC analogue, **7**.⁴⁸

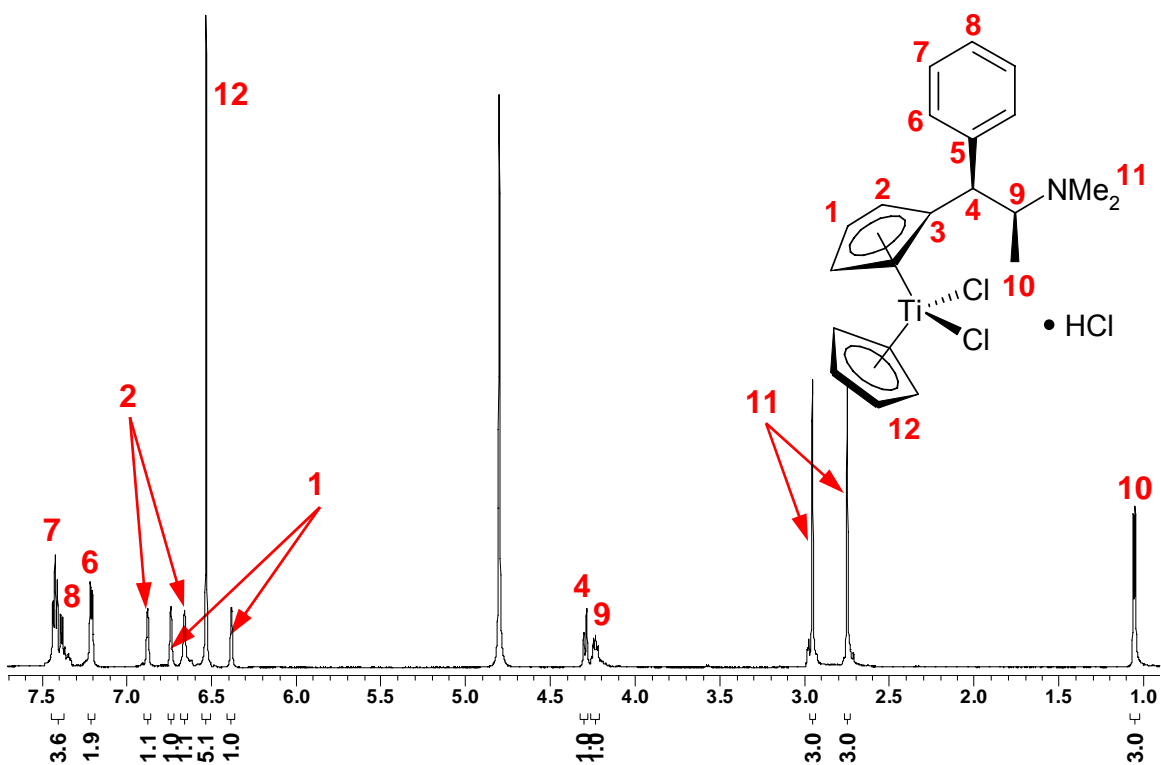


Figure 47 ¹H NMR spectrum and full assignment of **19c** showing the diastereotopic methine protons on the Cp ring and diastereotopic N,N-dimethyl proton resonances.

All other proton assignments were relatively straightforward, excluding the methine protons on the substituted Cp ring. The complete assignment of the methine protons (**1** and **2**) required a two-dimensional ¹H – ¹H correlation experiment (COSY) performed at high field (600 MHz) as shown in Figure 49. The differentiation between protons **1** and **2** could only be established by examining the correlations associated with neighbouring protons (Figure 48).

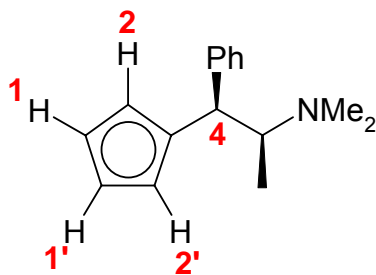


Figure 48 The substituted Cp ligand of **19c** illustrating three and four bond coupling.

In COSY spectra, protons that are separated by 3 bonds (3J) exhibit strong cross peaks (circled red), while protons that are separated by 4 (4J) or more bonds show weaker cross peaks (circled blue) in Figure 49. Protons **1** and **1'** were expected to have two strong correlations (3J , **1** – **2** and **1** – **1'**) and one weak correlation (4J , **1** – **2'**). On the other hand, protons **2** and **2'** are expected to have one strong correlation (3J , **2** – **1**) and two weak correlations (4J , **2** – **1'** and **2** – **2'**). These cross peaks identified proton **1** as the signals at 6.88 and 6.66 ppm and proton **2** as the signals at 6.74 and 6.38 ppm. Protons **1**, **1'** and **2**, **2'** could not be differentiated from each other using COSY experiments. An HMBC experiment showed long range coupling between carbons **2**, **2'** with proton **4** which also confirms the assignment of the methine protons.

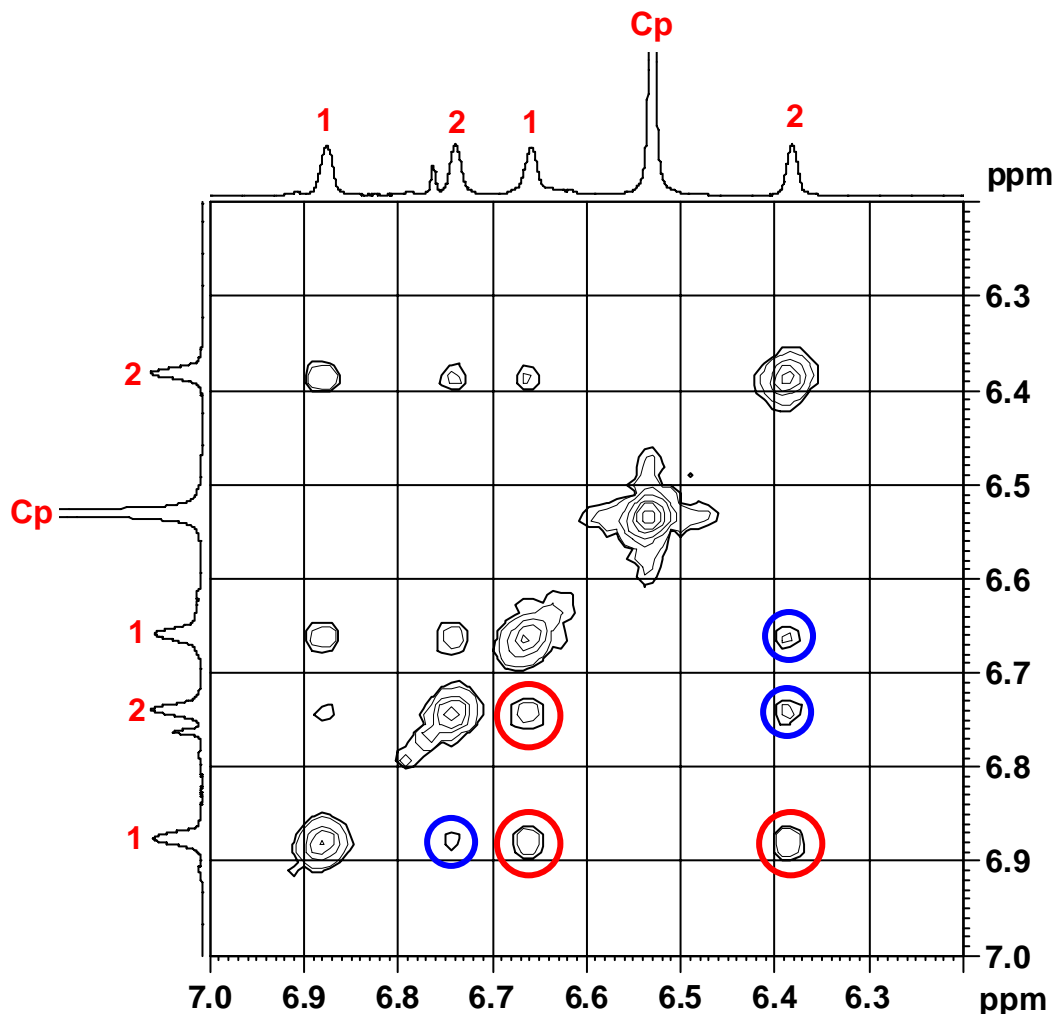


Figure 49 2D $^1\text{H} - ^1\text{H}$ COSY spectrum of **19c** in D_2O between 6.2 – 7.0 ppm. Red and blue circles denote ^3J and ^4J coupling, respectively.

Further analysis using ^{13}C NMR spectroscopy revealed a similar result. The ^{13}C NMR spectrum of **19c** had 15 signals that could only be explained by the appearance of diastereotopic carbons. The carbons associated with the two pairs of methines on the Cp ring and the pair of methyls bonded to the nitrogen showed chemical shift non-equivalence (Figure 50). A $^1\text{H} - ^{13}\text{C}$ single bond correlation (HSQC) experiment was used to fully assign all carbons bearing

protons, whereas a $^1\text{H} - ^{13}\text{C}$ multi-bond correlation (HMBC) experiment was used in order to assign all quaternary carbons. The methyls bonded to the nitrogen were assigned to the pair of signals that appeared at 42.6 and 36.4 ppm. Carbons **1** and **2** on the Cp ring were assigned to the signals appearing at 118.9, 114.4 and 119.7, 117.7, respectively. One of the singlets representing carbon **1** was overlapping the unsubstituted Cp ring. All of the proton and carbon-13 NMR assignments for complexes **19c**, (S)-**20c** and (R)-**20c** are displayed in Table 9. The enantiomers, (S)-**20c** and (R)-**20c**, of course, exhibited identical ^1H and ^{13}C NMR spectra.

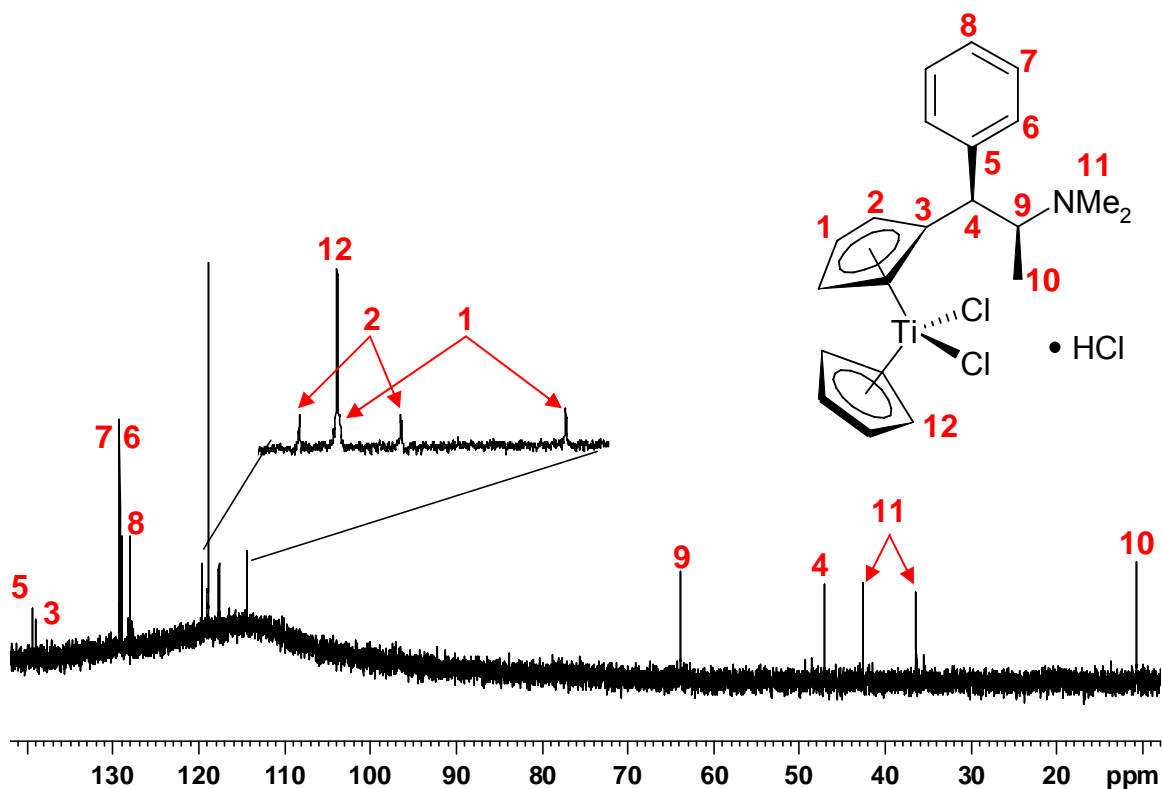


Figure 50 ^{13}C NMR spectrum of **19c** illustrating the three pairs of diastereotopic carbons.

Table 9 ^1H and ^{13}C NMR Data (δ) for titanocene derivatives (**19c** – **20c**).

Product	^1H NMR Assignment/(ppm)	^{13}C NMR Assignment/(ppm)
<p>19c</p>	7.42 (t, 2H, $^3J = 7.2$ Hz, 7), 7.38 (t, 1H, $^3J = 7.2$ Hz, 8), 7.21 (d, 2H, $^3J = 7.2$ Hz, 6), 6.88 and 6.66 (2 x s, 2H, 1), 6.74 and 6.38 (2 x s, 2H, 2), 6.53 (s, 5H, 12), 4.29 (d, 1H, $^3J = 10.2$ Hz, 4), 4.24 (m, 1H, 9), 2.95 and 2.75 (2 x s, 6H, 11), 1.05 (d, 3H, 3J = 6.0 Hz, 10)	139.4 (5), 138.9 (3), 129.2 (7), 129.0 (6), 128.1 (8), 119.7 and 117.7 (2), 118.9 and 114.4 (1), 118.9 (12), 63.9 (9), 47.1 (4), 42.6 and 36.4 (11), 10.7 (10)
<p>(S)-20c, (R)-20c</p>	8.19 (s, 3H, 7), 6.80 and 6.78 (2 x m, 2H, 1), 6.68 (s, 5H, 8), 6.43 (m, 2H, 2), 3.37 (m, 1H, 5), 3.05 (dd, 1H, 2J = -13.8 Hz, $^3J = 5.4$ Hz, 4), 2.77 (dd, 1H, $^2J = -13.8$ Hz, $^3J = 8.7$ Hz, 4'), 1.14 (d, 3H, $^3J = 6.6$ Hz, 6)	131.1 (3), 125.1 and 124.8 (2), 120.2 (8), 115.9 and 115.8 (1), 47.4 (5), 35.6 (4), 18.0 (6)

3.7 NMR spectroscopic characterization of the dicationic titanocene dichloride complexes **14d** – **20d**.

The proton and carbon-13 NMR spectra of the dicationic aminoalkyl substituted TDC derivatives were extremely similar to those of the monocationic analogues. The absence of the strong singlet representing the protons associated with the Cp ring at $\sim \delta$ 6.60 ppm was the most pronounced difference. A representative ^1H NMR spectrum for the cyclic alkylammonium TDC analogues (**14d**) is shown in Figure 51. The integrations of the signals accurately represent

the numbers of protons associated with each signal. The resonances for the eight protons on the Cp rings typically appeared as multiplets. The AA'BB' spin coupling system on the substituted Cp expectantly display multiplet spin coupling patterns, although in most cases even at high field (600 MHz), the multiplets were not well resolved. Complete assignment of the proton signals was aided by $^1\text{H} - ^1\text{H}$ COSY spectra and was relatively straightforward.

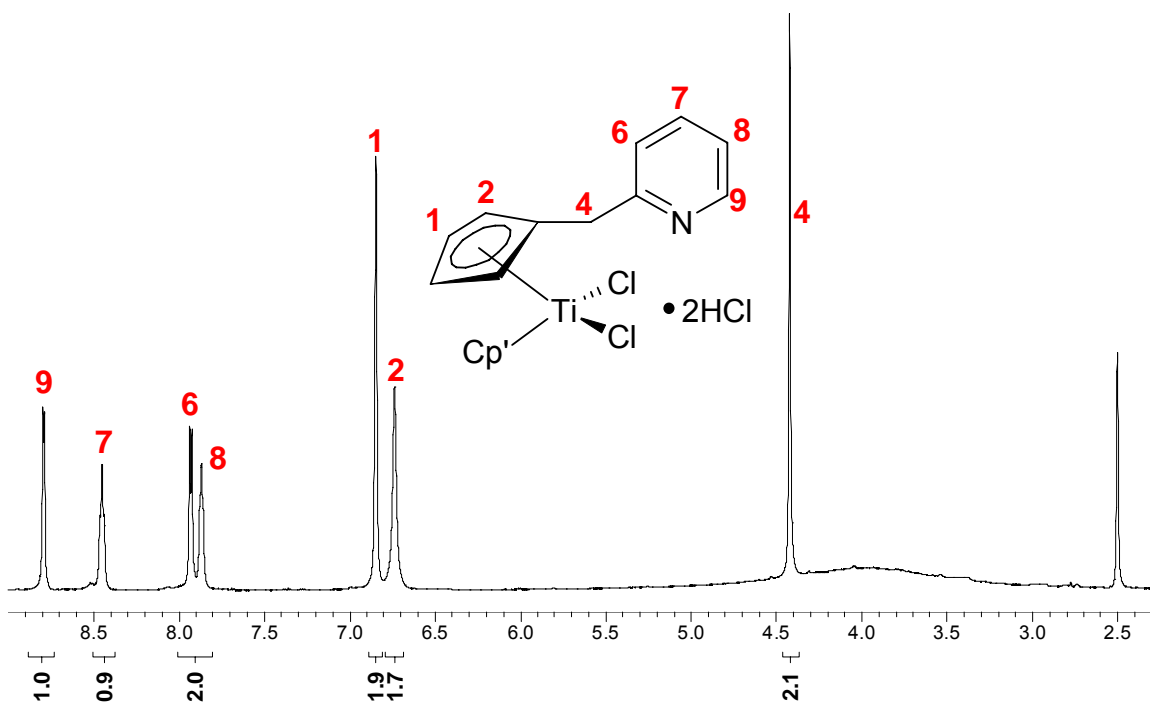


Figure 51 ^1H NMR spectrum of **14d** in $\text{DMSO-}d_6$ with all labeled assignments.

A complete summary of all proton and carbon-13 resonance assignments for the cyclic alkylammonium substituted titanocene complexes (**14d** – **18d**) is shown in Table 10. A comparison between the ^1H NMR spectra of all the monocationic and dicationic complexes revealed that the resonances of the

methine, methylene and methyl protons had the same coupling patterns and varied in chemical shift by less than 0.05 ppm. In addition, the resonances of the signals in the ^{13}C NMR spectra differed by less than 1 ppm when comparing the monocationic and dicationic complexes.

As with the monosubstituted complexes, the chiral alkylammonium dicationic analogues (**19d** and **20d**) provided interesting NMR spectra. A representative example of the ^1H NMR spectrum of (R,R)-**20d** is shown in Figure 52. The (S,S) enantiomer of **20d** displayed exactly the same NMR spectrum as (R,R)-**20d**, as expected. All of the integrations accurately represent the number

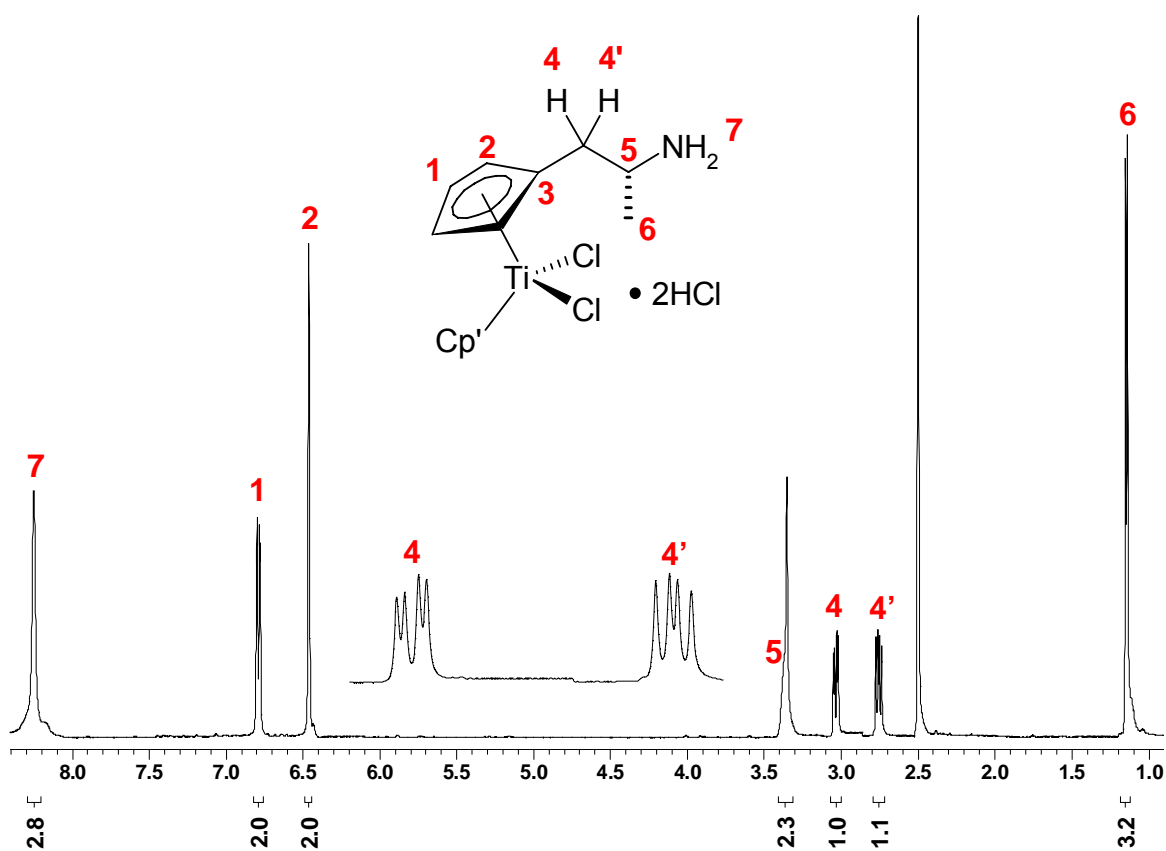


Figure 52 ^1H NMR spectrum of (R,R)-**20d** in $\text{DMSO-}d_6$ illustrating the diastereotopic protons **4** and **4'**.

of protons represented by the resonances except for the signal of proton **5**. The discrepancy in this particular integration is attributed to the presence of water in the sample. The protons associated with water have been shown to resonate at 3.33 ppm in DMSO- d_6 which overlaps with the signal representing proton **5**.¹³⁰ Water is frequently observed in the ^1H NMR spectra of these complexes because of their hygroscopic nature.

The presence of a chiral centre on carbon **5** caused the protons on carbon **4** to become chemically non-equivalent, or diastereotopic. Consequently, protons **4** and **4'** appear as a pair of doublet of doublets. The chiral centre also causes all of the methines on the Cp ring to be diastereotopic. The protons on carbon **1** appear as a pair of multiplets, while protons **2** appear to overlap even at

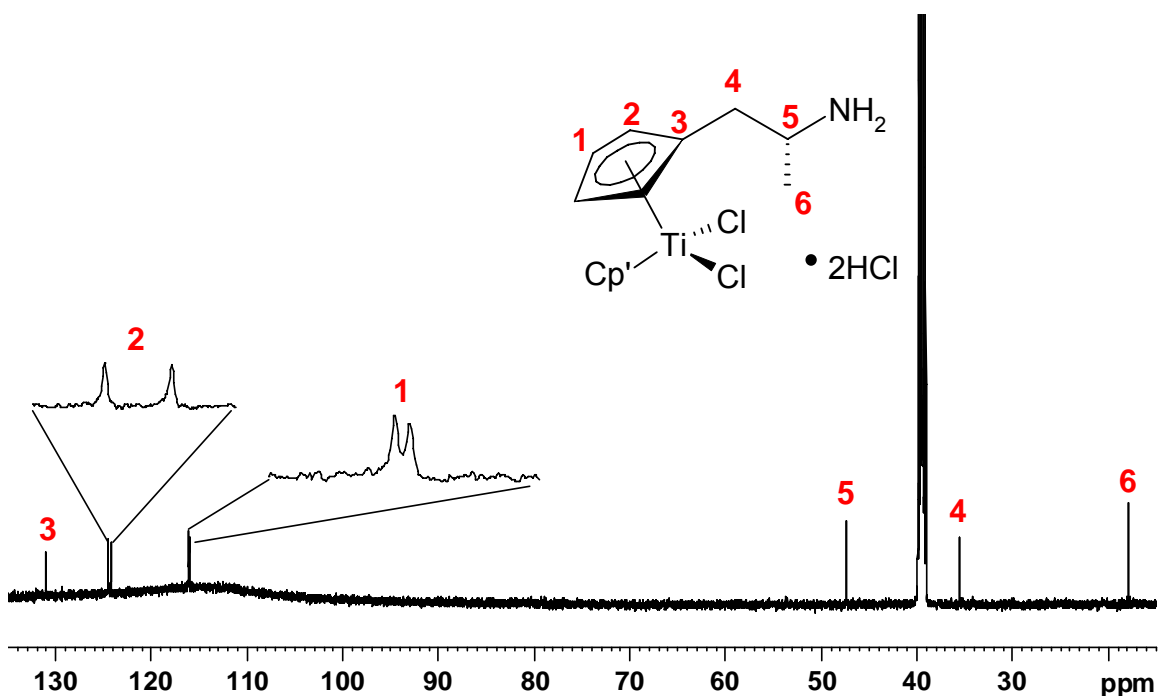


Figure 53 ^{13}C NMR spectrum of (R,R)-**20d** with insets illustrating the diastereotopic carbons on the Cp ring.

high field (600 MHz). However, in the ^{13}C NMR spectrum all four carbons on the Cp ring are magnetically non-equivalent and well resolved as shown in Figure 53. All of the proton and carbon-13 NMR data and assignments for the chiral complexes (**19d** – **20d**) are listed in Table 11.

The mixture of complexes, (Mix)-**20d**, was prepared by the reaction of an equimolar amounts of the lithium aminoalkyl substituted cyclopentadienide salts (R)-**20b** and (S)-**20b** with titanium tetrachloride. The resulting product mixture was expected to contain an equal amount of the following stereoisomers: (S,R), (R,S), (S,S) and (R,R) as illustrated in Figure 43. The stereoisomers, (S,R) and (R,S), are identical since the complex is meso and would be represented by one set of resonances. Similarly, the pair of enantiomers, (S,S) and (R,R) should exhibit the same proton resonances although, the two pairs of diastereomers should exhibit different NMR spectra.

Table 11 ^1H and ^{13}C NMR Data (δ) for titanocene derivatives (**19d** – **20d**).

Product	^1H NMR Assignment/(ppm)	^{13}C NMR Assignment/(ppm)
<p>19d</p>	7.43 (t, 4H, $^3J = 7.8$ Hz, 7), 7.39 (t, 2H, $^3J = 7.2$ Hz, 8), 7.23 (d, 4H, $^3J = 7.2$ Hz, 6), 6.52 and 6.39 (2 x s, 4H, 2), 6.43 and 5.95 (2 x s, 4H, 1), 4.30 (d, 2H, $^3J = 9.6$ Hz, 4), 4.07 (m, 2H, 9), 2.92 and 2.75 (2 x s, 12H, 11), 1.04 (d, 6H, $^3J = 6.6$ Hz, 10)	138.3 (5), 135.6 (3), 129.3 (6), 129.1 (7), 128.5 (8), 121.9 and 114.0 (1), 120.5 and 118.6 (2), 64.8 (9), 47.0 (4), 43.0 and 36.6 (11), 10.6 (10)
<p>(R,R)-20d, (S,S)-20d</p>	8.29 (s, 6H, 7), 6.79 and 6.77 (2 x m, 4H, 1), 6.46 (m, 4H, 2), 3.37 (m, 2H, 5), 3.04 (dd, 2H, $^2J = -13.8$ Hz, $^3J = 5.1$ Hz, 4), 2.76 (dd, 2H, $^2J = -13.8$ Hz, $^3J = 8.4$ Hz, 4'), 1.15 (d, 6H, $^3J = 6.0$ Hz, 6)	131.0 (3), 124.5 and 124.2 (2), 116.1 and 116.1 (1), 47.4 (5), 35.6 (4), 17.9 (6)
<p>(Mix)-20d</p>	8.34 (s, 6H, 8), 6.80 and 6.77 (2 x m, 4H, 1), 6.46 (m, 4H, 2), 3.36 (m, 2H, 5), 3.04 (dd, $^2J = 14.1$ Hz, $^3J = 5.1$ Hz, 2H, 4), 2.76 (m, 4'), 1.15 (d, $^3J = 6.6$ Hz, 6)	131.10 and 131.08 (3), 124.5 124.4 124.1 124.0 (2), 116.6 116.3 116.2 116.1 (1), 47.4 (5), 35.6 (4), 17.9 (6)
<p>(S,R)-20d</p>	8.34 (s, 6H, 8), 6.80 and 6.77 (2 x m, 4H, 1), 6.46 (m, 4H, 2), 3.36 (m, 2H, 5), 3.04 (dd, $^2J = -14.1$ Hz, $^3J = 5.1$ Hz, 2H, 4), 2.75 (dd, 2H, $^2J = -13.8$, $^3J = 9$ Hz, 4'), 1.15 (d, $^3J = 6.6$ Hz, 6)	131.08 (3), 124.4 and 124.0 (2), 116.6 and 116.3 (1), 47.4 (5), 35.6 (4), 17.9 (6)

The ^1H NMR spectrum of (Mix)-**20d** was measured in $\text{DMSO-}d_6$ and the data is reported in Table 11. A comparison between the ^1H NMR data of (R,R)-**20d** and (Mix)-**20d** showed striking similarities. The chemical shifts of protons that can hydrogen bond, such as those in ammonium groups, are sensitive to solvent conditions and can vary.¹²⁴ Aside from the difference in chemical shifts of the signals representing the protons on the ammonium group (~ 8.3 ppm), the only noticeable difference between the two spectra is with one of the diastereotopic protons (**4'**).

Even at high field (600 MHz), the splitting pattern of proton **4'** in the (Mix)-**20d** was not well resolved. In order to better resolve these signals, the free induction decays were processed using Gaussian Multiplication with a negative line broadening (LB) value of -2 Hz and a Gaussian broadening value of 0.13. A negative LB value has the effect of narrowing the signal lines and results in a significant resolution enhancement.¹³¹ This enhancement comes at the expense of the signal to noise ratio and, consequently, integrations of the peaks become meaningless. By processing the free induction decay of the (Mix)-**20d** NMR data the signal representing proton **4'** resolves into a pair of discernible doublet of doublet (dd) patterns (Figure 54, **b**) of equal intensity. Each doublet of doublet patterns must represent proton **4'** in either (R,R)/(S,S)-**20d** or (R,S)-**20d**. The equal intensity of the patterns also suggest that there is an equal amount of (R,R)/(S,S) and (R,S) stereoisomers. A comparison of the (Mix)-**20d** splitting pattern with the pattern generated by processing (R,R)-**20d** using identical conditions (Figure 54, **a**) clearly identifies the peaks belonging to (R,R)-**20d** in the

mixture. The remaining peaks labeled with red asterisks, were therefore assigned to (R,S)-**20d**. From this comparison, the chemical shifts of proton **4'** for both the (R,R)-**20d** and (R,S)-**20d** were determined to be 2.76 ppm and 2.75 ppm, respectively. The ^{13}C NMR assignment for (R,S)-**20d** was determined by the comparing the spectra of (R,R)-**20d** with (Mix)-**20d**.

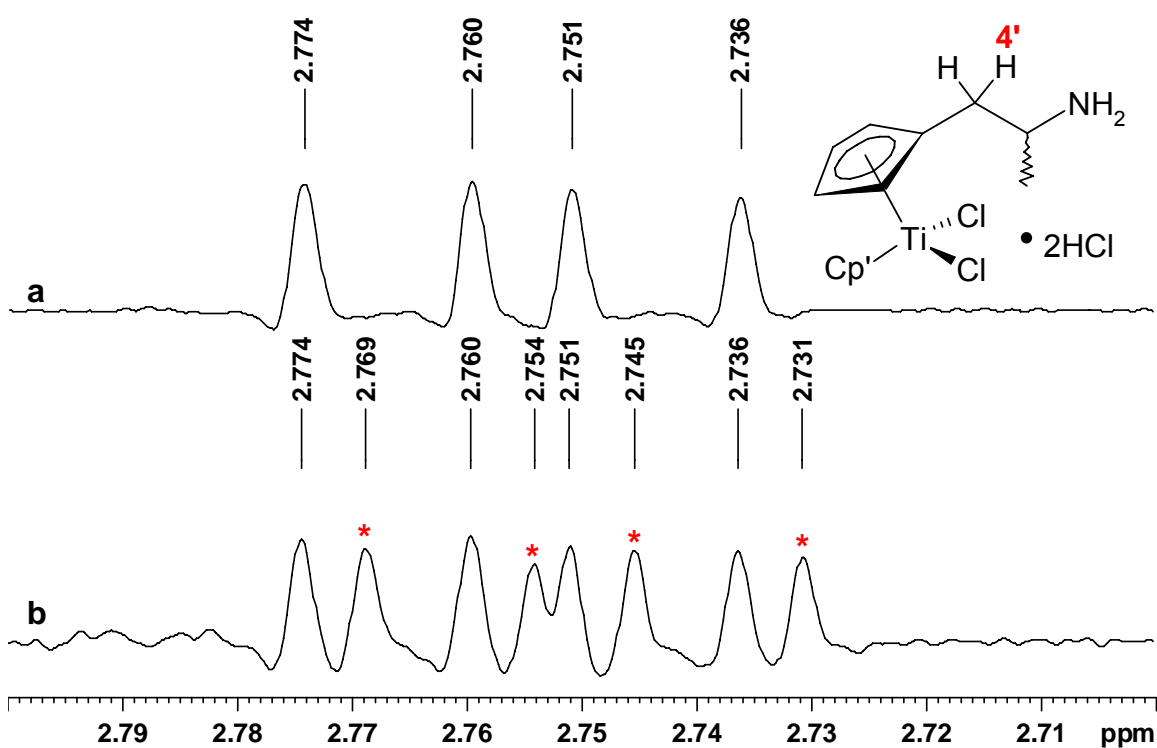


Figure 54 Comparison of the ^1H NMR signals of **4'** in (R,R)-**20d** (a) and (Mix)-**20d** (b) spectra. The red asterisks represent the peaks assigned to **4'** in (R,S)-**20d**.

3.8 Characterization of mono- and dicationic complexes (14c,d – 20c,d) by elemental analysis.

All of the mono- and dicationic TDC analogues were analyzed by elemental analysis to further characterize and verify the purity of the complexes. These hydrochloride salts were found to be hygroscopic. Although all of the complexes were dried in a drying pistol or an evacuated oven, a majority of them showed the presence of water by infrared analysis (IR). For those derivatives shown to contain water (by IR analysis), the expected elemental percentages reflected the inclusion of molecules of water. The results from the analyses of the monocationic (14c – 20c) and dicationic (14d – 20d) derivatives are shown in Table 12 and Table 13, respectively.

Table 12 Elemental analytical data for monocationic complexes 14c – 20c.

Complex, Molecular Formula	Elemental Analysis / %	H ₂ O present in IR
14c C ₁₆ H ₁₆ NTiCl ₃	Calc'd: C 51.04; H 4.28; N 3.72 Found: C 50.60; H 4.42; N 3.61	No
15c C ₁₆ H ₁₆ NTiCl ₃	Calc'd: C 51.04; H 4.28; N 3.72 Found: C 50.90; H 4.29; N 3.71	No
16c C ₁₆ H ₁₆ NTiCl ₃	Calc'd: C 51.04; H 4.28; N 3.72 Found: C 50.94; H 4.43; N 3.80	No
17c C ₁₆ H ₂₂ NOTiCl ₃ •H ₂ O	Calc'd: C 46.13; H 5.81; N 3.36 Found: C 45.78; H 5.52; N 3.71	Yes
18c C ₁₆ H ₂₂ NTiCl ₃	Calc'd: C 50.23; H 6.06; N 3.66 Found: C 50.55; H 5.57; N 4.40	No
19c C ₂₁ H ₂₆ NTiCl ₃ •H ₂ O	Calc'd: C 54.28; H 6.07; N 3.03 Found: C 54.29; H 5.93; N 2.95	Yes
(S)-20c C ₁₃ H ₁₈ NTiCl ₃ •½H ₂ O	Calc'd: C 44.42; H 5.16; N 4.35 Found: C 44.18; H 5.01; N 4.35	Yes
(R)-20c C ₁₃ H ₁₈ NTiCl ₃ •½H ₂ O	Calc'd: C 44.42; H 5.16; N 4.35 Found: C 44.59; H 5.33; N 4.11	Yes

Table 13 Elemental analytical data for dicationic complexes **14d – 20d**.

Complex, Molecular Formula	Elemental Analysis / %	H ₂ O present in IR
14d C ₂₂ H ₂₂ N ₂ TiCl ₄	Calc'd: C 52.42; H 4.40; N 5.56 Found: C 52.19; H 4.46; N 5.34	No
15d C ₂₂ H ₂₂ N ₂ TiCl ₄	Calc'd: C 52.42; H 4.40; N 5.56 Found: C 51.72; H 4.34; N 5.51	No
16d C ₂₂ H ₂₂ N ₂ TiCl ₄	Calc'd: C 52.42; H 4.40; N 5.56 Found: C 51.66; H 4.30; N 5.39	No
17d C ₂₂ H ₃₄ N ₂ O ₂ TiCl ₄ •2H ₂ O	Calc'd: C 45.23; H 6.56; N 4.79 Found: C 44.37; H 6.31; N 4.78	Yes
18d C ₂₂ H ₃₄ N ₂ TiCl ₄ •H ₂ O	Calc'd: C 49.46; H 6.79; N 5.24 Found: C 48.87; H 6.76; N 5.36	Yes
19d C ₃₂ H ₄₂ N ₂ TiCl ₄ •2H ₂ O	Calc'd: C 56.49; H 6.81; N 4.12 Found: C 56.63; H 6.67; N 4.01	Yes
(S,S)-20d C ₁₆ H ₂₆ N ₂ TiCl ₄ •2½H ₂ O	Calc'd: C 39.94; H 6.49; N 5.82 Found: C 39.93; H 6.11; N 5.50	Yes
(R,R)-20d C ₁₆ H ₂₆ N ₂ TiCl ₄ •2½H ₂ O	Calc'd: C 39.94; H 6.49; N 5.82 Found: C 39.41; H 5.85; N 5.39	Yes

3.9 Characterization of Mono- and Dicationic derivatives (14c,d – 20c,d) by Mass Spectrometric Analysis.

Another method of routine characterization for the mono- and dicationic complexes was analysis by mass spectrometry. All samples were prepared by dissolving the complexes in either dichloromethane or nitromethane with 1% methanol. A small amount of methanol was needed for each sample to help dissolve the complexes. A notable exception was the dicationic derivatives, **(S,S)-20d** and **(R,R)-20d**, which were instead analyzed in 100% methanol due to difficulties in solubility. The complexes were all analyzed using electrospray

mass spectrometry (ES-MS) and molecular ions were consequently observed as $[M+H]^+$ ions (where M represents the neutral or unprotonated complex). Upon analysis, the vast majority of the complexes produced observable amounts of the molecular ion. A couple notable exceptions to this were the dicationic complexes **14d**, (R,R)-**20d** and (S,S)-**20d** which predominantly showed fragmentation peaks.

The elements present in these complexes are composed of a number of isotopes. For example, naturally occurring chlorine exists primarily as two isotopes, ^{35}Cl and ^{37}Cl , with an abundance ratio of 3 to 1, respectively. The elements making up the titanocene derivatives (Ti, C, N, O, H and Cl) all exist with differing abundances of isotopes. The presence of these isotopes in molecules produces unique, isotopic patterns that are observable in mass spectrometry. These characteristic patterns help confirm the molecular formula of ions. An example of one of these isotopic patterns is shown in Figure 55. The calculated $[M+H]^+$ isotopic pattern of complex **15c** with the molecular formula $\text{C}_{16}\text{H}_{16}\text{NTiCl}_2$, is shown in the top spectrum and clearly matches the spectrum that was actually measured (bottom). These patterns helped confirm the identity of both the molecular and fragmentation ions. The results from the mass spectral analyses of the mono- and dicationic complexes are shown in Table 14 and Table 15, respectively.

The vast majority of the complexes generated a $[M - \text{Cl}]^+$ ion, corresponding to the cationic portion of the complex. A few notable complexes (**16c**, **14d**, **17d** and **19d**) generated dicationic molecular ions which were

observed at half the m/z value of the monocationic molecular ions. Additionally, a number of complexes exhibited $[M - Cl + MeOH]^+$ ions resulting from the loss of a chloride ligand and subsequent coordination of methanol.

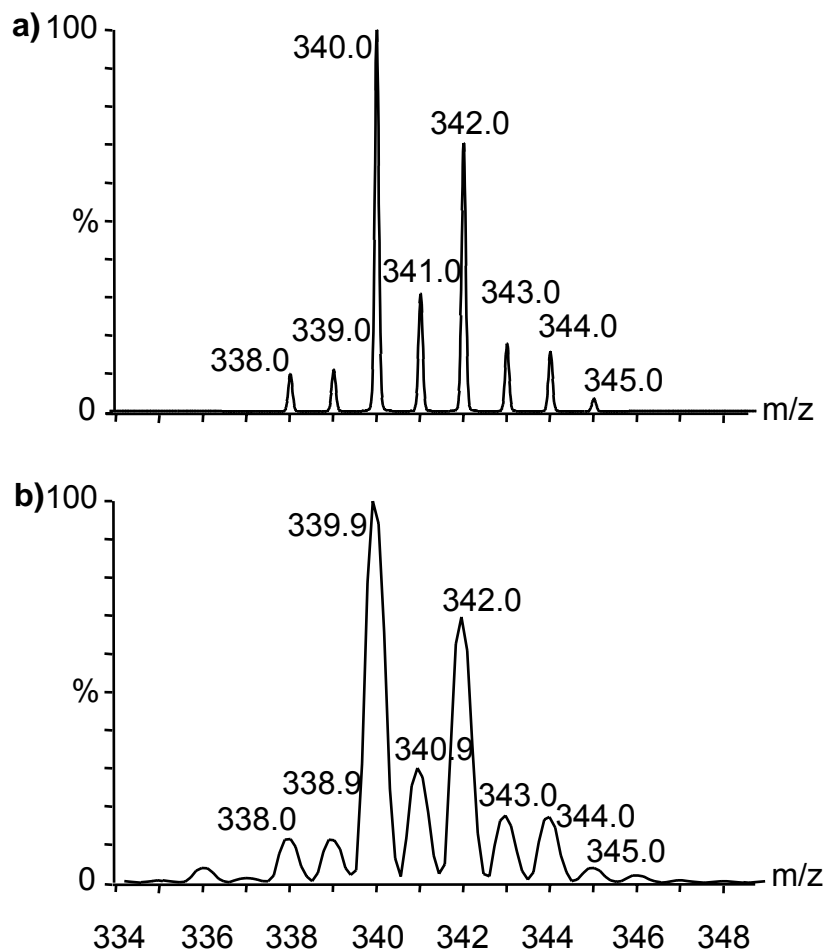


Figure 55 The predicted (a) and measured (b) isotopic patterns for the protonated molecular ion $[M+H]^+$ of **15c**.

Table 14 Mass spectral data for the monocationic complexes **14c** – **20c**.

Complex	Ion	Mass, (Intensity)
14c	$[M + H]^+$, $[M - Cl]^+$	340 (1), 304 (100)
15c	$[M + H]^+$, $[M - Cl]^+$	340 (90), 304 (20)
16c	$[M + H]^+$, $[M - Cl]^+$ $[M + H]^{2+}$	340 (30), 304 (100) 171 (10)
17c	$[M + H]^+$, $[M - H_2O]^+$ $[M - Cl]^+$	362 (25), 344 (90) 326 (100)
18c	$[M + H]^+$, $[M - Cl + MeOH]^+$ $[M - Cl]^+$	346 (80), 344 (10) 311 (10)
19c	$[M + H]^+$, $[M - Cl]^+$ $[M - Cp]^+$, $[M - N(CH_3)_2NHCl]^+$	410 (100), 374 (10) 345 (8), 227 (20)
(S)- 20c and (R)- 20c	$[M + H]^+$, $[M - Cl]^+$ $[M - 2Cl]^+$	306 (10), 270 (12) 235 (5)

Table 15 Mass spectral data for the dicationic complexes **14d** – **20d**.

Complex	Ion	Mass, (Intensity)
14d	$[M - Cl + MeOH]^+$, $[M - Cl]^+$ $[M + H]^{2+}$	429 (5), 395 (100) 216.5 (100)
15d	$[M + H]^+$, $[M - Cl + MeOH]^+$ $[M - Cl]^+$	431 (50), 427 (20) 395 (25)
16d	$[M + H]^+$, $[M - Cl + MeOH]^+$ $[M - Cl]^+$	431 (20), 429 (40) 395 (40)
17d	$[M + H]^+$, $[M - Cl + MeOH]^+$ $[M - H_2O]^+$, $[M]^{2+}$	475 (100), 471 (40) 457 (70), 238 (15)
18d	$[M + H]^+$, $[M - Cl]^+$	443 (40), 407 (90)
19d	$[M + H]^+$, $[M - CH_3]^+$ $[M - Cl]^+$, $[M]^{2+}$	571 (60), 555 (10) 535 (50), 286 (5)
(S,S)- 20d and (R,R)- 20d	$[M - 2Cl + OMe]^+$, $[M - 2Cl]^+$	323 (95), 292 (100)

3.10 Characterization of mono- and dicationic titanocene dichloride derivatives by X-ray crystallography.

The last method used in characterizing the TDC analogues was X-ray diffraction. All of the mono- and dicationic derivatives were purified using standard recrystallization techniques prior to full characterization. Only four of the sixteen complexes produced crystals that were suitable for X-ray crystallographic analysis. The molecular structures of complexes **14d**, **16c**, **18d** and **19c** are shown in Figures 54 – 57. Crystals for complexes **16c**, **18d** and **19c** were prepared by the layering technique. This technique involved dissolving the sample in a polar, aprotic solvent (dichloromethane) and carefully adding a less dense, non-polar solvent (benzene) so that the resulting mixture was made up of two distinct layers. As the solvents slowly diffuse over time, crystals begin to form at the interface. The dicationic derivative **14d** crystallized out of solution when it was dissolved in ethanol and consequently there are two molecules of ethanol in the crystal structure. Table 16 summarizes all of the particular crystal data and structure refinement parameters for all four products. Selected bond distances and angles of these complexes along with TDC are shown in Table 17.

The crystallographically determined mono- and dicationic complexes were shown in general to be structurally similar to the parent TDC.³¹ All of the complexes assumed a pseudotetrahedral arrangement of the two chloride and two η^5 -Cp ligands around the titanium centre. Because the Cp ligands have significant steric bulk, the centroid-Ti-centroid bond angle for the parent TDC (131.6°) is quite a bit larger than the Cl-Ti-Cl bond angles (94.43(6)° and

94.62(6)°). Neither mono- nor disubstitution on the Cp ring showed any significant effect on the centroid-Ti-centroid bond angle; all four complexes displayed angles between 128.8° – 133.4°. All of the observed angles for the Cl-Ti-Cl bonds were between 92.04° – 94.17°, with the notable exception of **19c** which had bond angles of ~97.5°. Furthermore, the bond lengths between titanium and its ligands for the novel complexes were shown to be similar to those of TDC. For the parent TDC the titanium-centroid bond distance was 2.058 Å. The comparable distance between the titanium centre and the Cp rings in the derivatives range from 2.046 – 2.101 Å. The titanium-chloride bond lengths for the derivatives range from 2.309(2) – 2.355(4) Å which is very similar to the average Ti-Cl bond length of 2.364 Å in TDC.

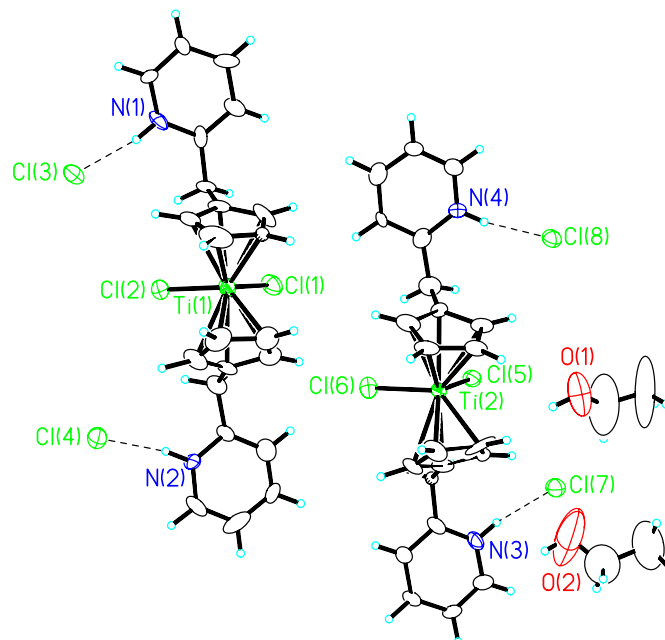


Figure 56 Molecular structure of **14d** showing two molecules per unit cell and two molecules of ethanol; thermal ellipsoids are shown at 50% probability level.

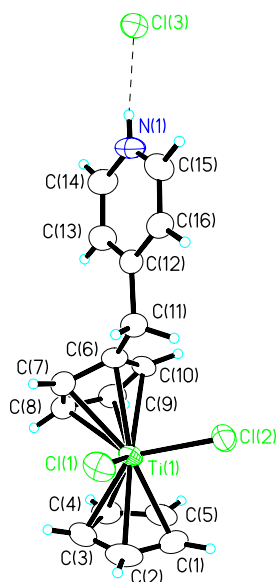


Figure 57 Molecular structure of **16c**; thermal ellipsoids are shown at 50% probability level.

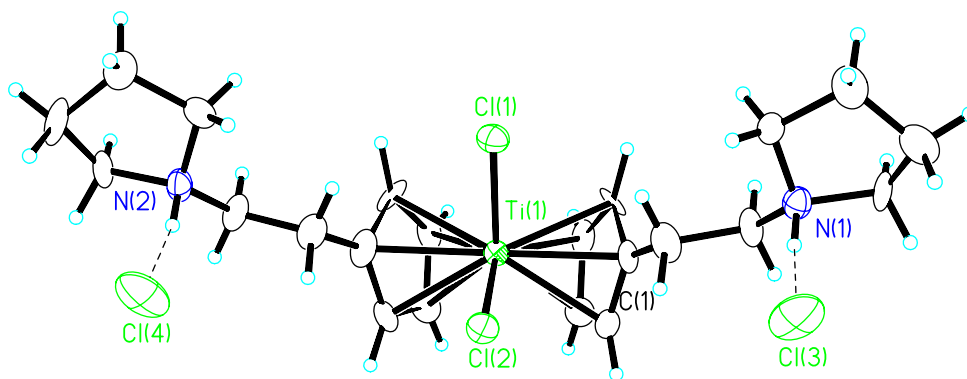


Figure 58 The crystal structure of **18d**; thermal ellipsoids are shown at 50% probability level.

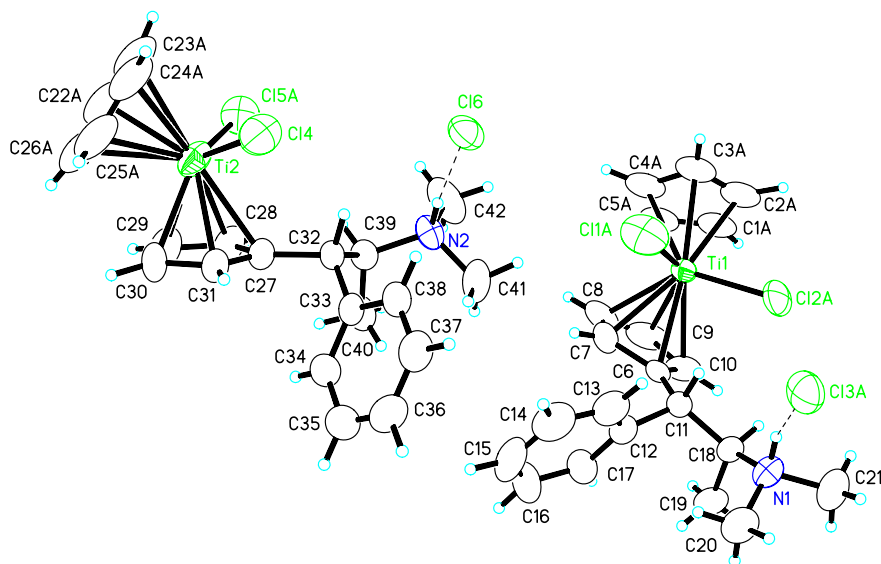


Figure 59 The molecular structure of **19c** showing two molecules per unit cell; thermal ellipsoids are shown at 50% probability level.

Table 16 Crystallographic data for compounds **14d**, **16c**, **18d** and **19c**.

Compound	14d	16c
Empirical formula	C ₂₄ H ₂₈ Cl ₄ N ₂ O ₂ Ti	C ₁₆ H ₁₆ Cl ₃ NTi
Formula Weight	550.18	376.55
Crystal System	Monoclinic	Triclinic
Lattice parameters		
<i>a</i> (Å)	10.692(3)	7.6841(9)
<i>B</i> (Å)	16.829(5)	9.6246(12)
<i>C</i> (Å)	28.000(9)	11.9385(15)
α°	90	108.374(2)
β°	93.751(6)	100.760(2)
γ°	90	93.465(2)
<i>V</i> (Å ³)	5027(3)	816.42(17)
Space Group	P2 ₁ /n	P-1
Z	8	2
ρ _{calc} (Mg m ⁻³)	1.454	1.532
μ (Mo Kα) (Å)	0.71073	0.71073
Temperature (K)	180(2)	180(2)
2θ _{max} (°)	52	50
Reflections collected	31347	4843
Data/restraints/parameters	9881 / 1 / 487	2851 / 0 / 254
<i>R</i> indices (<i>I</i> > 2σ <i>I</i>)		
R	0.0975	0.0445
<i>wR</i> ₂	0.1309	0.0916
<i>R</i> indices (all data)		
R	0.3240	0.0677
<i>wR</i> ₂	0.1679	0.0976
Largest peak final difference in map (e Å ⁻³)	0.510	0.472

Compound	18d	19c
Empirical formula	C ₂₂ H ₃₅ Cl ₄ N ₂ O _{0.5} Ti	C _{21.50} H ₂₇ Cl ₄ N ₂ Ti
Formula Weight	525.22	489.14
Crystal System	Orthorhombic	Monoclinic
Lattice parameters		
<i>a</i> (Å)	32.160(11)	7.2213(7)
<i>B</i> (Å)	11.639(4)	19.7152(18)
<i>C</i> (Å)	6.547(2)	16.7326(15)
α°	90	90
β°	90	98.8760(10)
γ°	90	90
<i>V</i> (Å ³)	2450.4(14)	2353.7(4)
Space Group	Ama2	P2(1)
Z	4	4
ρ _{calc} (Mg m ⁻³)	1.424	1.380
μ (Mo Kα) (Å)	0.71073	0.71073
Temperature (K)	180(2)	180(2)
2θ _{max} (°)	52	50
Reflections collected	7682	21817
Data/restraints/parameters	2130 / 1 / 135	8272 / 10 / 501
<i>R</i> indices (<i>I</i> > 2σ)		
R	0.0487	0.0465
<i>wR</i> ₂	0.0711	0.1241
<i>R</i> indices (all data)		
R	0.1093	0.0532
<i>wR</i> ₂	0.0821	0.1308
Largest peak final difference in map (e Å ⁻³)	0.536	0.373

Table 17 List of selected bond distances and angles of **14d**, **16c**, **18d**, **19c** and TDC.

Compound	Ti-Cl/(Å)	Ti-Cp (cent.)*/(Å)	Cl-Ti-Cl/(°)	Cent.-Ti- Cent./°)
14d	2.342(3), 2.360(3), 2.337(3), 2.355(3)	2.046, 2.063, 2.077, 2.057	94.17 (12) 92.43 (12)	133.4, 132.6
16c	2.3546(11), 2.3546(12)	2.061, 2.052	93.66 (4)	131.4
18d	2.355(4), 2.367(3)	2.048, 2.048	92.04(9)	132.5
19c	2.309(2), 2.3138(17), 2.385(10), 2.3337(13)	2.101, 2.066, 2.068, 2.059	97.98(11), 97.2(5)	128.8, 129.8
Cp₂TiCl₂ ³¹	2.367(2), 2.361(1), 2.363(1), 2.365(2)	2.058	94.43(6), 94.62(6)	131.6

* Cp' = Cp or substituted Cp; cent = ring centroid; ** angle calc using PLATON.¹³²

3.11 Summary of the Results for the Syntheses and Characterization of the Mono- and Dicationic titanocene dichloride derivatives.

A small library of mono- and dicationic TDC analogues bearing cyclic and chiral alkylammonium groups were prepared based on the structure activity relationship developed from cytotoxic activity studies of other titanocene derivatives. These complexes had significant improvements in aqueous solubility compared to the parent TDC; this is advantageous for clinical administration. Earlier work has shown that TDC derivatives bearing cyclic alkylammonium substituents such as **5** and **6** were more cytotoxic than acyclic analogues.⁴⁸ In order to exploit these apparent correlations, ten more novel derivatives bearing pendant cyclic alkylammonium groups (**14c,d** – **18c,d**) were prepared. These

analogues consist of picolyl stereoisomers, morpholinyl and pyrrolidinyl functional groups. The six chiral analogues (**19c,d** – **20c,d**) are derived from ephedrine and (S)/(R)-alaninol functionalities. The enantiomerically pure chiral derivatives were prepared in order to determine if there was a relationship between chirality (R or S) and cytotoxic activity, while the cyclic analogues would provide more insight into a possible structure activity relationship.

Following the syntheses of the above mentioned complexes, characterization was completed by ^1H , ^{13}C NMR spectroscopy, mass spectrometric and elemental analysis. Four of the sixteen complexes were also studied by X-ray crystallography. All of the complexes were subsequently evaluated for cytotoxic activity against a series of human cancer cell lines (A549, H69, HeLa and A2780).

3.12 Determination of Cytotoxicity for the Titanocene Dichloride Derivatives by MTT *in vitro* assays.

After all sixteen analogues (as seen in Figure 41 and Figure 44) were synthesized and fully characterized, their cytotoxic activities were evaluated by Kathy Sparks or Marina Chan in Dr. S.P.C. Cole's laboratory located in the Division of Cancer Biology and Genetics in the Cancer Research Institute at Queen's University. Complexes were tested against the cancer cell lines using the MTT chemosensitivity assay. This assay is a colorimetric test that measures the survival of cells after exposure to potentially cytotoxic agents. This method was originally developed by Mossman¹²⁰ and has since been adapted by Cole¹⁰⁹

and others for use with human tumour cells. The MTT assay is an *in vitro* test that measures the correlation between drug concentration and cell viability.

All sixteen of the complexes described here were initially screened against the non-small cell lung cancer cell line A549. The A549 cell line was used as a preliminary screening test partly because it is particularly robust. If the complex was found to be significantly cytotoxic against A549 cells, it was further tested against H69, HeLa, A2780, and H209 cells. These cell lines were used because they represent a mix both of standard cell lines for which many benchmarks of drug activities exist and of cell lines that represent solid tumour types for which more effective drugs are urgently needed. Furthermore, selected complexes were also evaluated against the cisplatin resistant derivatives of cell lines A2780 and H209, designated as A2780/CP and H209/CP. In addition, cisplatin and the clinical formulation of TDC (MKT-4) were also tested as a comparison. The *in vitro* assay results for all complexes are discussed below, with similar mono- and dicationic derivatives considered together, followed by a summary of the relative potencies for the entire series of complexes.

In all cases, an MTT assay was used to obtain IC_{50} values, i.e., the concentration of complex required to kill 50% of a cell population during the chosen time period. Absorbance values were determined at 570 nm using a UV spectrophotometer for the MTT assays. The software package GraphPad Prism 3.02 was used to calculate means and standard deviations for the wells that were treated with given drug concentrations which in turn generated dose response curves. Controls consisting of wells with untreated cells provided a baseline

absorbance and were assigned a value of 100%. IC_{50} values were obtained from the best fit of the data to a sigmoidal curve. The IC_{50} values that were determined from dose response curves were used to describe and compare the potencies of each complex against individual cancer cell lines. Typical representative dose response curves for cisplatin and the water soluble formulation of TDC (MKT-4) against A549 cells are shown in Figure 60a, for the mono- and dicationic complexes **15c** and **15d** in Figure 60b.

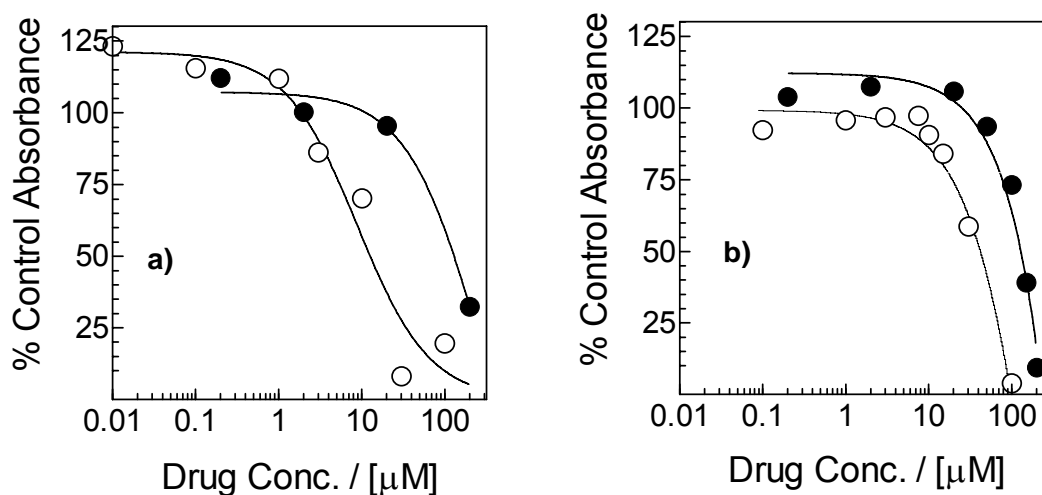


Figure 60 (a) Representative dose response curves for cisplatin (\circ) and TDC (\bullet) against A549 lung tumour cells; (b) Representative dose response curves for TDC derivatives **15c** (\bullet) and **15d** (\circ) against A549 lung tumour cells.

In general, cisplatin and the clinical formulation of TDC (MKT-4) were evaluated for cytotoxic activity against all of the cancer cell lines in order to allow for a comparison between the potency of the novel analogues of TDC that were synthesized. The IC₅₀ values obtained from testing cisplatin and MKT-4 against all of the above mentioned cancer cell lines are shown in Table 18 and Table 19. As another note of comparison, the cytotoxic activities of the previously prepared TDC derivatives containing cyclic alkylammonium groups (**5** and **6**) are also shown in Table 18.⁴⁸ For the chiral analogues, the IC₅₀ values of the previously tested complex **7** (consisting of stereoisomers) were included in Table 19 as a comparison. A majority of the cancer cell lines were shown to be highly sensitive to cisplatin with average IC₅₀ values of <9 μM for A549 cells, <2 μM for H69 cells, <0.1 μM for H209 and <2 μM for A2780 cells. A couple of notable exceptions were the HeLa cell line which only showed an IC₅₀ value of >30 μM and the cisplatin resistant cell line A2780/CP which was approximately 4 times more resistant to cisplatin than A2780.

The clinical formulation of TDC (MKT-4) was shown to be not nearly as potent as cisplatin. With all cancer cell lines, the IC₅₀ values for MKT-4 were >200 μM, which is above the concentration range (0 – 200 μM) tested.

The monocationic complexes **14c** – **16c** and dicationic complexes **14d** – **16d** contain picolyl functional groups and are constitutional isomers of each other. These complexes only differ as to where the nitrogen is present in the pendant pyridine ring. The mono- and disubstituted complexes **14c** and **14d** (containing an ortho substituted pyridinyl group) were initially screened against

the non-small cell lung cancer A549 as shown in Table 18. The IC₅₀ values for these complexes were greater than the highest concentration tested (>200 μM) and further testing of these complexes was abandoned.

Table 18 Effect of cyclic TDC analogues on human tumour cell viability

Complex	Cell line (IC ₅₀ ,/μM)*				
	A549	H69	HeLa	A2780	A2780/CP
14c	>200				
14d	>200				
15c	135.9 ± 23.9	29.2 ± 11.1	114.2 ± 57.0	22.9, 22.8	32.9, 61.2
15d	41.2 ± 16.9	28.1 ± 17.9	55.9 ± 16.2	21.1, 12.4	26.1, 12.8
15e	>200				
16c	>200				
16d	24.7 ± 6.9	13.3 ± 3.2	10.8 ± 0.6	12.1 ± 6.1	25.4 ± 7.7
17c	>200				
17d	>200				
18c	>200				
18d	>200				
5 ⁴⁸	66, 170			106, 17	112
6 ⁴⁸	38, 70			21	56
MKT-4	>200	>200	>200	>200	>200
Cisplatin	8.6 ± 2.5	1.9 ± 1.3	26.7, 18.9	0.9, 1.6	7.4, 4.0

* Data are means (± SD) of 3-5 independent experiments. Where <3 experiments were done, individual results are shown.

Table 19 Effect of chiral TDC analogues on human tumour cell viability.

Complex	Cell line (IC ₅₀ /μM)*		
	A549	H209	H209/CP
19c	571	62.0 ± 15.5	59.7 ± 4.7
19d	78, 66	31.7 ± 23.9	29.7 ± 12.5
(S)- 20c	>1000	>1000	>1000
(R)- 20c	>1000	>1000	>1000
(S,S)- 20d	>1000	>1000	>1000
(R,R)- 20d	>1000	>1000	>1000
(Mix)- 20d	>1000	>1000	>1000
7 ⁴⁸	94 ± 69	48 ± 16	
MKT-4	>200	>200	
cisplatin	8.6 ± 2.5	0.03 ± 0.01 ⁴⁸	

* Data are means (± SD) of 3-5 independent experiments. Where <3 experiments were done, individual results are shown.

Complexes **15c** and **15d** each contain a meta substituted pyridinyl group, mono- and disubstituted, respectively. Both complexes showed cytotoxic activity against A549 cells and were subsequently tested against four more cancer cell lines (H69, HeLa, A2780 and A2780/CP) as shown in Table 18. In general, the disubstituted derivative **15d** demonstrated better potencies compared to the monosubstituted complex **15c**. Complex **15c** showed moderate activity against A549 (IC₅₀ 136 μM) and HeLa (IC₅₀ 114 μM), and more pronounced activity against H69 (IC₅₀ 29 μM) and A2780 (IC₅₀ 23 μM). The dicationic complex **15d** showed similar cytotoxic activities against a four cancer cell lines (IC₅₀ 41 μM for A549, IC₅₀ 28 μM for H69, IC₅₀ 56 μM for HeLa and IC₅₀ 17 μM for A2780). For

HeLa and A2780 cell lines, both the mono- and di-substituted complexes showed equal IC_{50} values within experimental error.

The uncoordinated ligand **15a** was converted to its hydrochloride salt **15e** (as shown in Figure 61) and screened for cytotoxic activity against A549 cells. This hydrochloride salt showed no significant activity (Table 18) and confirmed that the cytotoxic activity demonstrated by the complexes **15c,d** is a result of the complex and not from the dissociation of the ligand. The complexes **15c,d** were also tested against the cisplatin resistant cell line A2780/CP. Complex 15d was shown to be just as effective against A2780/CP as it is against its non-cisplatin resistant variant.

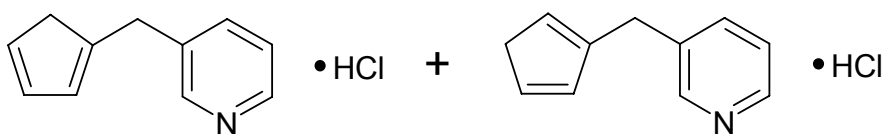


Figure 61 The two constitutional isomers making up **15e**.

Complexes **16c** and **16d** each contain a para substituted pyridinyl functional group. A summary of the IC_{50} values obtained for both **16c** and **16d** is shown in Table 18. The monocationic analogue **16c**, was initially screened against A549 cells and found to be ineffective over the concentration range that was studied (0 – 200 μ M). However, the dicationic derivative **16d** showed significant potency against A549 with an IC_{50} value of 25 μ M. Based upon the relatively greater cytotoxic activity of **16d**, it was subsequently tested against the other three tumour cell lines. The IC_{50} values obtained for complex **16d** against cell lines H69, HeLa and A2780 were 13 μ M, 10 μ M, and 12 μ M, respectively. In

fact, this particular complex was the most potent of all of the other TDC derivatives containing cyclic alkylammonium groups. Complex **16d** exhibits potencies that are vastly superior to the parent TDC and even come within an order of magnitude of cisplatin. Further testing of **16d** against the cisplatin resistant variant A2780/CP showed only a 2-fold decrease in activity compared to its parental cisplatin sensitive cell line.

Complexes **17c,d** incorporate a morpholinyl functional group while complexes **18c,d** contain a pyrrolidinyl functional group. None of these derivatives proved to have any cytotoxic activity when they were initially screened against A549 cells (Table 18). Due to the lack of activity against A549 cells, further testing of these four complexes was not pursued.

Complexes **19c** and **19d** both incorporate an ephedrine-type functional group consisting of two chiral centres. Overall, the monosubstituted derivative (**19c**) has two chiral centres and the disubstituted analogue (**19d**) has four chiral centres. A summary of their IC_{50} values is shown in Table 19. As in previous examples the disubstituted complex **19d** was shown to be more potent than the monosubstituted derivative (**19c**). In fact, complex **19d** ($IC_{50} \sim 72 \mu\text{M}$) was an order of magnitude more potent towards A549 cells than **19c** ($IC_{50} 571 \mu\text{M}$). Both complexes were subsequently tested against the H209 cell line and its cisplatin resistant variant H209/CP. The dicationic complex **19d** exhibited similar cytotoxicities against both strains of H209 with IC_{50} of $32 \mu\text{M}$ for H209 and $30 \mu\text{M}$ for H209/CP. Although the monocationic derivative was less potent than **19d**, it showed a similar trend with near identical IC_{50} values against both variants of

H209 (IC_{50} of 62 μ M for H209 and 60 μ M for H209/CP). These complexes are vastly more potent than TDC and the disubstituted derivative **19d** even improves upon the previously report chiral derivative **7**.

Finally, the enantiomerically pure complexes (S)-**20c**, (R)-**20c**, (S,S)-**20d** and (R,R)-**20d** were tested for cytotoxic activity in hopes of discovering a correlation between potency and chirality (Table 19). The complex (Mix)-**20d** which consists of 3 stereoisomers (R,R R,S and S,S in a ratio of 1:2:1, respectively) was also tested for potency as a point of comparison. It was found that none of these complexes exhibited any cytotoxic activity against the cell lines A549, H209 and H209/CP, even at an extended concentration range (0 – 1000 μ M).

3.13 Effect of substitution on Cytotoxicity of Titanocene Dichloride Derivatives 14c,d – 20c,d.

The majority of the prepared TDC derivatives exhibited very little cytotoxic activity. However, a few of the complexes proved to be quite potent and could provide some general insights regarding the effects of substitution on the Cp ring. In general, disubstituted derivatives were more potent than the corresponding monosubstituted species which is consistent with previously published studies.⁴⁸ Cisplatin was generally much more potent as a chemotherapeutic agent towards the tested cell lines than any of the TDC derivatives. The lower cytotoxic potencies of the titanocene analogues do not necessarily preclude them from further study considering that cisplatin has substantial toxic side effects. The

clinical formulation of TDC (MKT-4) was shown to be ineffective against the investigated cancer cell lines in the observed concentration range (0 – 200 μM).

Out of the sixteen complexes that were tested, only five showed any significant cytotoxic activity against the A549 cell line. As a general trend, the complexes bearing non-aromatic substituents (**17c,d** – **18c,d** and **20c,d**) were not cytotoxic. The derivatives containing picolyl groups, specifically those with meta and para substituted pyridine rings, were shown to have the most significant cytotoxic activity. In fact, complex **16d** was the most potent TDC derivative prepared in this lab to date with an IC_{50} value of $10.8 \pm 0.6 \mu\text{M}$ against the HeLa cell line. Against HeLa cells, the IC_{50} value of **16d** was even found to be more potent than cisplatin ($\text{IC}_{50} = 26.7, 18.9 \mu\text{M}$). Furthermore, the complexes containing an ephedrine type functional group were also shown to display significant cytotoxicity.

It was impossible to draw conclusions regarding the correlation between chirality and anticancer activity from the complexes **20c,d**. These complexes exhibited absolutely no cytotoxic activity over the concentration range studied (0 – 1000 μM). This complete lack of activity may be explained by the substitution of the pendant ammonium group. It has been previously shown that primary ammonium groups (like those in **20c,d**) have little to no cytotoxic activity.⁴⁸ Therefore it would be advantageous to prepare analogues of **20c,d** where the nitrogen has greater substitution (secondary or tertiary) for further cytotoxic testing.

It has been previously reported that TDC complexes exhibit activity against cisplatin resistant cancers both *in vitro* and *in vivo*.^{38,133} All analogues that were tested against both cisplatin resistant and non cisplatin resistant cell lines exhibited comparable activities, as shown in Table 18 and Table 19. This result is consistent with the proposed mechanism of action for titanium-based complexes which differs from that of platinum-based complexes. Accordingly, these titanocene derivatives should and do exhibit little to no difference in their activity against both parent and cisplatin resistant cancer cell lines.

Chapter 4: Summary and Conclusions

Previous research in this lab focussed on the preparation and cytotoxicity testing of a library of TDC derivatives with various alkylammonium substituents. These studies showed that TDC analogues bearing either cyclic or chiral alkylammonium groups were effective anti-tumour agents. In an effort to exploit these apparent correlations, the research presented here expands this library of TDC analogues focusing specifically on derivatives bearing cyclic and chiral alkylammonium groups. Sixteen novel water soluble monocationic and dicationic TDC derivatives, all similar in functionality to previous complexes which exhibit promising cytotoxic activities, were synthesized and characterized using ^1H and ^{13}C NMR spectroscopy, mass spectrometry and elemental analysis. In addition, four of the sixteen complexes were successfully crystallized for structural analysis by X-ray diffraction.

Following the syntheses of the library of complexes, all of the analogues were initially evaluated for cytotoxic activities against the human lung cancer cell line A549. The cyclic derivatives (**14c,d** – **18c,d**) that were found to exhibit potent IC_{50} values ($<200 \mu\text{M}$) against A549 cells were further evaluated against human cancer cell lines H69 (lung), HeLa (cervical), A2780 (ovarian) and A2780/CP (cisplatin resistant variant of A2780). The chiral analogues (**19c,d** – **20c,d**) were all evaluated against cancer cell lines H209 (lung) and H209/CP (cisplatin resistant variant of H209), regardless of their cytotoxicity against A549 cells.

The potencies of the complexes varied greatly, though there are some general trends. In general, it was found that the dicationic derivatives were more potent than their corresponding monocationic analogues and this result is consistent with the literature.⁴⁸ For the cyclic derivatives, it was found that those bearing 1,3- (**15c,d**) and 1,4-substituted (**16c,d**) pyridinyl groups were the most potent. The dicationic derivatives **15d** and **16d** exhibited IC₅₀ values as low as any for this class of complexes. Moreover, complex **16d** had an IC₅₀ value against HeLa cells ($10.8 \pm 0.6 \mu\text{M}$) that was comparable with that of cisplatin ($\sim 23 \mu\text{M}$). On the other hand, the derivatives bearing piperidinyl (**17c,d**) or morpholinyl (**18c,d**) groups were found to display no cytotoxic activity against the cancer cell lines assayed. The ephedrine substituted analogues (**19c,d**) were also found to exhibit promising cytotoxic activities. Conversely, the enantiomerically pure complexes (**20c,d**) exhibited no detectable cytotoxicity. This lack of activity is consistent with other TDC derivatives bearing primary substituted alkylammonium groups which also display no cytotoxic activity.

References

- (1) <http://www.bc.cancer.ca>, Canadian Cancer Centre
- (2) All statistics are taken from "National Cancer Instituted of Canada: Canadian Cancer Statistics 2007, Toronto, Canada, 2007"
- (3) B. Rosenberg, L. van Camp, J. E. Trosko and V. H. Mansour, *Nature* **1969**, 222, 385-386.
- (4) D. J. Higby, H. J. Wallace, D. J. Albert and J. F. Holland, *Cancer* **1974**, 33, 1219.
- (5) B. Rosenberg, *Plat. Met. Rev.* **1971**, 15, 42-51.
- (6) T. W. Hambley, *Coord. Chem. Rev.* **1997**, 166, 181-223.
- (7) E. Wong and C. M. Giandomenico, *Chem. Rev.* **1999**, 99, 2451-2466.
- (8) T. W. Hambley, R. A. Alderden and M. D. Hall, *J. Chem. Educ.* **2006**, 83, 728-733.
- (9) K. Siafaca, *Future Oncol.* **1999**, 5, 1045-1071.
- (10) R. B. Weiss and M. C. Christian, *Drugs* **1993**, 46, 360-377.
- (11) P. J. O'Dwyer, J. P. Stevenson and S. W. Johnson in *Cisplatin: Chemistry and Biochemistry of a Leading Anticancer Drug. Vol. B.* Lippert Ed; Verlag Helvetica Chimica Acta: Zurich, Weinheim, Germany, **1999**, 31-69.
- (12) D. P. Gately and S. B. Howell, *Br. J. Cancer* **1993**, 67, 1171-1176.
- (13) R. B. Martin in *Cisplatin: Chemistry and Biochemistry of a Leading Anticancer Drug. Vol. B.* Lippert Ed; Verlag Helvetica Chimica Acta: Zurich, Weinheim, Germany, **1999**, 183-206.
- (14) J. Arpalahiti in *Cisplatin: Chemistry and Biochemistry of a Leading Anticancer Drug. Vol. B.* Lippert Ed; Verlag Helvetica Chimica Acta: Zurich, Weinheim, Germany, **1999**, 207-222.
- (15) S. J. Lippard and E. R. Jamieson, *Chem. Rev.* **1999**, 99, 2467-2498.
- (16) T. W. Hambley, *Dalt. Trans.* **2001**, 2711-2718.
- (17) P. M. Takahara, C. A. Frederick and S. J. Lippard, *J. Am. Chem. Soc.* **1996**, 118, 12309-12321.

- (18) A. Eastman in *Cisplatin: Chemistry and Biochemistry of a Leading Anticancer Drug*. Vol. B. Lippert Ed; Verlag Helvetica Chimica Acta: Zurich, Weinheim, Germany, **1999**, 111-134.
- (19) F. Legendre and J.-C. Chottard in *Cisplatin: Chemistry and Biochemistry of a Leading Anticancer Drug*. Vol. B. Lippert Ed; Verlag Helvetica Chimica Acta: Zurich, Weinheim, Germany, **1999**, 223-246.
- (20) P. J. Sadler, A. I. Ivanov, J. Christodoulou, J. A. Parkinson, K. J. Barnham, A. Tucker and J. Woodrow, *J. Biol. Chem.* **1998**, *273*, 14721-14730.
- (21) F. Kratz in *Metal Complexes in Cancer Chemotherapy*. Vol. B. K. Keppler Ed; VCH, Weinheim, Germany, **1993**, 391-429.
- (22) R. C. DeConti, B. R. Toftness, R. C. Lange and W. A. Creasey, *Cancer Res.* **1973**, *33*, 1310-1315.
- (23) P. J. Sadler, K. J. Barnham, M. I. Djuran, P. d. S. Murdoch and J. D. Ranford, *Inorg. Chem.* **1996**, *35*, 1065-1072.
- (24) T. W. Hambley, R. C. Dolman and G. B. Deacon, *J. Inorg. Biochem.* **2002**, *88*, 260-267.
- (25) L. R. Kelland in *Cisplatin: Chemistry and Biochemistry of a Leading Anticancer Drug*. Vol. B. Lippert Ed; Verlag Helvetica Chimica Acta: Zurich, Weinheim, Germany, **1999**, 497-521.
- (26) M. J. Cleare and J. D. Hoeshcele, *Bioinorg. Chem.* **1973**, *2*, 187-210.
- (27) M. J. Cleare and J. D. Hoeshcele, *Plat. Met. Rev.* **1973**, *17*, 2-13.
- (28) D. Lebwohl and R. Canetta, *Eur. J. Cancer* **1998**, *34*, 1522-1534.
- (29) I. Judson and L. R. Kelland, *Drugs* **2000**, *59 Suppl.*, 29-36.
- (30) M. J. Clarke, F. Zhu and D. R. Frasca, *Chem. Rev.* **1999**, *99*, 2511-2533.
- (31) A. Clearfield, D. K. Warner, C. H. Saldarriaga-Molina, R. Ropal and I. Bernal, *Can. J. Chem.* **1975**, *53*, 1622-1629.
- (32) G. Wilkinson and J. M. Birmingham, *J. Am. Chem. Soc.* **1954**, *76*, 4281.
- (33) F. W. Siegert and J. De Liefde Meijer, *J. Organometal. Chem.* **1970**, *23*, 177.
- (34) J. C. Green, M. L. H. Green and C. K. Prout, *J. Chem. Soc., Chem. Commun.* **1972**, 421.
- (35) R. L. Cooper and J. L. H. Green, *J. Chem. Soc. A.* **1967**, 1155.

- (36) P. Köpf-Maier and H. Köpf, *Angew Chem Int Ed Eng.* **1979**, *18*, 477.
- (37) K. E. Dombrowski, W. Baldwin and J. E. Sheats, *J. Organometal. Chem.* **1986**, *302*, 281-306.
- (38) P. Köpf-Maier and H. Köpf, *Struct. and Bond.* **1988**, *70*, 103-185.
- (39) P. Köpf-Maier and H. Köpf, *Chem. Rev.* **1987**, *87*, 1137-1152.
- (40) M. M. Harding and G. Mokdsi, *Curr. Med. Chem.* **2000**, *7*, 1289-1303.
- (41) M. M. Harding and G. Mokdsi, *J. Inorg. Biochem.* **2001**, *83*, 205-209.
- (42) K. Mross, P. Robben-Bathe, L. Edler, J. Baumgart, W. Berdel, H. Fiebig and c. Unger, *Onkologie* **2000**, *23*.
- (43) A. Korfel, M. E. Scheulen, H.-J. Schmoll, O. Gründel, A. Harstrick, M. Knoche, L. M. Fels, M. Skorzec, F. Bach, J. Baumgart, G. Saß, S. Seeber, E. Thiel and W. Berdel, *Clin. Cancer Res.* **1998**, *4*, 2701-2708.
- (44) D. R. Ferry, D. W. Fyfe, A. Young, J. Doran, T. M. T. Sheehan, A. Eliopoulos, K. Hale, J. Baumgart, G. Sass, D. J. Kerr and C. V. Christodoulou, *J. Clin. Oncol.* **1998**, *16*, 2761-2769.
- (45) T. Schilling, K. B. Keppler, M. E. Heim, G. Niebch, H. Dietzfelbinger, J. Rastetter and A.-R. Hanauske, *Invest. New Drugs* **1996**, *13*, 327-332.
- (46) N. Kröger, U. R. Keleeberg, K. Mross, L. Edler, G. Saß and D. K. Hossfeld, *Onkologie* **2000**, *23*, 60-62.
- (47) G. Lümmer, H. Sperling, H. Luboldt, T. Otto and H. Rübber, *Cancer Chemother. Pharmacol.* **1998**, *42*, 415-417.
- (48) M. C. Baird, P. W. Causey and S. P. C. Cole, *Organometallics* **2004**, *23*, 4486-4494.
- (49) P. C. McGowan, O. R. Allen, L. Croll, A. L. Gott and R. J. Knox, *Organometallics* **2004**, *23*, 288-292.
- (50) T. J. Marks and J. H. Toney, *J. Am. Chem. Soc.* **1985**, *107*, 947-953.
- (51) M. M. Harding and G. Mokdsi, *J. Organometal. Chem.* **1998**, *565*, 29-35.
- (52) M. M. Harding and J. H. Murray, *J. Med. Chem.* **1994**, *37*, 1936-1941.
- (53) K. Döppert, *Naturwissenschaften* **1990**, *77*, 19-24.
- (54) M. M. Harding and G. Mokdsi, *Metal-Based Drugs* **1998**, *5*, 207-215.

- (55) M. M. Harding and P. M. Abeysinghe, *Dalt. Trans.* **2007**, 3474-3482.
- (56) B. W. Müller, R. Müller, S. Lucks and W. Mohr, US Pat. 5,296,237, **1994**
- (57) D. Osella, M. Ravera, C. Cassino, E. Monti and M. Gariboldi, *J. Inorg. Biochem.* **2005**, *99*, 2264-2269.
- (58) P. J. Sadler, M. Guo, H. Sun, H. J. McArdle and L. Gambling, *Biochemistry* **2000**, *39*, 10023-10033.
- (59) P. J. Sadler, H. Li and H. Sun, *Chem. Rev.* **1999**, *99*, 2817-2842.
- (60) P. J. Sadler, H. Li and H. Sun, *Eur. J. Biochem.* **1996**, *242*, 387.
- (61) H. M. Berman, J. Westbrook, Z. Feng, G. Gilliland, T. N. Bhat, H. Weissig, I. N. Shindyalov and P. E. Bourne, *Nucl. Acids Res.* **2000**, *28*, 235-242.
- (62) E. N. Baker and P. F. Lindley, *J. Inorg. Biochem.* **1992**, *47*, 147-160.
- (63) L. Messori, P. Orioli, V. Banholzer, I. Pais and P. Zatta, *FEBS Lett.* **1999**, *442*, 157-161.
- (64) E. Meléndez, L. M. Gao, R. Hernández and J. Matta, *J. Biol. Inorg. Chem.* **2007**, *12*, 959-967.
- (65) H. Li and Z. M. Qian, *Med. Res. Rev.* **2002**, *22*, 225-250.
- (66) A. D. Tinoco and A. M. Valentine, *J. Am. Chem. Soc.* **2005**, *127*, 11218-11219.
- (67) P. J. Sadler and M. Guo, *J. Chem. Soc. Dalton Trans.* **2000**, 7-9.
- (68) P. J. Sadler, M. Guo, H. Sun, S. Bihari, J. A. Parkinson, R. O. Gould and S. Parsons, *Inorg. Chem.* **2000**, *39*, 206-215.
- (69) P. K. Bali, O. Zak and P. Aisen, *Biochemistry* **1991**, *30*, 324-328.
- (70) F. Kratz and U. Beyer, *Drug Delivery* **1998**, *5*, 281-299.
- (71) M. Singh, *Curr. Pharm. Designs* **1999**, *5*, 443-451.
- (72) E. Wagner, D. Curiel and M. Cotten, *Adv. Drug Delivery Rev.* **1994**, *14*, 113-135.
- (73) P. Köpf-Maier and D. Krahl, *Chem.-Biol. Interact.* **1983**, *44*, 317.
- (74) P. Köpf-Maier and D. Krahl, *Naturwissenschaften* **1981**, *68*, 273.
- (75) P. Köpf-Maier, *J. Struct. Biol.* **1990**, *105*, 35.

- (76) P. J. Sadler, M. Guo and Z. Guo, *J. Biol. Inorg. Chem.* **2001**, 6, 698-707.
- (77) Z. Zhang, P. Yang and M. Guo, *Transition Met. Chem.* **1996**, 21, 322-326.
- (78) Z. Zhang, P. Yang, M. Guo and H. Wang, *J. Inorg. Biochem.* **1996**, 63, 183-190.
- (79) J. L. Vera, F. R. Román and E. Meléndez, *Anal. Bioanal. Chem.* **2004**, 379, 399-403.
- (80) J. C. Merrill, R. M. Lambrecht and A. P. Wolf, *Int. J. Appl. Radiat. Isot.* **1978**, 29, 115-116.
- (81) K. Ishiwata, T. Ido, M. Monma, M. Murakami, H. Fukuda, M. Kameyama, K. Yamada, S. Endo, S. Yoshioka, T. Sato and T. Matsuzawa, *Appl. Radiat. Isot.* **1991**, 42, 707-712.
- (82) A. L. Vavere, R. Laforest and M. J. Welch, *Nucl. Med. Bio.* **2005**, 32, 117-122.
- (83) A. L. Vavere and M. J. Welch, *J. Nucl. Med.* **2005**, 46, 683-690.
- (84) Q.-J. Meng, C.-S. Lu, Y. Zou, J.-L. Xie, Z.-P. Ni, H.-Z. Zhu and Y.-G. Yao, *Chem. Pharm. Bull.* **2003**, 51, 864-866.
- (85) Q.-J. Meng, Z. Lu, C.-S. Lu and X. Ren, *J. Organometal. Chem.* **2006**, 691, 5895-5899.
- (86) S. Lotz, R. Meyer, S. Brink, C. E. J. van Rensburg, G. K. Jooné and H. Görls, *J. Organometal. Chem.* **2005**, 690, 117-125.
- (87) U. Pindur, M. Haber and K. Sattler, *J. Chem. Educ.* **1993**, 70, 263.
- (88) M. C. Baird, J. R. Boyles, B. G. Campling and N. Jain, *J. Inorg. Biochem.* **2001**, 84, 159-162.
- (89) M. C. Baird, P. W. Causey, K. Sparks and S. P. C. Cole, Unpublished results
- (90) G. W. Coates, *Chem. Rev.* **2000**, 100, 1223.
- (91) P. Jutzi, C. Müller and D. Vos, *J. Organometal. Chem.* **2000**, 600, 127-143.
- (92) P. Jutzi, C. Müller, B. Neumann and H.-G. Stämmler, *J. Organometal. Chem.* **2001**, 625, 180-185.
- (93) P. Jutzi, T. Redeker, B. Neumann and H.-G. Stämmler, *Organometallics* **1996**, 15, 4153-4161.

- (94) P. C. McGowan and M. A. D. McGowan, *Inorg. Chem. Comm.* **2000**, 3, 337-340.
- (95) P. C. McGowan and R. J. Knox, International WO 2004/005305 A1, 2004
- (96) P. C. McGowan, O. R. Allen, A. L. Gott, J. A. Hartley, J. M. Hartley and R. J. Knox, *Dalt. Trans.* **2007**, 5082-5090.
- (97) M. Tacke, L. T. Allen, L. Cuffe, W. M. Gallagher, Y. Lou, O. Mendoza, H. Müller-Bunz, F.-J. K. Rehmann and N. J. Sweeney, *J. Organometal. Chem.* **2004**, 689, 2242-2249.
- (98) M. Tacke, F.-J. K. Rehmann, A. J. Rous, O. Mendoza, N. J. Sweeney, K. Strohfeltdt and W. M. Gallagher, *Polyhedron* **2005**, 24, 1250-1255.
- (99) M. Tacke, N. J. Sweeney, O. Mendoza, H. Müller-Bunz, C. Pampillón, F.-J. K. Rehmann and K. Strohfeltdt, *J. Organometal. Chem.* **2005**, 690, 4537-4544.
- (100) M. Tacke, C. Pampillón, N. J. Sweeney and K. Strohfeltdt, *J. Organometal. Chem.* **2007**, 692, 2153-2159.
- (101) M. Tacke, N. J. Sweeney, J. Claffey, H. Müller-Bunz, C. Pampillón and K. Strohfeltdt, *Appl. Organometal. Chem.* **2007**, 21, 57-65.
- (102) M. Tacke, N. J. Sweeney, W. M. Gallagher, H. Müller-Bunz, C. Pampillón and K. Strohfeltdt, *J. Inorg. Biochem.* **2006**, 100, 1479-1486.
- (103) M. Tacke, G. Kelter, N. J. Sweeney, K. Strohfeltdt and H.-H. Fiebig, *Anti-Cancer Drugs* **2005**, 16, 1091-1098.
- (104) M. Tacke, K. O'Connor, C. Gill, F.-J. K. Rehmann, K. Strohfeltdt, N. J. Sweeney, J. M. Fitzpatrick and R. W. G. Watson, *Apoptosis* **2006**, 11, 1205-1214.
- (105) M. Tacke, O. Obserschmidt, A. R. Hanauske, C. Pampillón, N. J. Sweeney and K. Strohfeltdt, *Anti-Cancer Drugs* **2007**, 18, 317-321.
- (106) P. Köpf-Maier and H. Köpf, *J. Organometal. Chem.* **1988**, 342, 167-176.
- (107) A. Gansäuer, D. Franke, T. Lauterbach and M. Nieger, *J. Am. Chem. Soc.* **2005**, 127, 11622-11623.
- (108) S. P. C. Cole, *Cancer Chemother. Pharmacol.* **1986**, 17, 259.
- (109) S. P. C. Cole, *Cancer Chemother. Pharmacol.* **1990**, 26, 250.
- (110) T. K. Panda, M. T. Gamer and P. W. Roesky, *Organometallics* **2003**, 22, 877-878.

- (111) D. Ranganathan, C. B. Rao, S. Ranganathan, A. K. Mehrotra and R. Iyengar, *J. Org. Chem.* **1980**, *45*, 1185-1189.
- (112) T. J. Clark, T. A. Nile, D. McPhail and A. T. McPhail, *Polyhedron* **1989**, *8*, 1804-1806.
- (113) C. Wang, International WO 2001/92346 A2, 2001
- (114) A. Döhring, J. Göhre, P. W. Jolly, B. Kryger, J. Rust and G. P. J. Verhovnik, *Organometallics* **2000**, *19*, 388-402.
- (115) L. Bernardi, B. F. Bonini, M. Comes-Franchini, M. Fochi, G. Mazzanti, A. Ricci and G. Varchi, *Eur. J. Org. Chem.* **2002**, 2776-2784.
- (116) A. Flores-Parra, P. Suárez-Moreno, S. A. Sánchez-Ruíz, M. Tlahuextl, J. Jaen-Gaspar, H. Tlahuext, R. Salas-Coronado, A. Cruz, H. Nöth and R. Contreras, *Tetrahedron: Asymmetry* **1998**, *9*, 1661-1671.
- (117) A. A. H. van der Zeijden, *Tetrahedron: Asymmetry* **1995**, *6*, 913-918.
- (118) A. A. H. van der Zeijden, *J. Organometal. Chem.* **1996**, *518*, 147-153.
- (119) Y. Minoura, M. Takebayashi and C. C. Price, *J. Am. Chem. Soc.* **1959**, *81*, 4689-4692.
- (120) T. Mosmann, *J. Immunol. Methods* **1983**, *65*, 55-63.
- (121) S. J. Coote, S. G. Davies, C. L. Goodfello, D. Middlemiss and A. Naylor, *Tetrahedron: Asymmetry* **1990**, *1*, 817-842.
- (122) A. J. Ashe III, *J. Am. Chem. Soc.* **1970**, *92*, 1233-1235.
- (123) E. W. Abel and M. O. Dunster, *J. Organometal. Chem.* **1971**, *33*, 161-167.
- (124) R. M. Silverstein and F. X. Webster, *Spectrometric Identification of Organic Compounds*, 6th Ed., John Wiley & Sons, Inc., **1998**.
- (125) J. Clayden, N. Greeves, S. Warren and P. Wothers, *Organic Chemistry*, Oxford University Press, New York, **2001**.
- (126) P. Jutzi and J. Kleimeier, *J. Organometal. Chem.* **1995**, *486*, 287-289.
- (127) P. Jutzi and T. Redeker, *Eur. J. Inorg. Chem.* **1998**, *6*, 663-674.
- (128) M. D. Rausch, J. F. Lewison and W. P. Hart, *J. Organometal. Chem.* **1988**, *358*, 161-168.
- (129) P. Jutzi and T. Redeker, *Organometallics* **1997**, *16*, 1343-1344.

- (130) H. E. Gottlieb, V. Kotlyar and A. Nudelman, *J. Org. Chem.* **1997**, *62*, 7512-7515.
- (131) J. K. M. Sanders and B. K. Hunter, *Modern NMR Spectroscopy 2nd Edition*, Oxford University Press, Oxford, **1993**. 30-33.
- (132) SHELXTL NT: Crystal Structure Analysis Package, version 5.10; Bruker AXS Inc.: Madison, WI, 1999
- (133) V. J. Moebus, R. Stein, K. D. G., I. B. Runnebaum, G. Saß and R. Kreienberg, *Anticancer Res.* **1997**, *17*, 815-822.